UNIVERSITY OF JYVÄSKYLÄ
DEPARTMENT OF CHEMISTRY

RESEARCH REPORT NO. 156

VIRPI NOPONEN

AMIDES OF BILE ACIDS AND BIOLOGICALLY IMPORTANT SMALL MOLECULES: PROPERTIES AND APPLICATIONS

Academic Dissertation for
the Degree of Doctor of Philosophy

UNIVERSITY OF JYVÄSKYLÄ
2012

DEPARTMENT OF CHEMISTRY, UNIVERSITY OF JYVÄSKYLÄ
RESEARCH REPORT No. 156

AMIDES OF BILE ACIDS AND BIOLOGICALLY IMPORTANT SMALL MOLECULES: PROPERTIES AND APPLICATIONS

BY

VIRPI NOPONEN

Academic dissertation
for the degree of
Doctor of Philosophy

To be presented, by permission of the Faculty of Mathematics and Science of the University of Jyväskylä, for public examination in Auditorium KEM4, on September 7th 2012, at 12 noon.

UNIVERSITY OF JYVÄSKYLÄ

Jyväskylä, Finland
ISBN 978-951-39-4836-8
ISSN 0357-346X

URN:ISBN:978-952-86-0189-0
ISBN 978-952-86-0189-0 (PDF)
ISSN 0357-346X

University of Jyväskylä, 2024

ABSTRACT

Noponen, Virpi
Amides of bile acids and biologically important small molecules: properties and applications
Jyväskylä: University of Jyväskylä, 2012, 85 p.
(Department of Chemistry, University of Jyväskylä, Research Report Series
ISSN 0357-346X; 156)
ISBN 978-951-39-4836-8

The research described in this thesis covers the synthesis and characterization of 18 bile acid derivatives of certain biologically important small molecules conjugated *via* an amide bond. The thread of the research has been the self-assembly studies of the compounds, along with the investigations of the formed systems.

A variety of self-assembled systems are shown to be formed by the investigated compounds. Seven of the compounds have been shown to be capable of self-assembly leading to organogelation. The nature of the compound conjugated to the bile acid moiety has proven to be the determinant factor for the gel-forming ability of the compounds.

Morphologies of the self-assembled systems have been investigated utilizing microscopic methods. Mainly two kinds of morphologies for the gel samples have been observed – fibrous structures or interconnected sphericals. Moreover, the sample preparation protocol has been shown to affect the sample appearance. NMR spectroscopic methods have been exploited to investigate the interactions involved in the gel formation. Additionally, solid state NMR studies have been performed for the native gel samples.

Solid state properties of the compounds have been investigated by means of both powder and single crystal X-ray diffraction along with solid state NMR spectroscopy. Single crystal structures for seven of the compounds have been solved. Moreover, a thermoreversible solid to solid phase transition for one of the compounds has been detected. The preliminary toxicological evaluation for the cysteamine conjugates has been performed. Finally, one of the compounds has been exploited in preparing steroid-capped gold nanoparticles *via* a single phase reduction process.

Basics of supramolecular gels, gold nanoparticles, and bile acids together with the most relevant achievements in the field of bile acid-based nanomaterials are reviewed in the literature part of the thesis.

Keywords: Bile acid, amino acid, cysteamine, amide, self-assembly, supramolecular gel, gold nanoparticle, SEM, TEM, NMR spectroscopy, ^{13}C CPMAS NMR, X-ray crystallography, toxicity tests

Author's address

Virpi Noponen
Department of Chemistry
P.O. Box 35
40014 University of Jyväskylä
Finland
virpi.noponen@jyu.fi

Supervisor

Academy Research Fellow, Adjunct Professor
Elina Sievänen
Department of Chemistry
University of Jyväskylä
Jyväskylä, Finland

Reviewers

Professor David K. Smith
Department of Chemistry
University of York
York, United Kingdom

Professor Julian X. X. Zhu
Department of Chemistry
University of Montreal
Montreal, Canada

Opponent

Professor Anthony P. Davis
School of Chemistry
University of Bristol
Bristol, United Kingdom

PREFACE

This work was carried out at the Department of Chemistry, University of Jyväskylä, Finland, between 2006 and 2012. Funding was received from the Magnus Ehrnrooth Foundation, University of Jyväskylä, and the Graduate School of Organic Chemistry and Chemical Biology (GSOCCB). Additionally, travelling grants were received from the Magnus Ehrnrooth Foundation, Emil Aaltonen Foundation, and GSOCCB. All of the above-mentioned instances are gratefully acknowledged for making this project financially possible.

I express my deepest gratitude to my supervisor, Academy Research Fellow, Adjunct Professor Elina Sievänen, who has been there for me all the way. I feel privileged because I have had the chance to work under her inspiring and encouraging guidance. I also would like to thank Professor Emeritus Erkki Kolehmainen, the initiator of the bile acid research in University of Jyväskylä, for the guidance and support he has given me throughout these years. Academy Professor Kari Rissanen is sincerely thanked for invaluable advices and support, as well.

Co-workers at the Department of Chemistry are warmly thanked for creating such a pleasant working atmosphere; I would be lying if I said that waking up in the morning and coming to the department to work with you has been a hard task. Especially the current and former members of the BA team – Kari Ahonen, Satu Ikonen, Ondřej Jurček, Juha Koivukorpi, Miika Löfman, Nonappa, Hana Svobodová, and Arto Valkonen – are sincerely thanked. Dr. Arto Valkonen is additionally acknowledged for kindly measuring and solving the single crystal X-ray structures for me. I also would like to thank Adjunct Professor Manu Lahtinen for his expertise, kind help, and contribution especially in the field of PXRD. In addition, I wish to thank all of the students whom I have supervised, who all have also taught me a lot. Especially I would like to thank M.Sc. Heini Belt for the excellent work done during her Master's project.

Laboratory technicians Mirja Lahtiperä, Elina Hautakangas, and Esa Haapaniemi are thanked for their assistance in mass spectrometry, elemental analysis, and NMR spectroscopy, respectively. Laboratory technician Hannu Salo is thanked for the time he has patiently spent staring at the SEM images with me, and for operating the equipment. Laboratory technicians Leena Koskela and already retired Reijo Kauppinen are especially acknowledged for their kind help considering whatever issue. I have considered you as my "spare parents" at the department. The administrative personnel at the Department of Chemistry are acknowledged for their invaluable help.

Professors David K. Smith (University of York, UK) and Julian X. X. Zhu (University of Montreal, Canada) are gratefully acknowledged for their detailed evaluation with kind and constructive comments of the present thesis. I feel privileged to have such experts on their own fields as the reviewers of my work.

I would like to thank my precious friends for your support and friendship, and to apologize, because I have totally neglected you during the past year. I owe my deepest gratitude to my parents Sisko and Aarno, and my brother

Kimmo, for the love and support they have given me throughout my whole life. I also wish to thank Pirkko and Kauko, my parents-in-law, for their support and help whenever needed. Finally, my husband Harri, son Jimi, and daughter Inka: I would be nothing without you. I love you.

Jyväskylä, August 17th 2012

Virpi Noponen

LIST OF ORIGINAL PUBLICATIONS

This thesis is based on the following original publications, which in the text are referred to by their Roman numerals.

I H. Svobodová, V. Noponen, E. Kolehmainen, and E. Sievänen, Recent advances in steroidal supramolecular gels, *RSC Adv.*, **2012**, *2*, 4985 – 5007.
https://doi.org/10.1039/C2RA01343F

II V. Noponen, Nonappa, M. Lahtinen, A. Valkonen, H. Salo, E. Kolehmainen, and E. Sievänen, Bile acid–amino acid ester conjugates: gelation, structural properties, and thermoreversible solid to solid phase transition, *Soft Matter*, **2010**, *6*, 3789 – 3796.
https://doi.org/10.1039/B925795K

III V. Noponen, A. Valkonen, M. Lahtinen, H. Salo, and E. Sievänen, Self-assembling properties of bile acid derivatives of L-cysteine, L-valine, and L-serine alkyl esters, *submitted*.
https://doi.org/10.1080/10610278.2012.735365

IV V. Noponen, H. Belt, M. Lahtinen, A. Valkonen, H. Salo, J. Ulrichová, A. Galandáková, and E. Sievänen, Bile acid–cysteamine conjugates: Structural properties, gelation, and toxicity evaluation, *Steroids*, **2012**, *77*, 193 – 203.
https://doi.org/10.1016/j.steroids.2011.11.006

V V. Noponen, S. Bhat, E. Sievänen, and E. Kolehmainen, Novel two-step synthesis of gold nanoparticles capped with bile acid conjugates, *Mater. Sci. Eng., C*, **2008**, *28*, 1144 – 1148.
https://doi.org/10.1016/j.msec.2007.10.001

Author's contribution

In paper I, the author has written the chapters about hydrogels and organogels. The author has carried out all of the syntheses and the self-assembly studies in papers II and III. The syntheses and the self-assembly studies in paper IV have been performed under her supervision. In papers II and III, the author has either performed or participated in most of the experimental work, apart from the X-ray crystallographic measurements. In paper IV, she has supervised the experimental work, apart from the X-ray crystallographic, DSC, and biological studies. In paper V, she has synthesized the compound **25a** and performed the NMR spectroscopic and mass spectrometric characterization for the compound. The author is the corresponding author of papers II–IV and the primary author of paper V. She is responsible for writing the papers II–V.

ABBREVIATIONS

1D	One-dimensional
3D	Three-dimensional
AcOH	Acetic acid
AFM	Atomic force microscopy
AgNP	Silver nanoparticle
AOT	Sodium bis(2-ethylhexyl) sulfosuccinate
ATP	Adenosine triphosphate
AuNP	Gold nanoparticle
CA	Cholic acid
CD	Circular dichroism
CDCA	Chenodeoxycholic acid
cmc	Critical micellar concentration
CPMAS	Cross polarization magic angle spinning
DCA	Deoxycholic acid
DHCA	Dehydrocholic acid
DHN	2,3-Dihydroxynaphthalene
DLS	Dynamic light scattering
DMF	*N*,*N*-Dimethylformamide
DMSO	Dimethylsulfoxide
DNA	Deoxyribonucleic acid
DSC	Differential scanning calorimetry
EM	Electron microscopy
Et_3N	Triethylamine
EtOAc	Ethyl acetate
FRET	Fluorescence resonance energy transfer
FT-IR	Fourier transform infrared spectroscopy
HRTEM	High-resolution transmission electron microscopy
IR	Infrared
LCA	Lithocholic acid
LDI-MS	Laser desorption–ionization mass spectrometry
MeCN	Acetonitrile
MeOH	Methanol
MGC	Minimum gelation concentration
MWCNT	Multi-walled carbon nanotube
NaDC	Sodium deoxycholate
nanoGUMBOS	Nanoparticles from a group of uniform materials based on organic salts
NH_4LC	Ammonium lithocholate
NIR	Near infrared
NMR	Nuclear magnetic resonance
NP	Nanoparticle

NR	Neutral red dye
OPV	Oligo(*p*-phenylenevinylene)
PEG-400	Polyethylene glycol 400
PEI	poly(ethylene-imine)
ppm	Parts per million
PXRD	Powder X-ray diffraction
RNA	Ribonucleic acid
SANS	Small-angle neutron scattering
SAXS	Small-angle X-ray scattering
SEM	Scanning electron microscopy
SERS	Surface-enhanced Raman scattering
SPB	Surface plasmon resonance band
SPR	Surface plasmon resonance
STM	Scanning tunneling microscopy
SWCNT	Single-walled carbon nanotube
TEM	Transmission electron microscopy
TEOS	Tetraethoxysilane
TGA	Thermogravimetric analysis
T_{gel}	Gel–sol transition temperature
THF	Tetrahydrofuran
TLCA	Taurolithocholic acid
TNF	2,4,7-Trinitrofluorenone
TOAB	Tetraoctylammonium bromide
TRIS	Tris(hydroxymethyl) aminomethane
UDCA	Ursodeoxycholic acid
UV	Ultraviolet
UV-Vis	Ultraviolet–visible spectroscopy
VT NMR	Variable-temperature NMR
XPS	X-ray photoelectron spectroscopy

TABLE OF CONTENTS

1 REVIEW OF THE LITERATURE

1.1 Supramolecular gels

A simple approach to the spontaneous generation of nanomaterials is offered by the use of organic building blocks able to self-assemble into nanoscale architectures. Of particular interest in this regard has been the rapid development of gel-phase materials constructed *via* the hierarchical assembly of molecular building blocks.[1]

Gels can be found in our everyday life in a variety of forms. The wet soft solids encountered in the form of commercial products such as soap, toothpaste, hair gel, and contact lenses are all gels derived from polymeric compounds, the gelation properties of which have been known for centuries. However, the gels derived from low molecular weight compounds, called physical or supramolecular gels, although known for a long time, have started to gain an increasing interest only during the past 20 years or so.[2,3]

Gels are, in general, viscoelastic solid-like materials comprised of an elastic cross-linked network, and a solvent as the major component. The formation of the cross-linked network can either result from the chemical cross-linking or physical interactions. The gels formed by strong chemical bonds cannot be redissolved and are thermally irreversible, whereas the gels formed by the weak non-covalent interactions are reversible. The gels derived from low molecular weight compounds (Fig. 1) are formed by the self-assembly of the gelator molecules through a combination of non-covalent interactions like hydrogen bonding, π-π stacking, donor-acceptor interactions, metal coordination, solvophobic forces, and van der Waals interactions, and are thus supramolecular in the strictest sense.[2]

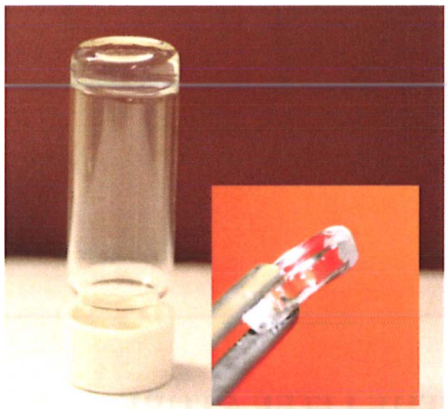

Figure 1. Photographs of a supramolecular gel.[11]

As already mentioned the process of gelation is often described as hierarchical and depends on a number of steps. Usually, the process involves the self-association of the gelator molecules to form long, polymer-like fibrous aggregates, which get entangled during the aggregation process forming a matrix, which traps the solvent mainly by surface tension. However, in spite of extensive investigations, several aspects of the gel forming process are poorly understood and thus remain as an area of intense interest. The power of the hierarchical assembly is demonstrated by the fact that very small amounts (typically < 2% w/v) of the gelator compound often achieve complete solvent immobilization.[1]

1.1.1 Building blocks

Gelation is highly dependent on the choice of the solvent. Gels can be broadly divided into two categories: in aqueous solutions forming hydrogels, and organogels, that form in organic solvents. In addition, there exists a structurally varied group of ambidextrous gelators,[4-9] which are able to form gels both in polar and apolar solvents.

The design of a gelator molecule is typically a challenging task, and very often the gelators are discovered by serendipity. However, some broad conclusions about the requirements for a molecule to be capable of self-assembly leading to gelation can be drawn. First, the molecule should be partly soluble in the solvent of choice. However, at the same time the compound should be partly insoluble, as well. Second, the molecule should have the potential to self-assemble *via* multiple non-covalent interactions, which should occur in a directional manner. Van der Waals forces are usually needed to support the gelation process.[1] In addition, chirality has been shown to play an essential role in the molecular packing, and thus the gel formation in many cases.[10] In recent years, more and more effort has been put to achieve the goal of rational design and

synthesis of gelator molecules.[11] Two approaches, namely molecular engineering and crystal engineering can be utilized to design the gelators.

The –CONH– group found in the amide, urea, and carbamate type of compounds has both a hydrogen bond donor (N–H) and a hydrogen bond acceptor (C=O), and is thus ideal for the formation of intermolecular hydrogen-bonded networks. Hydroxyl groups, likewise, contain both a hydrogen bond donor and an acceptor. Carbohydrates, as naturally occurring building blocks having multiple hydroxyl groups with different organizations and chiralities, are particularly interesting. Normally, for the formation of organogels, some of the sugar hydroxyl groups are protected, whereas in hydrogelators the fully deprotected carbohydrate is employed. Steroids, such as cholesterol and bile acids, as naturally occurring lipid molecules having apolar tetracyclic skeletons and relatively planar rigid structures, have been widely explored as gelators.[1] Nucleobases, for one, represent interesting structures for the preparation of gel-phase materials, because they are able to form hydrogen bonding interactions within the plane of the heteroaromatic ring, and π-π interactions perpendicular to the plane. Moreover, an interesting feature of nucleobase derivatives is their ability to form specific interactions with their complementary nucleobase partner, by which the self-assembly process and hence the properties of the formed gel can be modified. Alkyl chains are nearly ubiquitous in the gel-phase systems, since they provide a simple way of tuning the solubility of the molecular building blocks. Alkyl chains pack together *via* van der Waals forces, which may enhance gelation by supporting other intermolecular forces, particularly during the organogel formation. In hydrogels, for one, alkyl chains are often the driving forces in the aggregation process as a consequence of the hydrophobic effect. Yet another interesting group of compounds explored as gelators are dendritic molecules that possess multiple functional groups within their branched structure, and are thus capable of forming multiple intermolecular interactions.[1] Selected examples of molecules capable of self-assembly leading to gelation are presented in Figure 2.

Two-component gelation systems[12] are of considerable interest, since the extra level of supramolecular control in the hierarchical self-assembly of these materials provides additional tunability and controllability in comparison to the one-component systems. In two-component gels, the self-assembly relies on the initial interaction between two complementary components to form a complex, which subsequently self-assembles into a gel-phase material. Variation of one of the two components provides a simple way to build functionality into the material. Moreover, the ratio of the components is yet another parameter that can be varied in order to generate new morphologies and tune the materials' behavior.

Metallogels, the gels that in some way incorporate a metallic element into the system, have recently become highly topical.[13,14] In these systems, the metal ions can form part of the covalent structure of the gelator, or be bound by the coordination interactions.

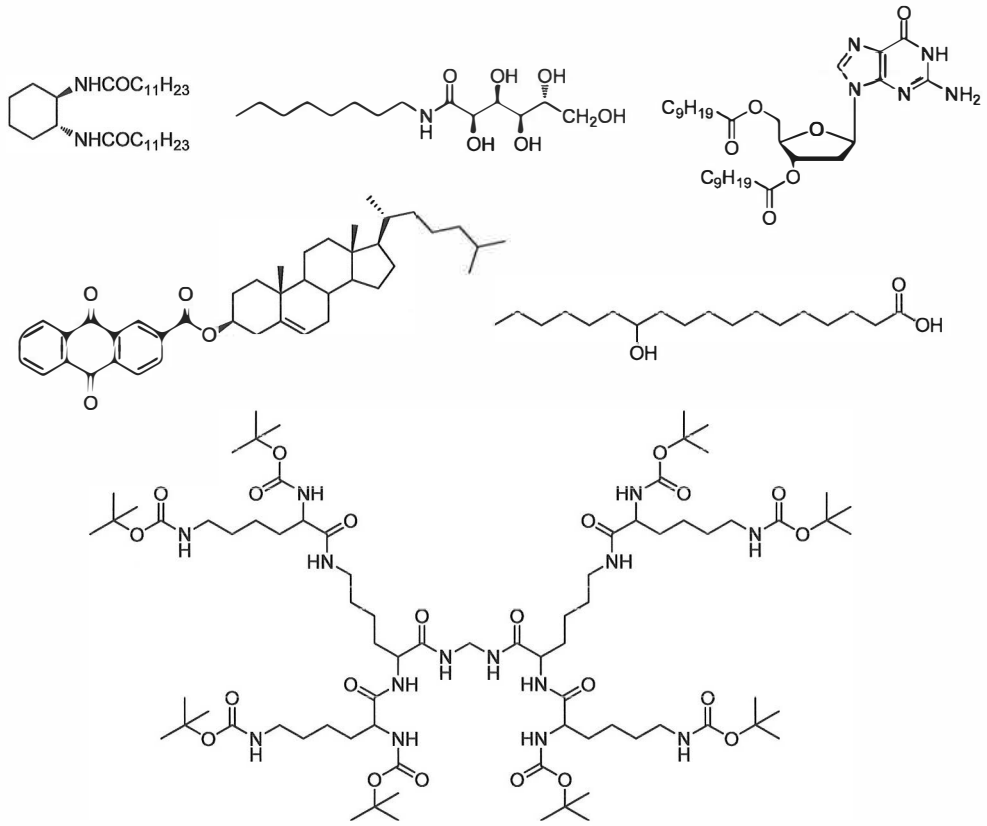

Figure 2. Examples of molecules capable of forming supramolecular gels.[1]

1.1.2 Preparation of the gels

Supramolecular gels are often formed by heating the solid low molecular weight gelator in an appropriate solvent resulting in the solubilization of the gelator. Sometimes sonication either exclusively or in addition to heating is applied. The solution transforms into a gel upon (preferably controlled) cooling. In some cases, the gel forms instantly on dispersing the gelator in the appropriate solvent. Since the gel properties may vary depending on the precise details of preparation, the accurate reporting of the gel preparation method is essential.[1]

1.1.3 Analysis of the systems

Among the most interesting features of supramolecular gels are the connectivity between the molecular structure, nanoscale self-assembled morphology, and macroscopic materials' properties. There are many techniques across the full range of length scales available in order to investigate the materials.

Two simple parameters widely used to define the macroscopic properties of the gels are minimum gelation concentration (MGC) and gel–sol transition temperature (T_{gel}). MGC represents the minimum concentration of a gelator required to form a sample-spanning self-supporting gel at a given temperature. T_{gel} can be determined by monitoring the gelation with the use of a thermoregulated heating–cooling bath either by using the tube inversion or the dropping ball method.[1]

The macroscopic behavior of the gels can also be explored utilizing rheology. Typically, the magnitudes and ratios of the elastic (G′) and loss (G″) moduli determined under oscillatory shear are the parameters studied. The ability of the deformed material to regain its shape is indicated by the elastic modulus, whereas the loss modulus represents the ability of the material to flow under stress. Rheological studies performed for a number of supramolecular gels have proven that the gels can be rheologically classified as cellular solids, fractal/colloidal systems, or soft glassy materials depending on their behavior. Differential scanning calorimetry (DSC) provides yet another way to examine the macroscopic properties of the gels. DSC provides a way to directly measure the enthalpy of the phase-change ($\Delta H_{gel-sol}$) and gives an insight into the thermodynamics of the gelator–gelator interactions.[1]

The utilization of electron microscopy gives an insight into the nanostructures of the gel-phase materials. Scanning electron microscopy (SEM, Fig. 3) is by far the most applied technique. For SEM the gel sample is first allowed to dry on a substrate, and then coated under vacuum with a thin metallic layer, after which the imaging is performed. Usually the drying of the gel sample causes the gel network to collapse to yield a xerogel. Besides this collapse, also some other changes in the nanostructure may occur during the drying process; however, the effects of these changes are often assumed to be minor. Using SEM, a wide variety of morphologies (fibers, tapes/ribbons, helical objects, platelet-like structures, *etc.*) is observed. In general, transparent gels exhibit nanoscale structuring, whereas opaque gels have microscale features. Transmission electron microscopy (TEM) is also applicable to gel imaging, although normally it requires a heavy metal staining agent to be applied in order to enhance the image contrast. Moreover, it is possible to utilize cryo-electron microscopic techniques, which use a rapid freezing step to prevent the thermal motion of the assembled network. This leads to significantly diminished disruption of the gelator network, and therefore a more expanded and "solvated" network is visible in a cryo-EM image, compared to the EM images of xerogel samples.[1]

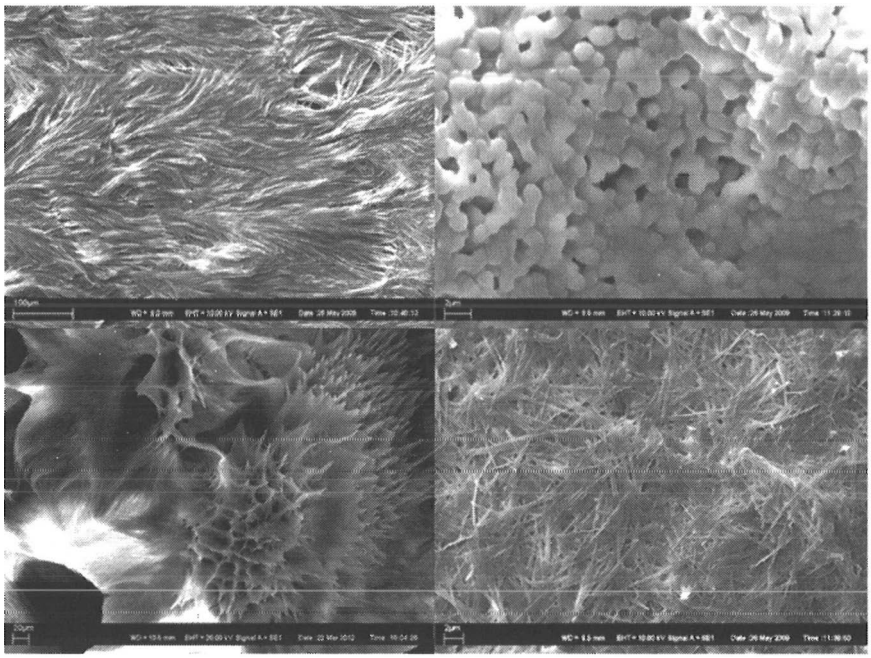

Figure 3. SEM images of dried supramolecular gels (xerogels).[II-IV]

X-ray scattering analysis of gel-phase materials provides a way of "visualizing" the molecular-scale fibrils, which underpin the morphology observed by electron microscopy. Further, X-ray diffraction can be utilized to study the dried gels (xerogels) in order to obtain a more precise understanding of the molecular packing within the fibrils. However, the results must again be treated with some care, as the drying process may lead to morphological changes. Computer modeling is often used as a complementary tool to X-ray diffraction (as well as the other techniques used) to study the supramolecular gels. In some cases, such approaches can be used to predict the fibril/fiber packing and even lead to pictorial models describing the self-assembled systems.[1]

Spectroscopic methods, such as NMR, IR, and fluorescence spectroscopy are useful tools when investigating the molecular scale assembly.[1] NMR data gives information on the chemical nature as well as on the molecular or collective mobility of an observed component.[15] In most cases attention is paid to the analysis of the variation of chemical shifts, spin relaxation times, or intensity of the NMR signals along with concentration, solvent composition, or temperature. Besides information on the intermolecular interactions, NMR data can be used to obtain information on the critical concentration values, the change in the motion of the molecules, or thermodynamic parameters associated within the gel formation.

Infrared (IR) spectroscopy is very useful for probing the hydrogen bond interactions between the molecular building blocks. Also van der Waals interactions can be detected by monitoring the changes in the C–H stretching interactions. Typically the IR spectra of a gelator in both the solution and the gel phase

are compared in order to determine the main non-covalent interactions. Fluorescence spectroscopy can be utilized to track the aggregation of gelators that bear a fluorophore in their structures. Both variable temperature IR and fluorescence can be useful techniques to study, which spectral features are responsive to the aggregation process.[1]

Circular dichroism (CD) spectroscopy provides a way to monitor both molecular and nanoscale chirality. The self-assembled nanostructures often give rise to much larger CD bands than their isolated molecular building blocks, and therefore the presence of a CD signal provides a good evidence for the presence of a chiral nanoscale object. In the case of well-characterized chromophores, it is sometimes possible to use CD spectroscopy to predict whether the molecules within the helical assembly are packed in a clockwise or anticlockwise manner. Moreover, CD spectroscopy provides an ideal method for probing the assembly of enantiomeric mixtures of molecular building blocks into gels.[1]

1.1.4 Stimuli-responsive systems

Supramolecular gels are thermoreversible, which makes them thermoresponsive. In addition to that, the incorporation of a receptor site or a photoresponsive group in the gelator molecule might give sensitivity towards external stimuli, such as chemicals or light. Azobenzene and anthracene units have often been exploited as the photoresponsive entities, whereas pH-responsiveness is commonly achieved by the introduction of acidic or basic sites in the gelator compound. Gel-phase materials responsive to other stimuli, such as mechanical stress or oxidation state, are also known. The most common response of the systems is a transition from solution to gel (or *vice versa*). Other responses include changes in chemical or physical properties, such as conductivity, color, or light emission. Stimuli-responsive gels are of great potential in designing and constructing new functional materials, such as sensors, actuators, molecular devices, or drug delivery vehicles, as described later in this thesis.[16-18]

1.1.5 Hybrid materials derived from supramolecular gels

The design of inorganic–organic hybrid materials, in which the matrix of supramolecular gels is exploited to organize the nanoparticles into two- or three-dimensional architectures, has been of considerable interest. These materials have potential applications in optics, electronics, ionics, mechanics, biology, fuel and solar cells, catalysis, sensors, *etc*.[16]

One of the earliest reports has described the incorporation of superparamagnetic ferrite and semiconducting CdS nanoparticles into an organogel formed by the addition 4-chlorophenol to a solution containing the reverse micellar aggregates of the well-known surfactant bis(2-ethylhexyl)sulfosuccinate (AOT).[19] Kimura and Shirai with their co-workers were the first to describe the self-organization of gold nanoparticles (AuNPs) into a gel network structure. The organogelator contained two functional groups, a *trans*-1,2-bis(alkylamide)-cyclohexane unit and two thiol groups. The octanethiol-stabilized AuNPs were

prepared separately. When the gel components and the AuNPs were mixed, the octanethiol residues were shown to be replaced by the thiol groups of the gelator by site-exchange reactions, as depicted in Figure 4. An interlocked 3D structure of fibrous aggregates consisting of individual AuNPs was observed by TEM.[20]

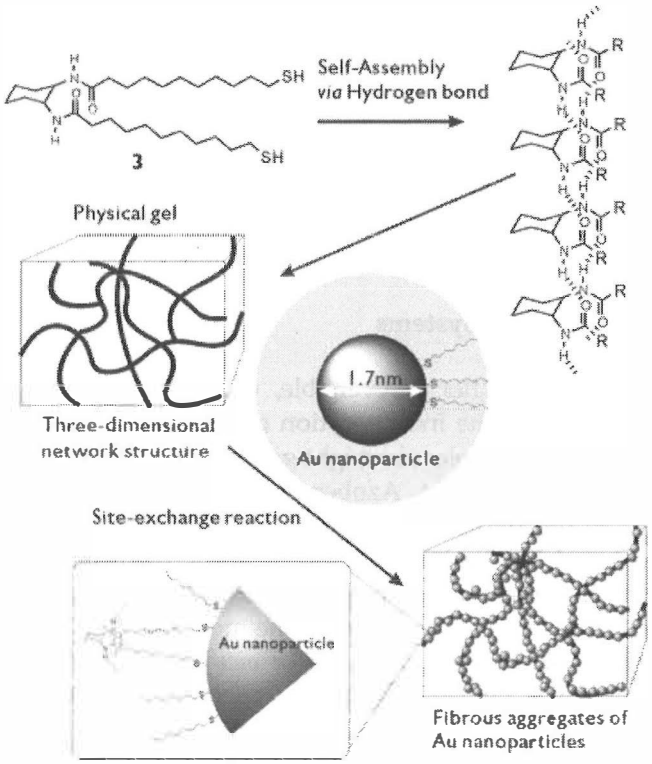

Figure 4. Schematic illustration of the organization of AuNPs around the gel fibers.[20] Reprinted with permission. Copyright © 2004 WILEY-VCH Verlag GmbH & Co. KGaA, Weinheim

A number of ways to incorporate Au/AgNPs into the gel network structures have been reported. The materials can be prepared either by mixing the pre-formed nanoparticles with the gel components[21-25] or synthesizing the nanoparticles within the supramolecular gel network.[26-31]

The influence of the gold nanoparticle capping agent on the morphological features and viscoelastic properties of the gel–AuNP hybrid materials has been investigated by Bhattacharya and co-workers.[22] A fatty acid amide of L-alanine was used as the gel-forming component. Different sets of capping agents based on *n*-alkanethiols, a cholesterol-based thiol, and *p*-thiocresol were utilized in order to investigate the gel–AuNP interactions. The incorporation of the AuNPs in the gel was shown to have a notable impact on the morphological features of the resulting hybrid materials as evidenced by SEM. Moreover, the rheological characterization of the materials revealed interesting viscoelastic properties. The incorporation of the alkanethiol- and cholesterol thiol-capped AuNPs led to

the hybrid materials with increased rigidity compared to the native gel. However, the thiocresol-based AuNPs in the gel were shown to decrease the rigidity of the resulting hybrid material. It was proposed that the van der Waals interactions of the gel fibers with the alkyl chains or cholesteryl units on the surface of the AuNPs collated the gel fibers into the close-packed aggregates resulting in increased rigidity of the materials.

The gelator compound discussed above has also been exploited for the preparation of novel near IR (NIR)-responsive organogel–single-walled carbon nanotube (SWCNT) hybrid materials.[32] In order to improve the solubility of the SWCNTs in the gel matrix, a variety of SWCNTs funtionalized with different aliphatic and aromatic chains were synthesized. SEM investigations of the prepared materials revealed that the texture and organization of the gel aggregates were altered upon the incorporation of SWCNTs. The nature of the SWCNT used was shown to determine the microstructure of the hybrid material. The sol-to-gel phase transition temperature was shown to decrease with increasing chain length of the functionalized SWCNTs, suggesting greater miscibility of such nanotubes in the organogels due to the enhanced induction of the chain interdigitation of the pendant chains with the fatty acid amides of L-alanine. Also the flow behavior of the materials was found to depend on the length of the hydrocarbon chain of the functionalized SWCNTs. Finally, by using the near IR laser irradiation at 1064 nm for 1 min at room temperature, it was possible to selectively induce a gel-to-sol phase transition of the hybrid materials, whereas the native gel did not show similar melting behavior even after irradiating for a longer time.

Also Ajayaghosh and co-workers prepared novel nanotube-containing hybrid materials by dispersing the carbon nanotubes (both SWCNTs and MWCNTs) in oligo(*p*-phenylenevinylene) (OPV) gels in nonpolar solvents.[33] The gelation of the OPV derivatives in toluene was shown to be induced below their normal critical gelation concentration when the carbon nanotubes were dispersed. In addition, the hybrid gels were found to be both thermally and mechanically more stable compared to the native gels. This is expected to be caused by the strong π-π stacking interactions between the OPV moieties of the gelators and the carbon nanotubes.

1.1.6 Applications

A myriad of applications exploiting the nanoscale architectures of supramolecular gels *e.g.* in the fields of optoelectronics, light harvesting, hybrid materials (discussed above), tissue engineering, and regenerative medicine have been reported and reviewed.[2,16,17,34,35] In this section, a very general introduction to the theme is given.

The self-assembly of organic building blocks is able to generate a variety of supramolecular structures showing diversity in size, shape, chemical composition, and function. The transcription of these structures may lead to the development of novel inorganic materials. Several reports concerning the transcrip-

tion of the supramolecular gel structure into silica have been published. In some studies even the chirality of the materials has been transcribed in the resulting inorganic systems. Many studies reporting the synthesis of metal oxide/sulfate/sulfide materials with a wide variety of morphologies using supramolecular gels as templates have been published.[16,36] One of the most interesting findings was introduced by Stupp and co-workers,[37] who designed a nanostructured organic template to study the mineralization of bone material (Fig. 5). The self-assembled peptide amphiphile fibers were shown to be able to nucleate hydroxyapatite on their surfaces in a manner that is analogous to the alignment observed between the collagen fibers and hydroxyapatite crystals in bone. This observation could find use in designing of materials for mineralized tissue repair.

As already mentioned, stimuli-responsiveness of the gels provides accessibility for the design and construction of new functional materials, such as sensors, actuators, molecular devices, *etc.* Several stimuli-responsive gels have been designed by coupling chromophores to cholesterol-based gelators. In many of the systems irradiation with light of different wavelengths can reversibly induce the gel–sol transition of the system.[16] Hamachi and co-workers[38,39] have demonstrated the immobilization of artificial receptors in a hydrogel matrix of the glycosylated amino acid derivative for both sensing and discriminating phosphate derivatives, such as phosphate ion, phosphate esters, ATP, *etc.* Urea-based systems, in particular, represent anion-tunable systems, in which the self-association and anion binding are tensioned against one another to allow the anion binding to modulate the urea self-association and hence the bulk materials behavior of the gels.[40] This phenomenon was recently exploited by Steed and co-workers, who described the use of supramolecular gels as media for controlling the pharmaceutical crystal growth (Fig. 6). It was shown in many cases that the supramolecular nature of the gels allowed facile recovery of the formed crystals upon the addition of acetate anion without any damage to the crystals.[41]

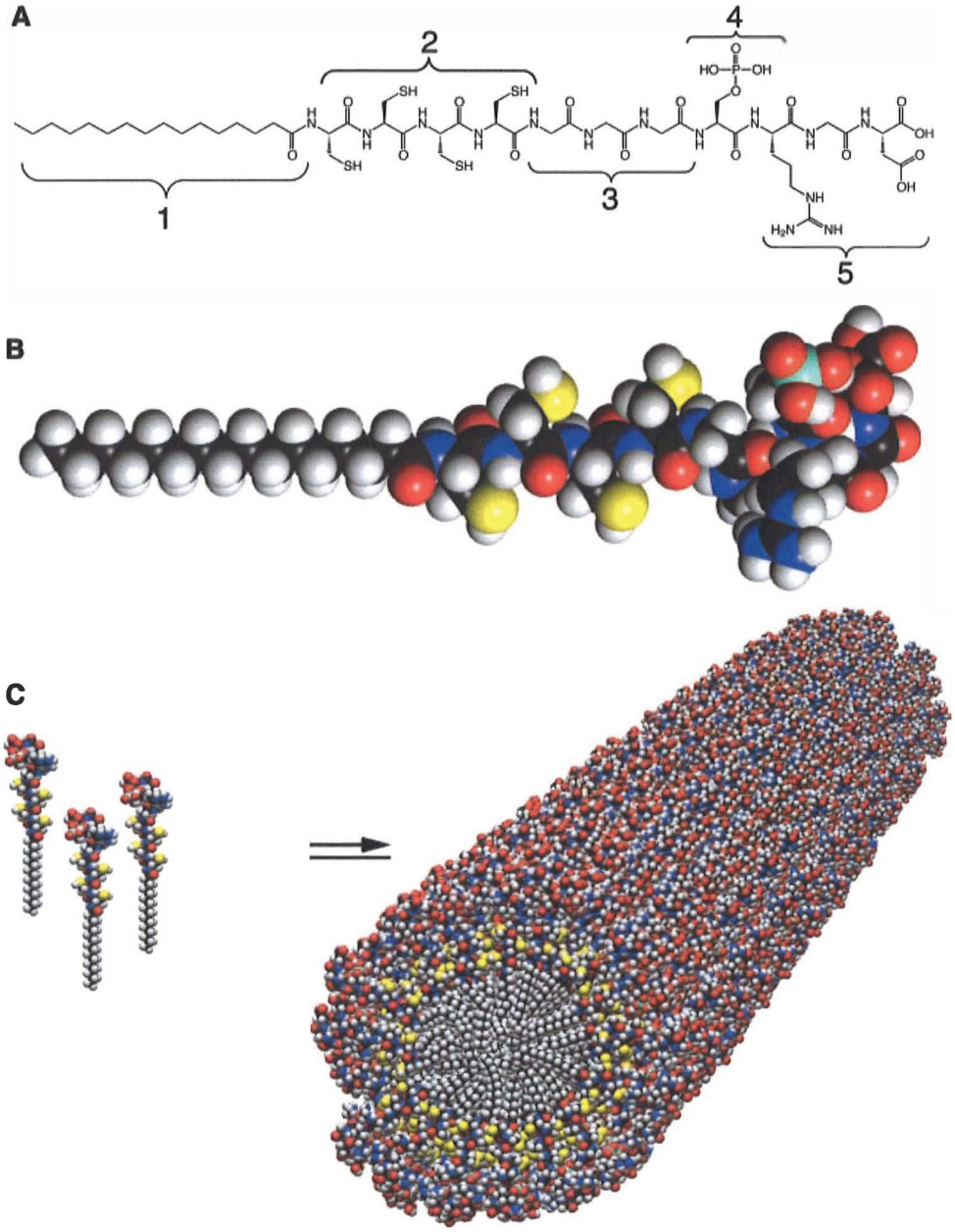

Figure 5. Chemical structure (A) and molecular model (B) of the peptide amphiphile reported by Stupp *et al.* (C) Schematic model showing the self-assembly of the peptide amphiphile molecules into a cylindrical micelle.[37] Reprinted with permission. Copyright © The American Association for the Advancement of Science

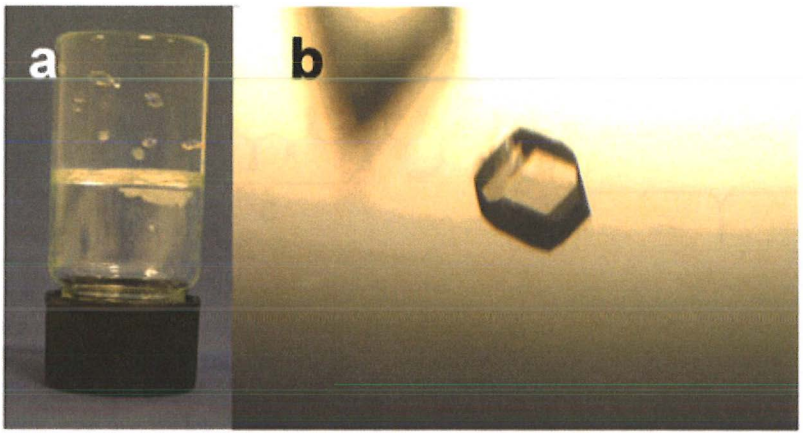

Figure 6. Photographs of carbamazepine crystals grown in a supramolecular organogel.[3,41] Reproduced by permission of The Royal Society of Chemistry

Carrying out reactions in the supramolecular gel medium has considerable potential, since the constrained environment provided by this approach can bring the advantage of specific interactions between the reactants, thus leading to better selectivity.[16] In supramolecular gels, the reactions can take place within the gel phase, on the surface of the fibrillar network, or in solution, depending on the relative affinity between the reagents, solvent, and gelator. In the case of catalytic supramolecular gels, non-covalent interactions are used for the construction of a multitopic catalyst, catalytic centers of which can be metals coordinated to the gel fibers (metallocatalysts) or catalytic organic fragments (organocatalysts).[42]

The creation of artificial architectures to mimic photosynthesis, the natural light harvesting process, has been an active area of research. The gel matrix of a supramolecular system as a scaffold may help in the proper organization of the donor and acceptor chromophores in order to gain efficient energy transfer. Additionally, the energy transfer in the supramolecular gels can be controlled by changing the temperature. Several studies concerning the use of supramolecular gels in light harvesting systems, that show promise for the design of electronic devices, have been reported. However, certain practical problems, such as long-term stability, should be addressed before real applications can be expected.[16]

Construction of 1D ordered assembly of electroactive molecules through non-covalent interactions may give rise to conducting supramolecular materials. The favorable electronic and optical properties of the molecules together with the proper spatial positioning of them leads to efficient electron mobility, which may find use *e.g.* in solar cells, light-emitting diodes, or field-effect transistors. There are many reports on the use of π-conjugated molecules like tetrathiafulvalene, thiophene, and phthalocyanine for forming electroactive self-assembled nanofibers. In addition, the physical gelation of ionic liquids is of current interest, as the materials hence prepared are attractive replacements for generally

volatile and flammable organic electrolytes. Grinding or sonication of a suspension of single-walled carbon nanotubes (SWCNTs) with imidazolium-based ionic liquids has led to the formation of physical gels, the so-called "bucky gels" (Fig. 7).[43] These gels bear good potential for electrochemical applications, since they contain both dispersed nanotubes (π-conjugated materials) and an electrolyte (the ionic liquid) in the very same system. Finally, the physical gels of liquid crystals represent an important class of compounds for optoelectronic applications.[16]

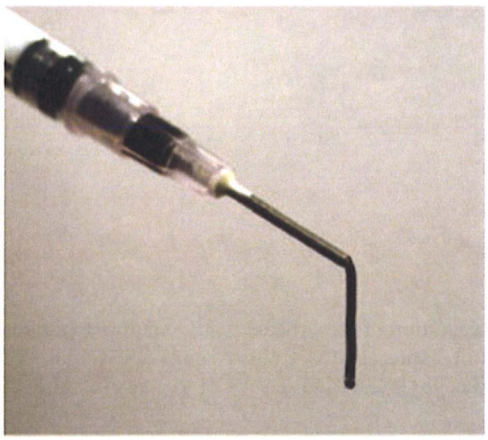

Figure 7. "Bucky gel" formed by mixing SWCNTs and imidazolium-based ionic liquid.[43] Adapted with permission. Copyright © 2007 WILEY-VCH Verlag GmbH & Co. KGaA, Weinheim

Natural and synthetic gel-like materials have appeared in the development of biomaterials for wound healing and other tissue engineering purposes. As a consequence of the expansion of supramolecular gel research, also their use for biomaterials purposes has gained ever increasing interest. When mixed with, or conjugated to therapeutic drugs or other bioactive molecules, these materials hold great promise for treating/curing various diseases, such as cancer, osteoarthritis, and neural injuries. Numerous potential applications for self-assembled (hydro)gels in the fields of 3D cell-culturing,[44,45] drug delivery,[46-48] tissue engineering,[49] and regenerative medicine,[50] for example, have been outlined in the literature. When compared to the polymeric gels traditionally exploited for these purposes, the self-assembled hydrogels possess a variety of advantages. From the chemical perspective, these include their easily controlled gel-to-sol state reversibility and the fact that their chemistry is a lot easier to manipulate than that of polymer hydrogels. Further, as a result of their dynamic nature, the supramolecular hydrogels can easily change their pore sizes and thus readily reassemble during shrinkage/swelling processes. Self-assembled hydrogels are also readily biodegradable due to the weak forces that hold their supramolecular structure together. High water content of the gels, together with mostly naturally occurring components comprising them, further assist

their biodegradability.[35] Figure 8 represents a schematic description of an enzyme-triggered β-peptide hydrogel, which could be of use when designing biomaterials for long-term biostability.[51]

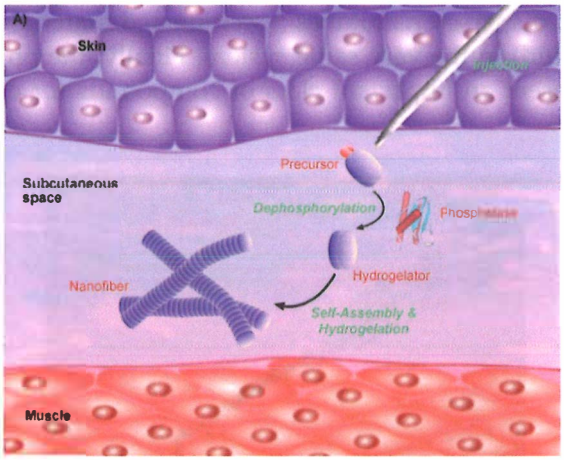

Figure 8. A schematic depiction of the process using enzyme to control the balance between hydrophilic and hydrophobic interactions to form a supramolecular hydrogel *in vivo*.[51] Adapted with permission. Copyright © 2007 WILEY-VCH Verlag GmbH & Co. KGaA, Weinheim

1.2 Gold nanoparticles

Gold nanoparticles (AuNPs) and their arrays are perhaps the most studied nanomaterials, with promising applications *e.g.* in the fields of chemistry, biology, engineering, and medicine. The history of AuNPs dates back to the ancient Roman times, where they were used for staining glasses for decorative purposes. Over 150 years ago, Michael Faraday was probably the first to observe that colloidal gold solutions have properties that differ from bulk gold. Over the last half-century, reliable and high-yielding methods for the synthesis of AuNPs have been developed. AuNPs possess unique properties, such as size- and shape-dependent optical and electronic features, a high surface-to-volume ratio, and surfaces that can be readily modified with ligands that show affinity for gold surfaces.[52,53]

1.2.1 Synthesis, surface functionalization, physical properties, and characterization

Numerous methods for preparing AuNPs have been reported. In 1951, Turkevich developed one of the most popular approaches for the synthesis of AuNPs, namely citrate reduction of $HAuCl_4$ in water.[54] This method provides AuNPs with diameters of 20 nm, and utilizes citric acid as both reducing and stabilizing agent. The Brust–Schiffrin method[55] reported in 1994 was a signifi-

cant breakthrough in the field of AuNP synthesis. The method relies on a two-phase strategy in which $AuCl_4^-$ is transferred from aqueous phase to toluene using tetraoctylammonium bromide (TOAB) and reduced by sodium borohydride ($NaBH_4$) in presence of dodecanethiol (Fig. 9). Easily handled, characterized, and functionalized AuNPs with controlled diameters in the range of 1.5–5 nm are generated by this method. By varying the reaction conditions, such as gold/thiol ratio, temperature, and reduction rate, the particle size can be tuned. This method has been further modified into a single-phase system. Place exchange method reported by Murray *et al.*[56,57] describes the substitution of thiol ligands by different thiols. This technique can be used for introduction of chemical functionality onto the AuNP monolayer in a divergent fashion. While most functionalization of AuNPs has been done utilizing thiol/thiolated ligands, a variety of other ligands have also been used as reducing/capping agents. Those include *e.g.* other sulfur containing ligands (disulfides, multivalent di- and trithiols, thioethers, xanthates, and resorcinarene tetrathiols), amines, amino acids, porphyrins, certain polymers, and dendrimers.[58] In a recent study, the controlled synthesis of AuNPs in quaternary ammonium ionic liquids by simple heating has been described.[59]

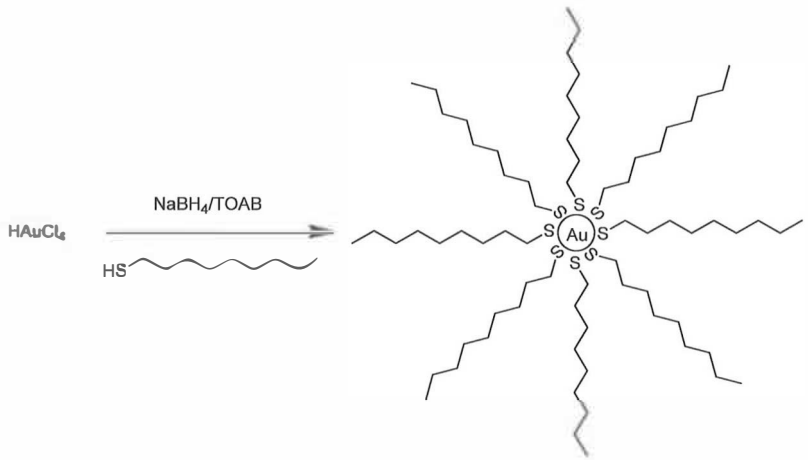

Figure 9. Brust–Schiffrin method for two-phase synthesis of AuNPs by reduction of gold salts in the presence of thiol ligands.[58]

Besides chemical methods, physical methods for the manipulation of the structure and hence the properties of AuNPs are available, as well. These include *e.g.* thermolysis, digestive and conventional ripening, UV and laser irradiation, sonication, and radiolysis. Further, the formed nanoparticles can be separated by shape and size utilizing size-exclusion chromatography.[52,58]

AuNPs possess quantum size effect, which arises when the de Broglie wavelength of the valence electrons is of the same order as the size of the particle itself. The particles behave electronically as zero-dimensional quantum dots (or quantum boxes) relevant to quantum-mechanical rules. Freely mobile elec-

trons are trapped in such metal boxes and show a characteristic collective oscillation frequency of the surface plasmon resonance (SPR), giving rise to the so-called plasmon resonance band (SPB) observed near 530 nm for the AuNPs with the diameter of 5–20 nm.[52] The SPR frequency is sensitive to the proximity of other nanoparticles. The aggregation of nanoparticles results in significant red-shifting and broadening in the SPB, thus changing the solution color from red to blue due to the interparticle plasmon coupling. This phenomenon is utilized in AuNP-based colorimetric sensors.[58]

The most utilized characterization technique for AuNPs is high-resolution transmission electron microscopy (HRTEM), by which an image of the gold core of the AuNPs is obtained. The core dimensions can also be determined using scanning tunneling microscopy (STM), atomic force microscopy (AFM), small-angle X-ray scattering (SAXS), laser desorption–ionization mass spectrometry (LDI-MS), and X-ray diffraction. The histogram obtained from the TEM images provides the size distribution of the cores and gives information on the dispersity of the AuNPs. The mean number of gold atoms, N_{Au}, can be determined when the mean diameter, d, of the cores is known: $N_{Au} = 4\pi(d/2)^3/v_{Au}$. From these data, the elemental analysis, giving the Au/S ratio, allows calculation of the average number of S ligands. Same information is obtainable by X-ray photoelectron spectroscopy (XPS) or thermogravimetric analysis (TGA), whereas UV-Vis, IR, and NMR spectra give information on the ligand moiety.[52]

1.2.2 Chemical and recognition properties

As already mentioned in the previous section, some of the thiolate ligands in alkanethiolate-stabilized AuNPs can be substituted, and various functional thiols can be incorporated into AuNPs by this way. For example, chelating properties of incorporated carboxylate groups have been utilized for metal detection and formation of AuNP films.[60,61] Various simple groups, such as halides, nitriles, alkenes, and sulfonates, as well as electro- and photoactive groups, spin labels, and catalysts can be introduced to the AuNPs using this method. Further, nucleophilic substitution of bromide in ω-bromoalkanethiolate-functionalized AuNPs with alkylamines or ω-hydroxyl-functionalized AuNPs with alkyl halides gives rise to modification of the ligand moiety. By the nucleophilic addition of ω-maleimido thiol–AuNPs onto sulfhydryl groups the AuNPs can be attached to proteins, peptides, and oligonucleotides. Moreover, polymerization of AuNPs can be achieved by appropriate functionalization. Finally, the thiolate-stabilized AuNPs can be decomposed for example by the reaction of cyanide by photoirradiation in the presence of bromine-containing trihalomethanes yielding mononuclear gold cyanide and the free thiols.[52]

AuNPs offer a suitable platform for functionalization with a wide range of organic or biological ligands for selective binding and detection of small molecules and biological targets. Detection of chemical and biological agents plays a significant role in biomedical, forensic, and environmental sciences as well as in

anti-bioterrorism actions. In general, sensors are composed of two functional components: a recognition element to provide selective/specific binding with the target analytes and a transducer component for signaling the binding event. Tunable recognition properties of AuNPs together with their straightforward synthesis, stability, unique optoelectronic properties, and high surface-to-volume ratio make excellent scaffolds for the fabrication of novel chemical and biological sensors. Moreover, the binding event between the recognition element and the analyte can alter the physicochemical properties (plasmon resonance absorption, redox behavior, conductivity, *etc.*) of the transducer AuNPs, which in turn can generate a detectable response signal (Fig. 10). AuNP-based sensors are discussed further in the following section.[58]

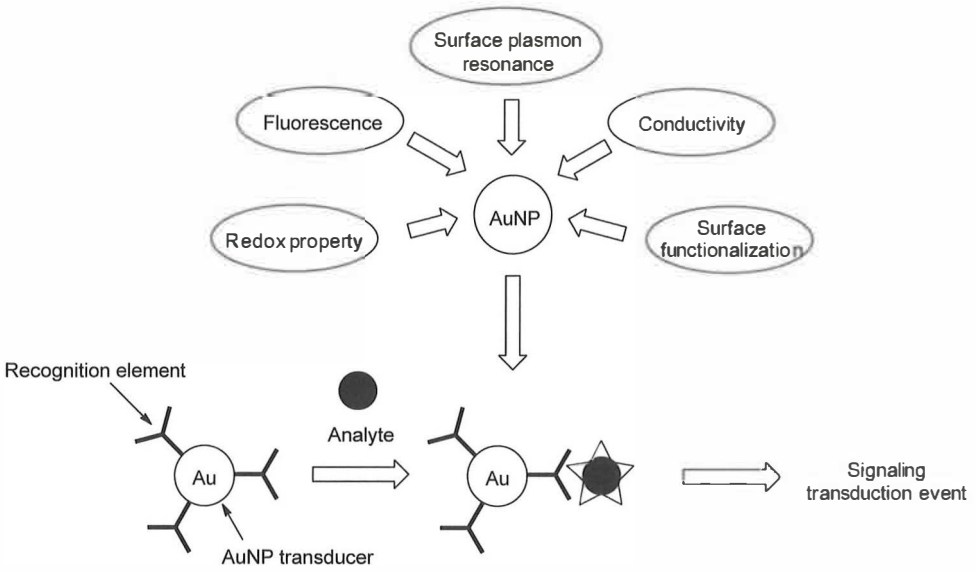

Figure 10. Physical properties of AuNPs and a schematic illustration of a AuNP-based detection system.[58]

1.2.3 Applications

As already mentioned, the aggregation of AuNPs of appropriate sizes induces interparticle surface plasmon coupling, resulting in a visible color change from red to blue at nanomolar concentrations. This provides a basis for absorption-based colorimetric sensing of a target analyte that directly or indirectly triggers the AuNP aggregation/redispersion. AuNPs have many applications in fluorescence-based sensors, and they can serve as excellent fluorescence quenchers for FRET-based assays for detecting *e.g.* various metal ions, certain small organic molecules, or nucleic acids.[58] Rotello and co-workers have developed a sensor array of six non-covalent AuNP–fluorescent polymer conjugates which, based on a "chemical nose" strategy, is able to detect, identify, and quantify protein targets (Fig. 11).[62] The polymer fluorescence is quenched by the AuNPs, but the

presence of proteins disrupts the nanoparticle–polymer interaction and produces distinct fluorescence response patterns. Analogous AuNP–polymer systems have been developed to detect and identify bacteria, and similar systems have also been used for rapid and effective differentiation between normal, cancerous, and metastatic cells.[58]

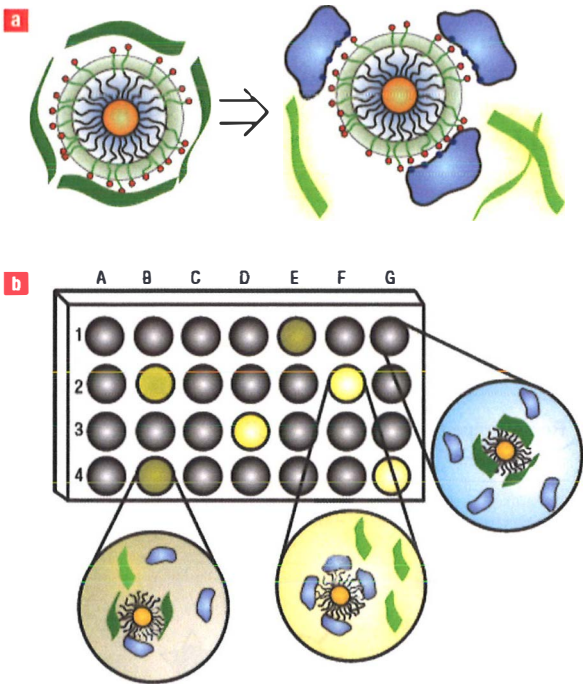

Figure 11. Schematic illustration of the "chemical nose" sensor array based on fluorophore displacement.[62] Reprinted with permission from Macmillan Publishers Ltd., copyright 2007.

Excellent conductivity, high surface area, and catalytic properties make AuNPs excellent materials for electrocatalytic and electrochemical sensing of a wide range of analytes. Chemiresistors are solid-state devices that rely on the sensitivity through changes in electrical resistance upon interaction with a chemical species. A number of chemiresistor vapor sensors based on AuNPs have been developed. In addition, the combination of electroactive AuNPs and macrocyclic compounds has shown to provide useful sensor systems. Further, AuNPs have been exploited in electrochemical detection of numerous small molecules, toxic chemicals, drugs, and even mammalian cells. Additionally, AuNP-based electrochemical enzymatic biosensors and immunosensors for the detection of a wide variety of analytes have been developed. AuNP-based sensors taking advantage of surface plasmon resonance or surface-enhanced Raman scattering (SERS) have been investigated, as well.[58] Very recently, a review article describing the exploitation of functionally modified gold colloids in the detection of a broad range of threat agents, including radioactive substances,

explosive compounds, chemical warfare agents, biotoxins, and biothreat pathogens, has been published.[63]

Gold is chemically very inert and resistant to oxidation, and it is indeed one of the most stable metals in the group 8 elements. However, catalysis with AuNPs, particularly the very active oxide-supported ones, is an expanding area with a large number of new catalytic systems for a variety reactions being under study. Most of the research on the catalytic activity of oxide-supported AuNPs concerns CO oxidation. Catalysis by functional thiolate-stabilized AuNPs in addition to other miscellaneous catalytic applications exploiting AuNPs has been investigated, as well.[52]

Gold nanoparticles represent attractive vehicles for the delivery of drugs, genetic materials, proteins, and small molecules. The inert, non-toxic, and biocompatible gold core is ideal starting point for the carrier construction. As already mentioned many times, AuNPs with a wide range of core size with controlled dispersity are rather easily synthesized. Moreover, the high surface area-to-volume ratio of AuNPs enables dense loading of the delivered materials. The highly tunable and multivalent surface structures offer the diversity to incorporate delivered items by covalent or non-covalent fashion. Moreover, the ability to tailor the surface makes AuNPs effective in both active and passive targeting. Finally, a variety of release strategies using internal or external stimuli, such as glutathione, pH, heat, and light, may be provided by the variety of functional monolayers. AuNPs intended for delivery applications can be roughly divided into two categories based on the type of functionalities present on the NP surface, namely synthetic monolayers and biomolecule coating.[64]

Organic monolayer coated AuNPs have been utilized *e.g.* in DNA/RNA binding, protein delivery, drug delivery (Fig. 12), and targeted delivery.[64,65] For example, AuNPs functionalized with cationic quaternary ammonium headgroups bind plasmid DNA *via* electrostatic interaction and can inhibit the transcription of DNA.[66] AuNPs with engineered monolayer are thought to be able to overcome the issues of poor permeability through the cell membrane or digestion of the proteins by enzymes. The high surface area and tunability of AuNPs provide an excellent platform for attachment of drugs for controlled and sustained release. Both covalent and non-covalent strategies have been employed for loading drugs onto AuNPs; both approaches having their advantages and disadvantages. Stable delivery systems are provided by the covalent attachment, but intracellular processing of the prodrug is typically required. However, intracellular activation of the prodrug enables the delivery of inert forms of the drug, resulting in reduced side effects. Non-covalent loading of drugs, for one, allows direct release of active drug forms, but the premature release might cause problems. AuNP surfaces can be modified with a variety of biomolecules, such as oligonucleotides, peptides/proteins, carbohydrates, and lipids, thus leading to efficient transport of biomacromolecules with minimal cytotoxicity.[64]

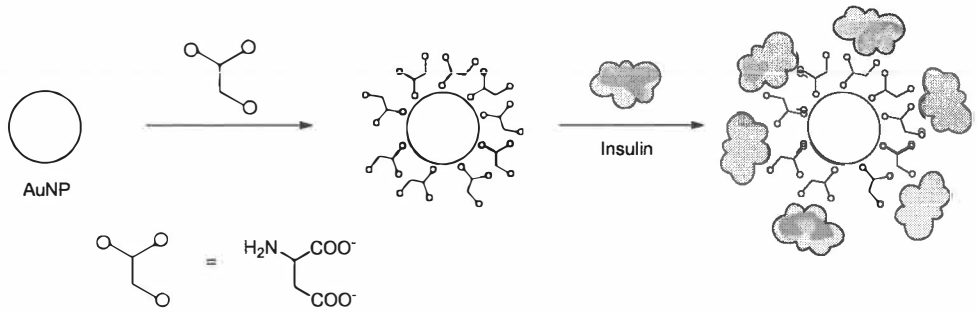

Figure 12. Functionalization of AuNPs with aspartate ligands followed by loading of insulin protein leading to enhanced reduction in blood glucose levels of diabetic rats.[67]

Antibody-labeled gold nanoconjugates have been used in immunohistochemistry for a long time. However, as a consequence of the development of gold nanoconjugates for live cell studies, interest in them has risen further. AuNPs modified with antibodies specific to cancer-associated proteins can be used to image cancerous cells, whereas gold nanorods and nanoshells conjugated with antibodies are being developed as photothermal therapy agents.[53]

Novel hybrid materials with interesting properties for various applications, such as catalysts and gas sensors as well as electronic and magnetic devices, have been prepared by attaching AuNPs to carbon nanotubes. The materials can be prepared by two ways: the AuNPs can be grown and/or incorporated into the hollow cavities of the carbon nanotubes (endohedral approach) or the AuNPs can interact on the outer part of the carbon nanotubes (exohedral approach).[68,69]

1.3 Bile acids

1.3.1 Chemistry and biology

Bile acids are a group of steroidal compounds biosynthesized in the liver from cholesterol through several complementary pathways. Although their best-known role is their participation in the emulsion and absorption of dietary fats and liposoluble vitamins, they play important roles in several other physiological processes. Bile acids, for example, facilitate intestinal calcium absorption, are known to modulate pancreatic enzyme secretion and cholecystokinin release, and are potent antimicrobial agents that prevent bacterial overgrowth in the small bowel. Moreover, they have been discovered to act as signaling molecules modulating the expression of proteins involved in the cholesterol homeostasis.[70,71]

After their biosynthesis from cholesterol, bile acids are conjugated with either glycine (75%) or taurine (25%). This amidation increases the aqueous solu-

bility of bile acids under physiological conditions. The bile acids biosynthesized in the liver are stored in the gall bladder, from which the bile, being composed of bile acids as the main component, is secreted through the bile duct into the intestine when food passes from stomach to the duodenum. In the intestine, bile acids emulsify dietary fat droplets through the formation of mixed micelles, making the fat available for digestion by lipases. Most of the bile acids secreted into the upper region of the small intestine are absorbed along with dietary lipids at the lower end of the small intestine. Then the bile acids are separated from the dietary lipids and the majority of them returned to the liver for recirculation. This movement of bile acid molecules between the liver and intestine is termed as enterohepatic circulation.[70]

Bile acids consist of two connected units; a rigid steroidal nucleus composed of four rings and a short aliphatic side chain (Fig. 13). The steroidal nucleus contains three six-membered rings (A, B, and C) and a five-membered ring (D). In addition, there are angular methyl groups attached to the positions C-10 and C-13. The side chain is attached to the position C-17. In higher vertebrates the rings A and B are in a *cis*-fused configuration causing curvature to the skeleton. In mammals, commonly from one to three hydroxyl groups at positions C-3, C-7, and/or C-12 are attached to the steroidal nucleus.[71]

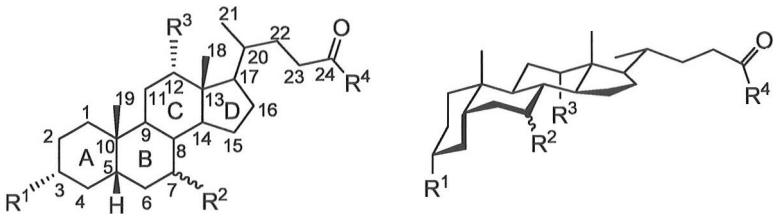

Name	R^1	R^2	R^3	R^4
Cholanoic acid **1**	H	H	H	OH
Lithocholic acid, LCA **2**	OH	H	H	OH
Chenodeoxycholic acid, CDCA **3**	OH	α-OH	H	OH
Ursodeoxycholic acid, UDCA **4**	OH	β-OH	H	OH
Deoxycholic acid, DCA **5**	OH	H	OH	OH
Cholic acid, CA **6**	OH	α-OH	OH	OH
Glycocholate **7**	OH	α-OH	OH	$NHCH_2COO^-$
Taurocholate **8**	OH	α-OH	OH	$NHCH_2CH_2SO3^-$

Figure 13. Structures of the most common bile acids, together with the glycine and taurine salts of cholic acid.

1.3.2 Bile acid/salt self-assembly in aqueous solutions

The salts of bile acids self-assemble to form micelles in aqueous environments, similar to classical amphiphiles. However, the structure of bile acids deviates quite a lot from the classical amphiphiles, which have hydrophilic head groups consisted of relatively small polar or charged groups in addition to typically long, flexible, and apolar hydrocarbon chains as hydrophobic tails. In bile salts

the polar hydroxyl groups are oriented to the concave α-face of the rigid steroidal ring system, which is thus rendered hydrophilic. The convex β-face, for one, has the three methyl groups and is hydrophobic. Because of this facial amphiphilicity, the hydrophilic and hydrophobic domains of bile salts are not as clearly separated as in classical amphiphiles. Moreover, the rigidity of the steroidal core often results in an incomplete separation of the hydrophilic and hydrophobic domains in aggregates.[72]

The hydroxyl and acidic groups of bile acids may, beyond providing polar domains, participate in intermolecular hydrogen bonding. Co-operative hydrogen bonding between several hydroxyl groups is typically allowed by their positions and orientations. The directed, specific nature of the hydrogen bonds limits the possible orientations consequently introducing additional rigidity into the aggregates. The micellization is thus driven by the interplay of two modes of interaction – hydrogen bonding and hydrophobic effect – latter of which, in the case of bile salts, is relatively weak and complex. Bile salts are ionic amphiphiles, since the carboxylic acid group is dissociated under physiological conditions. This leads to electrostatic interactions between the bile salt molecules both in bulk and aggregates.[72]

Precise determination as well as quantitative comparison of critical micellar concentration (cmc) values of bile salts has proven to be difficult due to the very small size of the aggregates. In addition, because of the low aggregation numbers, the aggregates are very susceptible to external influences. However, the cmc of bile salts has been extensively determined under various conditions.[72-80] It has been shown that the cmc values exhibit similar general trends on solution parameters (*e.g.* ionic strength, pH, and temperature) as classical amphiphiles. Increasing the ionic strength reduces the electrostatic repulsion between charged groups, and hence favors aggregation and decreases cmc. Charges are also controlled by the pH. A change in the pH has a significant effect, if the ionization state of the bile salt molecules is thereby changed. At pH close to the pK_a of the bile acid both dissociated and undissociated, *i.e.* charged and uncharged, molecules participate in micelle formation thus reducing the cmc. The temperature dependence of the cmc has shown to be very weak. The minimum value for cmc is obtained around room temperature and it is shown to increase at higher temperatures. The micellization also depends on the bile salt species, the more hydrophobic deoxycholate and chenodeoxycholate having smaller cmc values compared to the more hydrophilic cholate. The number, position, and orientation of the hydroxyl groups have a great impact on the cmc values.[72]

Several models have been used to describe the unusual self-assembly of bile salts (Fig. 14).[72] The earliest model proposed the formation of primary and secondary micelles. The primary micelles are suggested to be formed by the hydrophobic association of the hydrophobic faces of the bile salts. The hydroxyl and acidic groups are pointing outside and are in contact with water, thus shielding the hydrophobic parts from water. Without creating a cavity, a maximum of ten bile salt molecules can assemble in this manner. At higher concen-

trations these primary micelles form hydrogen bonds leading to the formation of elongated, secondary micelles. The nature of the interaction leading to the aggregate formation has been debated though.[72,81] In the disclike model,[72] the bile salt molecules are thought to associate with their hydrophobic faces oriented towards the micelle interior and the hydrophilic faces towards the water. The long axes of the molecules are approximately parallel, and the molecules are alternatingly oriented. Yet another suggested model is based on the structure of the crystalline state.[82] The crystal structure determined by X-ray diffraction suggests a helical arrangement of the molecules driven by polar interactions. The interior of the helix is filled with cations surrounded by water molecules. However, this model requires that the arrangement of the bile salt molecules is not significantly affected by the presence/absence of forces due to the crystalline order and that the dynamics of the molecules in the crystalline and liquid state are comparable.[72]

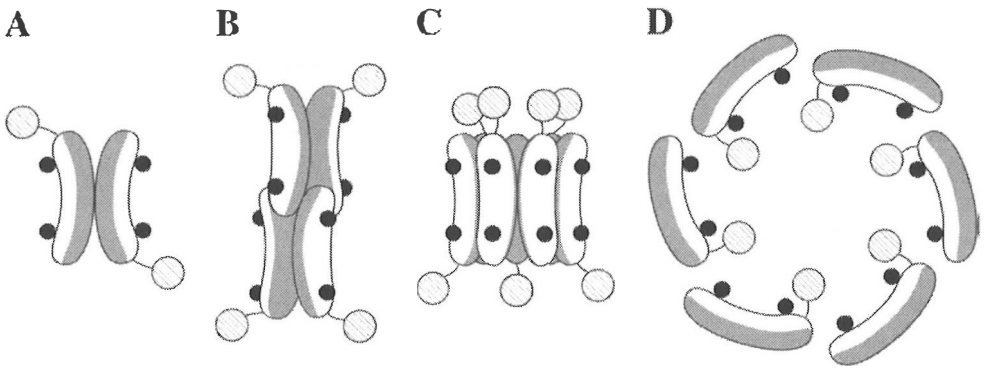

Figure 14. Schematic representation of different models for the bile salt micellar structure. Different primary micelles (A and B), disclike micelle (C), and helical micelle (D, seen from the top).[72] Reprinted with permission from Elsevier.

Besides micelles, in aqueous solutions bile acids and their salts have shown to form a variety of self-assembled structures such as helical fibers,[83] tubules,[84-86] and tubular spherulites.[87] Blow and Rich[83] reported in 1960 that in the aqueous solution of deoxycholate at lowered pH some of the deoxycholate molecules are protonated, and arranged into helical fibers, with the helical diameter of 36 Å. It was also shown, that if the complex forms in an undisturbed medium, these structures will grow in all directions and form a matrix of high viscosity, eventually recognized as a gel.

Sodium lithocholate, for one, has been shown to form organic nanotubes exhibiting monodisperse cross sections with a large inner cylindrical cavity of 49 nm in alkaline aqueous solutions.[84] Furthermore, the tubules have shown to be easily oriented under a weak elongational stress. Fang *et al.* have also studied the self-assembly of lithocholic acid in alkaline solutions.[85] When dissolved in alkaline aqueous solution with pH 12.0, the LCA molecules were after 2 h shown to form vesicles with an external diameter of about 1.5 μm, as evidenced by the optical microscope imaging. These initially formed vesicles then linearly

aggregated, and the fusion of the vesicles led to the formation of hollow cylindrical tubes. The LCA tubes were shown to continuously grow until all of the vesicles were consumed. Furthermore, the tubes were shown to coil into 3D spirals as their lengths increased. The coiling of the tubes was shown to be a slow process and take a few days to complete. The formed tubes were stable in aqueous solution at pH 12.0. However, as the pH of the solution was reduced to 7.4 by adding HCl, the tubes were shown to transit into a straight shape. When the pH was adjusted back to 12.0 by adding NaOH, the straight tubes switched back to the spiral ones. These pH-switchable tubes may act as supramolecular springs in response to chemical and environmental stimuli.

Smart organic tubes have also been shown to be formed by the co-assembly of lithocholic acid and taurolithocholic acid (TLCA) in aqueous solution at pH of ~8.[86] After two days of ageing the sample prepared by mixing solutions of LCA dissolved in aqueous NaOH and TLCA in water, formation of fibers with a diameter of about 150 nm was observed. These fibers were then shown to laterally aggregate and fuse into sheets over time, finally leading to the formation of tubes after two weeks. The formed tubes were able to transit into flat sheets after being dried on a glass surface. This was shown to result from a longitudinal unzipping of LCA/TLCA tubes induced by the capillary force. The tubes were tested for the encapsulation and release of guest molecules (red dye #40). Indeed, the guest molecules could be loaded into the tubes, and the dried tubes were shown to release the guest molecules *via* unzipping of the tubes. After the release of the guests, the LCA/TLCA sheets were shown to zip back into tubes by the hydration with aqueous solution.

The self-assembly of lithocholic acid at pH 7.5 has also been studied by Fang *et al.* (Fig. 15).[87] They first prepared the 0.1% (w/w) solution of LCA in aqueous NaOH with pH 12.3 at room temperature. After ageing of the sample in a sealed vial for 2 h, the pH of the LCA solution was reduced to 7.5 by adding water. The sample was then allowed to stand for two months, after which optical microscopy revealed the formation of self-assembled rod-like structures, interestingly showing splitting at both ends. The splitting was shown to progress to the middle of the rods in the process of time, resulting in the formation of sheaf-like bundles in which the hollow tubules developed from the intensive splitting were tied in the middle. Finally spherulites in which the tubules radiate from the spherulite center were formed. The tubular spherulites were shown to be metastable, and the disassembly of the spherulites through brief sonication led to the well-dispersed crystalline tubules in solution. When the pH of aqueous solution was increased to above 12.0 by the addition of NaOH, the LCA tubules were shown to coil into three-dimensional spiral or helical shapes, depending on their diameters. Also the tubules, which were tied at the center of the spherulites, were shown to display the pH-switchable shape transition. As the pH of the aqueous solution was increased to 12.0, the tubules in the spherulites became flexible and the free ends of the tubules were shown to coil into a worm-like shape. Moreover, when the pH was adjusted back to 7.5 by adding HCl the worm-like tubules were straightened.

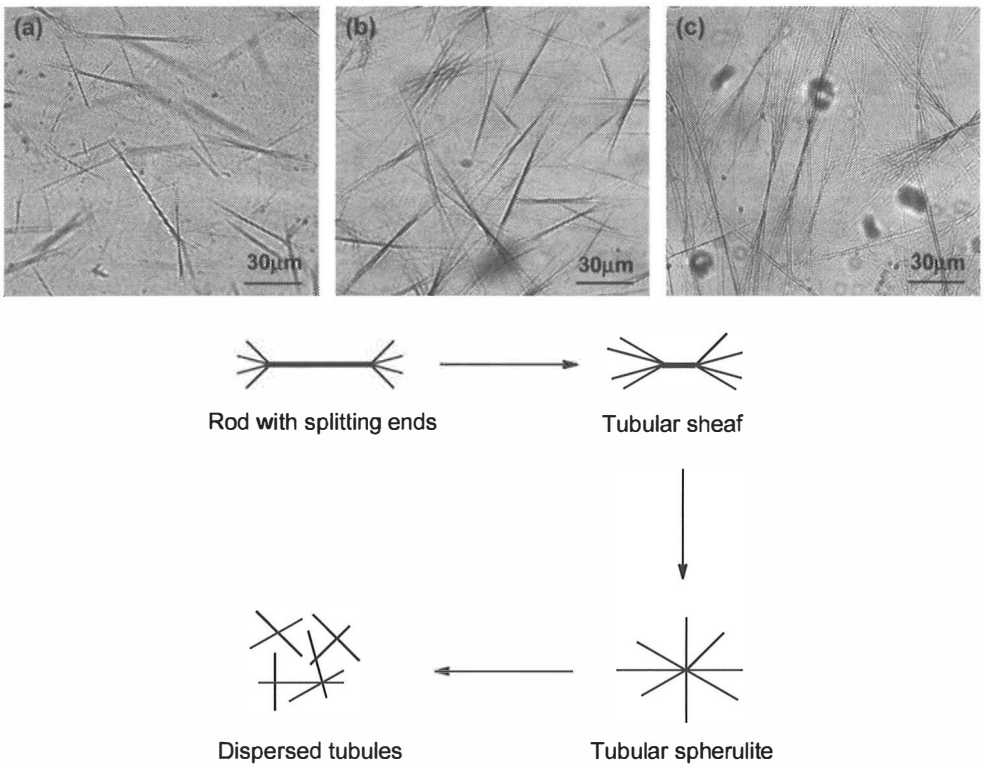

Figure 15. Top: Bright-field optical microscope images of self-assembled LCA rods with splitting ends in aqueous solution at pH 7.5. Images were taken after 60 (a), 65 (b), and 70 (c) days. Bottom: Schematic representation for the formation of dispersed LCA tubules through the self-assembly and disassembly of tubular spherulites in aqueous solution at pH 7.5.[87] Microscopy images reproduced by permission of The Royal Society of Chemistry.

1.3.3 An overview of applications of bile acids and their derivatives in pharmacology, synthesis, and supramolecular chemistry

The enterohepatic circulation of bile acids – a complex process involving numerous transport proteins – is one of the most efficient recycling routes in the human body. The exploitation of the tremendous transport capacity and organ specificity of enterohepatic circulation combined with versatile derivatization possibilities, high stability of the steroidal skeleton, enantiomeric purity, biocompatibility, availability, and low cost have raised interest to utilize bile acids in designing pharmacological applications.[88-92] Certain bile acids are used therapeutically as such to correct deficiency states, to decrease the cholesterol saturation of bile, or to decrease the cytotoxicity of retained bile acids in cholestatic liver disease.[93] The utilization of bile acid transport proteins in drug delivery and targeting, and the applicability of bile acids as building blocks in prodrug design have been widely studied and several reviews on the topic have been

published.[91,94,95] Molecular umbrellas prepared from bile acids have been found to be capable of transporting certain hydrophilic peptides, nucleotides, and oligonucleotides across liposomal membranes by passive diffusion. They have also been shown to increase water solubility and hydrolytic stability of a hydrophobic drug, and to exhibit significant antiviral activity.[96] In addition to the above-mentioned molecular umbrellas, several other bile acid derivatives have been shown to possess antimicrobial and/or antifungal activity. These studies and other advances in the field of bile acid medicinal chemistry have been extensively reviewed recently.[92]

Achieving high levels of stereoselectivity is one of the major challenges in modern organic synthesis. The transfer of chirality *via* the utilization of chiral auxiliaries has proven to be an effective way for preparing homochiral molecules. Facial amphiphilicity of chiral bile acids with a rigid backbone and the unique disposition of hydroxyl groups have led to the discovery of their usage as chiral templates, organocatalysts, and chiral ligands.[97-99] They are also able to act as enantioselective host compounds in solid state; deoxycholic acid being the classical example by forming crystalline inclusion compounds with various organic guests. In addition, bile acids are capable of generating supramolecular chirality in achiral molecules by causing the molecules to be fixed in a chiral conformation or to be arranged in a chiral manner in the crystal lattice.[100] Moreover, bile acids have been utilized as enantioselective receptors in solution.[99]

A massive number of both cyclic and acyclic bile acid-based compounds have been designed to act as receptors for molecular and ionic recognition.[89,98,101,102] In addition, bile acids have found use in certain oligo- and polymeric structures, such as dendrons, which might be exploited for example in drug delivery or in artificial light harvesting systems.[98,103,104]

Gelation of organic or aqueous solvents by low molecular weight compounds has received an enormous interest in recent decades,[3] as already mentioned earlier in this thesis. A vast number of bile acids and their derivatives have been shown to be capable of self-assembly leading to gel formation.[105,I] Nanomaterials derived from bile acids and their derivatives including supramolecular gels, gold/silver nanoparticles, and hybrid materials combining them are further discussed in the following section.

1.4 Bile acid-based nanomaterials

There exists a vast number of bile acid-derived compounds capable of forming nanoscale materials, most of which originate from the compounds' unique ability to self-assemble leading to a variety of structures. Numerically the largest group of bile acid-based materials is undoubtedly the supramolecular gels. However, exploitation of bile acids and their derivatives as capping and/or reducing agents in gold/silver nanoparticle synthesis, and in hybrid materials combining supramolecular gels and gold/silver nanoparticles or carbon nano-

tubes are attracting an ever increasing attention. Besides the before-mentioned, there are many other nanoscale materials, some of which have been briefly described in the following sections. In this context one has to mention the bile acid-derived polymeric materials,[106,107] which have proven to be promising mostly in biomedical and pharmaceutical fields. This thesis, however, concentrates on materials relying on weak interactions.

1.4.1 Supramolecular gels[1]

The earliest reports on the gel formation by cholic acid salts in water date back to the early 20th century.[108-110] The gelation of aqueous solutions of the salts of deoxycholic acid and lithocholic acid, for one, was observed in the 1950's.[111] As already mentioned in section 1.3.2, the helical fiber formation of deoxycholic acid eventually leading to gelation in aqueous solution of lower pH was reported in 1960.[83] Forty years later, the use of sodium deoxycholate hydrogel for drug delivery applications was investigated.[112] However, the interest in the gel formation of bile acids and their derivatives has grown rapidly only during the last two decades. In fact, one of the earliest reports on bile acid-based organogelators introduced the organogelation properties of *N*-isopropyl cholamide not until in 1998.[113]

Organic salts are found to be popular in supramolecular gel research because of their relatively easy and fast preparation, which enables rapid scanning of their gelation ability. Moreover, the self-assembly in such salts is typically based on strong and directional hydrogen bonding as well as stronger but less directional electrostatic interactions between the charged species.[5] Maitra and co-workers have reported a series of cationic analogues of bile salts as hydrogelators. The majority of the investigated compounds have been shown to require the use of NaCl for better gelation of aqueous solvents, but one of the compounds has been shown to form a stable gel even in pure water at concentrations above 0.8%. The authors suggest that besides providing the ionic environment, NaCl is also responsible for salting out effect. In addition to NaCl solutions, gels have been obtained in 1 M aqueous solutions of several other inorganic salts.[114] A combinatorial library approach has been applied in preparing 60 organic salts by reacting five bile acids and 12 secondary amines. Gelation tests revealed that six of the salts were ambidextrous displaying the ability to form gels with organic as well as aqueous solvents. Didodecylammonium cholate was found to be the most versatile gelator of the series displaying gelation ability with a maximum number of solvents. The authors were able to classify the gelation process into three stages: 1) a dispersion of the gelator molecules (solution), 2) fibrous structures of the associations (pregel), and 3) a pseudo-infinite network (gel), based on dynamic light scattering (DLS) and small-angle neutron scattering (SANS) investigations.[5] Bhattacharya and co-workers, for one, have demonstrated the formation of two-component gel systems by simply mixing lithocholic acid in aqueous solution in the presence of various dimeric or oligomeric amines. FT-IR studies were shown to confirm the involvement of the carboxylate and ammonium residues in the salt formation leading to the

formation of a continuous hydrogen-bonded network eventually giving rise to a hydrogel. The morphology of the network was shown to be controllable by varying the amine component.[115] Yet another example of a two-component gel system described sodium deoxycholate-assisted gel formation of a two-tailed anionic surfactant, sodium bis(2-ethylhexyl) sulfosuccinate (AOT), in nonpolar solvents.[116]

Huang and co-workers have rather recently reported temperature-controlled, one-dimensional hierarchical architectures including nanotubes, coiled-coil rope-like structures, nanohelices, and nanoribbons fabricated by supramolecular self-assembly of lanthanum cholate (Fig. 16).[117] The entanglement of these nanostructures has been found to generate "super" hydrogels with the lowest gelation concentration of as low as 0.04 wt-%. Moreover, the gels have been shown to display unprecedented "heating-enhanced stiffness" and "heating-promoted gelation" behavior.

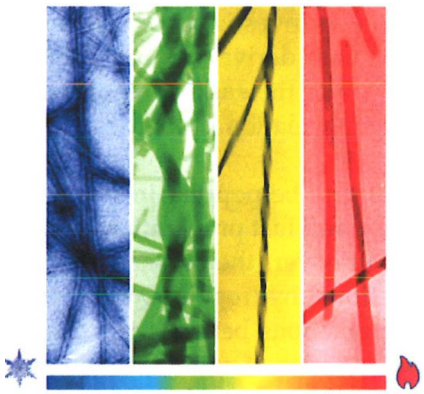

Figure 16. Representation of temperature-dependent nanostructural evolution of lanthanum cholate hydrogel.[117] Copyright © 2010 American Chemical Society

Lanthanide ions as an integral part of the gel matrix have also been exploited by Maitra and co-workers in novel luminescent materials composed of cholic acid-based lanthanide hydrogels. In a preliminary study, hydrogels were found to be formed from mixtures of variable compositions of europium acetate and sodium cholate. The gelation process was shown to efficiently increase the sensitization of the Eu(III) emission by accommodating a hydrophobic chromophore, pyrene, on the hydrophobic gel fibers.[118] In a subsequent study, hydrogel formation by several other lanthanide cholates was reported. The hydrogel matrix was utilized for the sensitization of Tb(III) by doping a non-coordinating chromophore, 2,3-dihydroxynaphthalene (DHN). Tunable multi-color emissions were shown to be achieved from mixed cholate gels of Tb(III) and Eu(III) both in the gel phase as well as in dried xerogels.[119] Very recently, a novel "pro-sensitizer" based sensing of two completely different enzymes (lipase and β-glucosidase) using a cholate gel-based Tb(III) luminescence assay was reported (Fig. 17).[120]

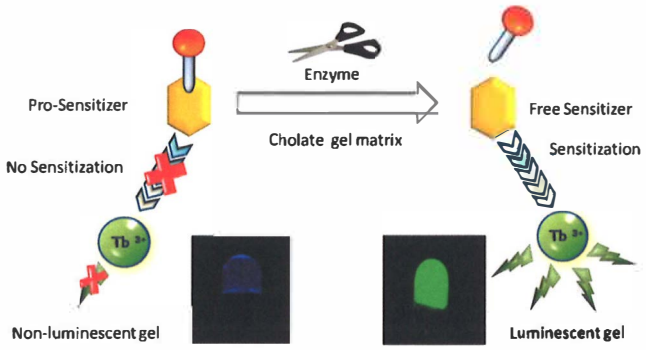

Figure 17. A strategy presented by Bhowmik and Maitra towards the design of enzyme-induced luminescent gel.[120] Reproduced by permission of The Royal Society of Chemistry.

An interesting example of light-responsive hydrogel systems has been reported by Zhao and Stoddart (Fig. 18).[121] They showed that the formation of a supramolecular inclusion complex by a deoxycholic acid-modified β-cyclodextrin derivative and an azobenzene-branched poly(acrylic acid) is accompanied by the formation of a hydrogel. In the hydrogel state, the *trans*-azobenzene units of the copolymer are included inside the cavity of the β-cyclodextrin derivative. Upon photoirradiation with UV-light of 355 nm, the hydrogel is converted into the sol phase because of the photochemical conversion of the *trans*-azobenzene units into the *cis*-configuration, which causes the *cis*-azobenzene units to dissociate away from the β-cyclodextrin rings. The hydrogel formation is reversible, and the gel can be recovered *via* photoirradiation with visible light of 450 nm.

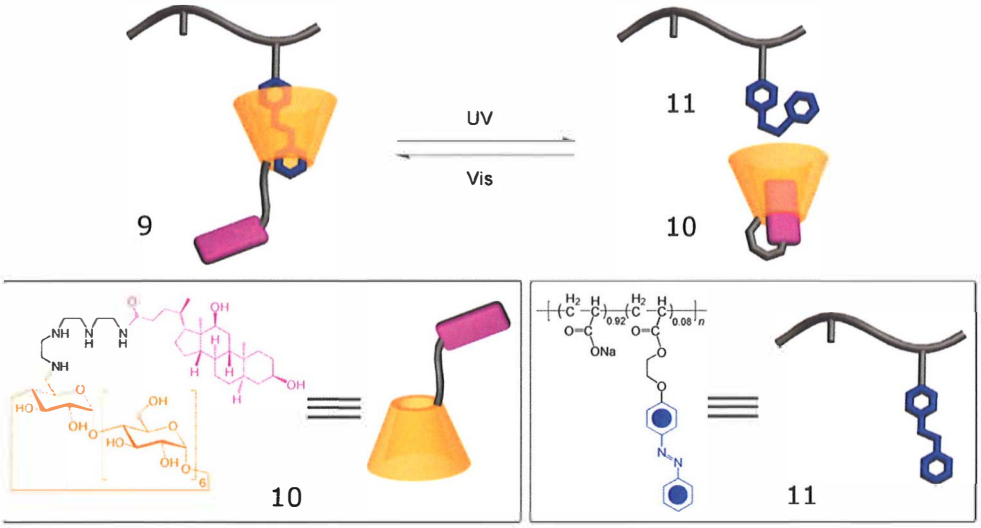

Figure 18. Supramolecular inclusion complex **9** formed from deoxycholate-β-cyclodextrin derivative **10** and azobenzene-branched poly(acrylic acid) copolymer **11**.[121] Copyright © 2009 American Chemical Society

Recently, a novel method for the modification of sodium deoxycholate hydrogels, their application as templates for nanomaterial synthesis, as well as their potential applications in biotechnology and drug delivery was presented.[122] In the presence of increasing concentrations of tris(hydroxymethyl) aminomethane (TRIS) the gel crystallinity and rigidity were shown to be enhanced. Cyanine-based fluorescent nanoGUMBOS (nanoparticles from a group of uniform materials based on organic salts) were synthesized utilizing hydrogel microstructures obtained under various conditions as templates. In addition, the release profiles of the gel systems were studied in order to evaluate their utilization for drug delivery purposes.

Maitra and co-workers were the first to design and synthesize a bile acid analogue with a neutral hydrophilic side chain capable of forming gels in aqueous solvent mixtures. The amide conjugate of deoxycholic acid and 2-amino-2-hydroxymethyl-1,3-propanediol was shown to be insoluble in water, but formed stable, thermoreversible, and transparent gels when varying amounts of polar organic solvents were added.[123] Maitra and co-workers have also prepared a series of 23- and 24-phosphono-bile salts from cholic, deoxycholic, chenodeoxycholic, ursodeoxycholic, and lithocholic acids (**12a**–**j**, Fig. 19), all of which have been shown to form hydrogels at rather narrow pH ranges. These materials might be useful for drug delivery and other pH-responsive systems.[124] Certain cholic acid esters with hydrophilic tails represent yet additional examples of neutral bile acid derivatives capable of hydrogel formation. To form the gels, the compounds synthesized by a simple esterification of cholic acid with tri(ethylene glycol) and tetra(ethylene glycol) (**13a**–**b**, Fig. 19) are dissolved in a small amount of organic solvent, followed by the addition of water. The turbid solutions are successively heated and cooled down to room temperature, after which the gel is formed.[125] A tripodal cholamide **14** (Fig. 19) has turned out to be a supergelator of aqueous fluids with the minimum gel concentration of as low as 0.15 mM.[126] Transparent and thermally stable gels have been obtained in acetic acid water systems ranging from 0.01 to 30% of AcOH in water. A variety of physical techniques have been exploited in order to understand the structure and dynamics of the gels. In addition, the gel formed by the tripodal cholamide has been utilized in preparing gold nanoparticle–hydrogel hybrid materials, as further discussed in a later part of this thesis.[21,127,128]

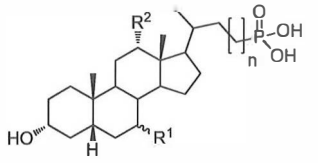

12a R^1 = α-OH R^2 = OH n = 1
12b R^1 = H R^2 = OH n = 1
12c R^1 = α-OH R^2 = H n = 1
12d R^1 = β-OH R^2 = H n = 1
12e R^1 = H R^2 = H n = 1
12f R^1 = α-OH R^2 = OH n = 2
12g R^1 = H R^2 = OH n = 2
12h R^1 = α-OH R^2 = H n = 2
12i R^1 = β-OH R^2 = H n = 2
12j R^1 = H R^2 = H n = 2

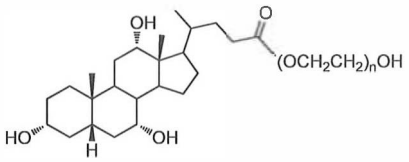

13a n = 3
13b n = 4

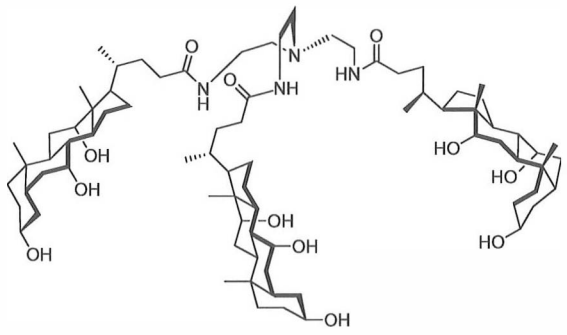

14

Figure 19. Structures of selected hydrogel-forming bile acid derivatives.[124-126]

A new class of efficient gelators of organic and aqueous–organic media, namely perfluoroalkyl bile esters, were recently introduced.[129] Three different bile acid moieties (LCA, DCA, and CA) were exploited in the syntheses, and the perfluoroalkyl chains of different lengths were attached through two different ester linkages (Fig. 20a). The presence of CO_2-philic perfluoroalkyl group is expected to enhance the solubility of the studied compounds in supercritical CO_2, thus making the compounds promising candidates for forming aerogels. The organogelation ability of certain conventional bile acid esters were serendipitously discovered by Maitra *et al.*,[130] and the systems further studied by solid state NMR and X-ray powder diffraction methods to reveal a close resemblance in the packing pattern between the gelators and the bulk solid, xerogel, and the gel in its native state.[131] Alkyl esters of cholic acid with chain lengths of 8, 10, and 12 carbon atoms studied by Marcelis and co-workers were not shown to be able to undergo self-assembly leading to organogelation. However, these compounds were shown to form thermoreversible two-component gels with carbohydrates isomannide and isosorbide in apolar solvents, such as hexane or octane (Fig. 20b).[132]

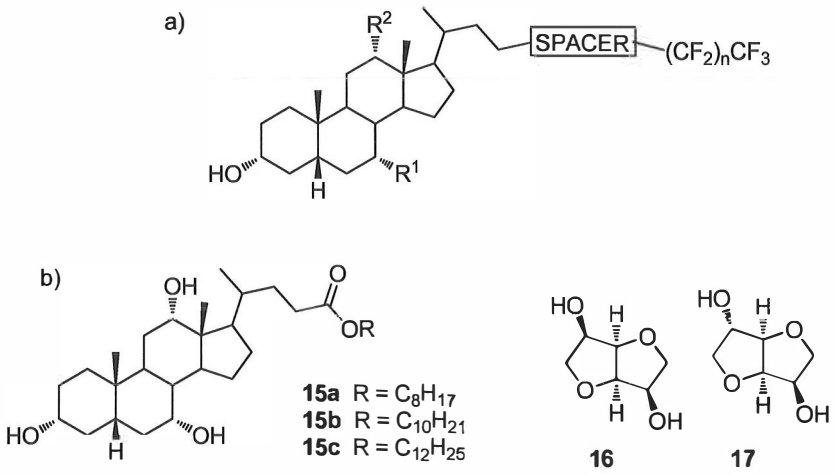

Figure 20. General structure of fluorinated bile acid-based gelators by Maitra *et al.* (a)[129] and alkyl cholates (**15a–c**) and carbohydrates (**16,17**) used for forming two-component gels (b).[132]

The majority of the bile acid-based compounds capable of forming organogels have the amide functionality in their side chain. As already mentioned previously, the amide group is ideal for the formation of intermolecular hydrogen-bonded networks.[1] Besides the above-mentioned alkyl esters, a group of amide and urea derivatives of cholic acid were prepared and tested for their gelation ability by Marcelis *et al.*[132] The compounds gelated aromatic solvents and cycloalkenes. The direction of the amide bond was shown to have a minor influence on the gelation ability, as was demonstrated by preparing compounds with a reversed amide bond. However, the introduction of an aryl group was shown to decrease the gelling capability.

A series of *N*-cholyl amino acid alkyl esters were reported to act as organogelators for aromatic solvents and cyclohexene.[133] The compounds capable of gel formation were cholic acid derivatives of selected hydrophobic or aromatic amino acid esters (Fig. 21). L-Leucine methyl ester conjugates of LCA, CDCA, and DCA were prepared in order to study the effect of the bile acid moiety in the gel-forming properties. These reference compounds did not form any gels. Detailed network structures of certain gels formed by the CA-derivatives were further studied by SANS.[134]

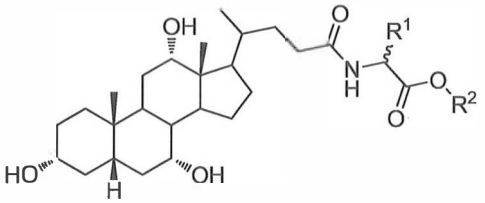

Compound	R^1	R^2
18		Me
19		Me
20a	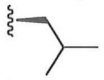	Me
20b	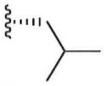	Me
20c	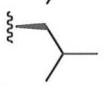	*n*-Bu
21a	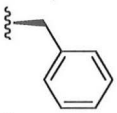	Me
21b	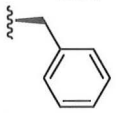	Et
21c	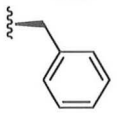	*n*-Bu
22	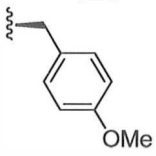	Me

Figure 21. *N*-Cholyl amino acid alkyl ester organogelators reported by Sudhölter and co-workers.[133]

Structurally related groups of aminoalkyl and (di)hydroxyalkyl amides of certain bile acids have been prepared and their gelation properties investigated in our laboratory. Amides of lithocholic and deoxycholic acids with 2-aminoethanol and 3-aminopropanol have been shown to be effective gelators for mainly chlorinated organic solvents or aromatic solvents.[135] LCA- and DCA-derivatives of dihydroxypropyl amine, for one, have not been able to form gels.[136] However, during the extensive investigation of aminoalkyl amides of bile acids (LCA, DCA, and CDCA) several gel-forming systems have been obtained. Apart from one exception, the compounds capable of gel formation have shown to be lithocholic acid derivatives. A correlation between the values of

Kamlet–Taft parameters and solvent preferences for gelators has been observed as depicted in Figure 22.[136] The Kamlet–Taft parameters for the gel-forming solvents (1–14) show rather uniform values compared to values for solvents which do not form gels (15–36). Additional examples of organogel-forming compounds from our laboratory provide the monomeric and dimeric alkylamide–phenylurea derivatives of DCA,[137] and structurally very interesting and rather rare bile acid-derived monoketals of pentaerythritol.[138]

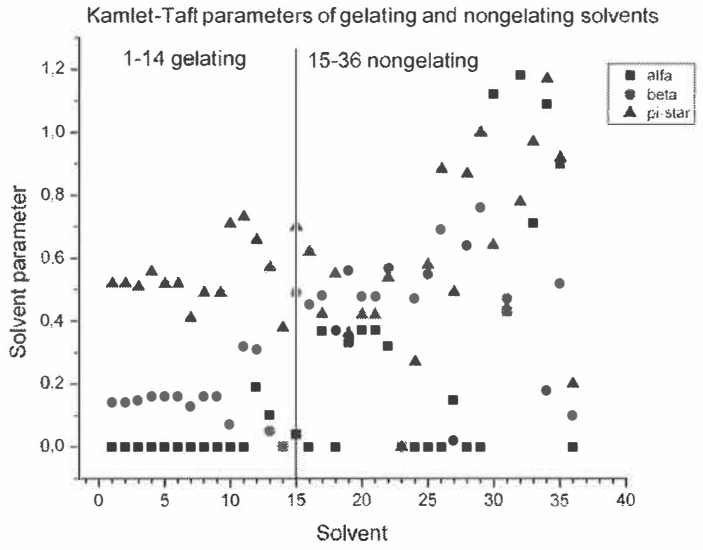

Figure 22. A correlation between the Kamlet–Taft parameters and solvent preferences for certain bile acid-based gelator compounds observed by Löfman and Sievänen with co-workers.[136]

Maitra and co-workers have observed that the 3α-esters of 1-pyrene butyric acid of certain DCA-alkylamide/esters are effective gel-forming compounds in many organic solvents when the gelation is triggered by the addition of a charge transfer agent 2,4,7-trinitrofluorenone (TNF).[139] The same research group also reported two bile acid-derived compounds containing a basic amino group in their structures to act as efficient gelators for organic and aqueous solvents. The organogelator has been shown to be a non-gelator in its neutral form. However, as its iodide salt the compound forms strong gels in 1,2-dichlorobenzene and chlorobenzene. For the hydrogelator the situation has shown to be reversed; as its neutral form the compound is able to form gels in certain aqueous mixtures of organic solvents, but the salt formation has been shown to disrupt the gel network.[140] A bile acid-based anion receptor (Fig. 23), which forms a stable gel in $CHCl_3$/DMSO mixture in the presence of HSO_4^- anion and can thus be used for the recognition of hydrogen sulfate anions, has been recently reported.[141]

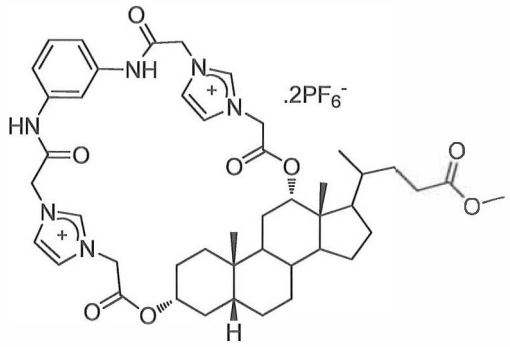

23

Figure 23. A bile acid-based anion receptor reported by Pandey and Tripathi.[141]

1.4.2 Gold/silver nanoparticles

Maitra and co-workers were the first to report gold nanoparticles with bile acid-derived thiols as capping agents.[21,142] The AuNPs utilizing bile acid derivatives as stabilizers were prepared by the $NaBH_4$ reduction of $HAuCl_4$ in methanol. Molar ratio of 1:1 between the gold salt and the steroidal thiol was employed. The prepared steroid-capped AuNPs were shown to be stable through several cycles of drying and re-dissolution. The shapes of the observed surface plasmon resonance bands and the sizes of the spherical nanoparticles were shown to depend on the structure of the steroidal capping agent. Further, the steroidal AuNPs exhibited a tendency to agglomerate in aqueous medium due to the amphiphilic nature of the stabilizing agent. The exploitation of the steroid-capped AuNPs in preparation of nanoparticle–gel hybrid materials was further investigated,[21] as presented in the following section. Acetylation as one of the simplest reactions was chosen to carry out on the steroidal AuNPs. Nanoparticles stabilized by the lithocholic acid-derived thiol bearing a single hydroxyl group at the position C-3 of the steroidal backbone were acetylated in pyridine–acetyl chloride in order to demonstrate a functional group transformation on the capped AuNPs. The same research group also prepared silver nanoparticles (AgNPs) employing the same bile acid-derived thiols as stabilizing agents.[142]

A novel strategy for the synthesis of silver and gold nanoparticles using naturally occurring sodium salts of taurocholate and glycocholate as both reducing and capping agents was presented rather recently.[143] The size and the shape of the nanoparticles were shown to be determined by the nature as well as the concentration of the bile salt employed. Thereafter the synthesis of AuNPs employing sodium cholate and sodium deoxycholate as reducing and capping agents has been reported.[144] Variation of the sodium cholate concentration was shown to provide control over the size and shape of the nanoparticles formed (Fig. 24). At concentrations below cmc the formed nanoparticles were shown to be exclusively anisotropic in nature. However, at concentrations

above cmc the NPs were essentially shown to be spherical. The formation of AuNPs was shown to proceed at greater rate in the presence of sodium cholate in comparison to sodium deoxycholate at identical concentrations of bile salts. This was suggested to indicate the important role of the hydroxyl groups in the reduction of Au^{3+} ions. Further evidence supporting this hypothesis was achieved by FT-IR. The combination of steady-state and time-resolved quenching studies using fluorescent probes revealed the hydrophobic interaction between the sodium cholate micelles and AuNPs. Finally, the prepared AuNPs were evaluated as a colorimetric sensor for the detection of Gemini viral DNA using degenerate probes.

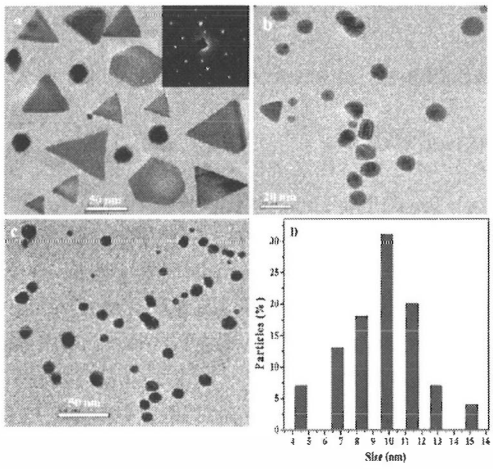

Figure 24. TEM images of AuNPs prepared by varying the sodium cholate concentration ((a) 0.0015, (b) 0.008, and (c) 0.033 M). Particle size distribution of 0.033 M sodium cholate-capped AuNPs is also seen.[144] Reprinted with permission.

Very recently, the one-step "green" process for the formation of AuNPs with sodium cholate as the reducing and stabilizing agent in aqueous conditions at ambient temperature was reported.[145] The size and shape of the AuNPs can be tuned by changing the cholate/$HAuCl_4$ ratio and solution pH (Fig. 25). The cholate-capped AuNPs prepared by this way have shown to exhibit good electrocatalytic activity toward methanol oxidation. Thin films prepared from the AuNPs have shown to be capable of serving as efficient substrates for surface-enhanced Raman scattering (SERS).

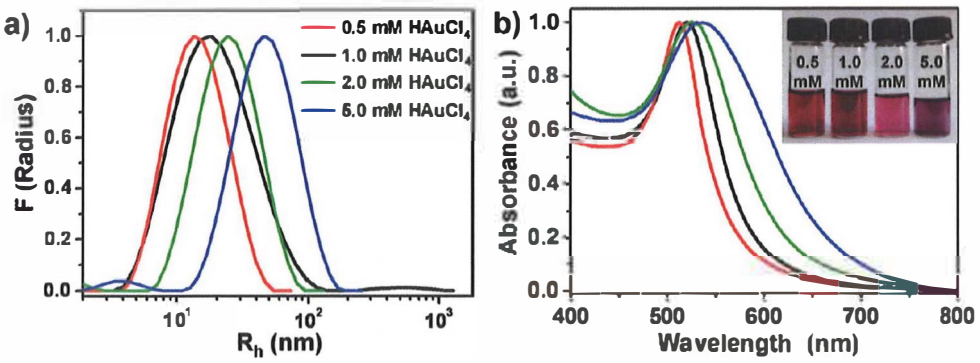

Figure 25. Sodium cholate-capped AuNPs prepared by varying the initial $HAuCl_4$ concentration: (a) DLS analysis; (b) UV–vis spectra. Inset in (b) shows the macroscopic appearance of AuNPs in solution.[145] Reprinted with permission. Copyright © 2011 American Chemical Society

Bile acid-based polymers prepared by click chemistry have shown to stabilize silver nanoparticles. Moreover, the AgNPs of 4.0–4.2 nm of average size were shown to be capable of selective colorimetric sensing for the iodide ion.[146]

1.4.3 Hybrid materials

As already mentioned in the previous section, Maitra and co-workers utilized the steroidal thiol-capped AuNPs for preparing novel AuNP–hydrogel hybrid material.[21] A bile acid-derived hydrogelator **14**[126] (Fig. 19) that forms a fibrillar network upon aggregation in AcOH/water medium was chosen as the gel-forming part. The hybrid material was prepared by dissolving the nanoparticles and the gelator compound in AcOH first, and then diluting the system with four volumes of water. The dispersion was shown to form a gel within 4–5 h. TEM images of the hybrid material revealed the steroid-capped NPs being well immobilized on the gel fibers (Fig. 26).

A single-step synthesis of narrowly dispersed AgNPs by reducing $AgNO_3$ in the presence of natural light in a hydrogel system composed of cholic acid conjugate of polyethylene glycol 400 (CA–PEG400) has been introduced by Wang, Li, and co-workers.[147] The gelator compound was shown to act not only as a stabilizer preventing the silver particles from further growth and aggregation, but also as a reducing agent. Yet another example from the same research group described the formation of narrow-dispersed gold nanospheres, regular single crystal nanoplates, and nanobulks, respectively, by reducing $HAuCl_4$ within the above-mentioned hydrogel system under UV-irradiation.[148] The initial concentration of $HAuCl_4$ and the microenvironment of the gel matrix were shown to determine the geometric shape and size of the gold products.

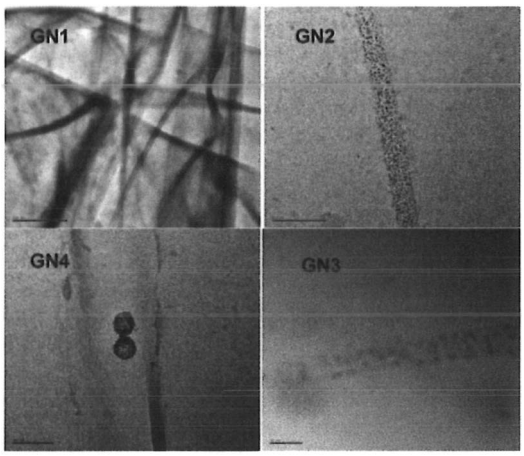

Figure 26. TEM images of AuNP gel hybrids prepared by Maitra and co-workers.[21] Scale bars: 200 nm (GN1), 100 nm (GN2), 20 nm (GN3), and 10 nm (GN4). Reprinted with permission. Copyright © 2006 American Chemical Society

Self-assembled organic/inorganic hybrid tubes are attractive since they can display dual physical properties; the inorganic fraction might, for example, enhance the mechanical strength of the tubes allowing them to sustain harsh conditions, while the organic fraction may provide biocompatible environment. Fluorescent hybrid tubes in which the *in situ*-formed cadmium sulfide (CdS) nanoparticles are embedded in lithocholic acid tube walls have been presented by Fang and co-workers.[149] As already mentioned earlier, LCA can in aqueous solutions self-assemble into tubular structures with different morphologies and shapes by controlling the experimental conditions in which the self-assembly occurs.[85-87,150] The self-assembly of LCA-CdS tubes has been carried out in a mixed solution of LCA, $Cd(ClO_4)_2{\cdot}2H_2O$, and C_2H_5NS. At pH 9.5 the negatively charged COO^- groups coordinate with Cd^{2+} ions, which then react *in situ* with S^{2-} to form CdS seeds during the self-assembly of LCA-Cd molecules, eventually growing into CdS nanoparticles inside the walls of the LCA tubes. The fluorescence of the hybrid tubes has been shown to originate from the embedded CdS nanoparticles with the cubic (zinc blende) crystal structure. The shape of the tubes has shown pH-dependency, since at pH 9.5 the self-assembled tubes display a straight shape (Fig. 27), while at pH 13.0 the tubes coil into a left-handed helix. These fluorescent hybrid tubes with pH-controlled shapes show promise for a variety of materials and biological applications.[149]

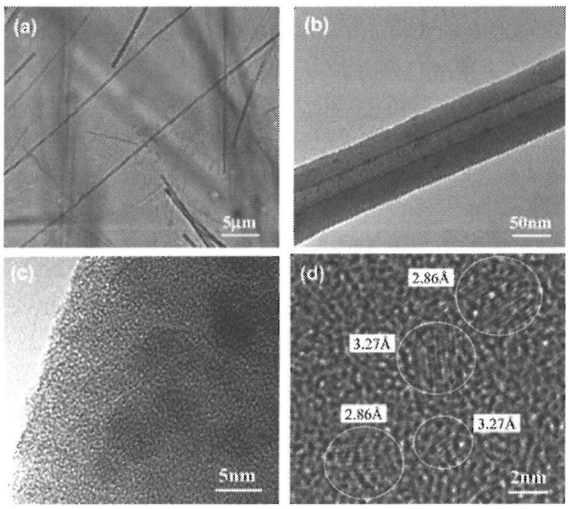

Figure 27. (a) Optical microscopy image of hybrid LCA/CdS tubes in aqueous solution at pH 9.5. (b) Low-resolution TEM image of a tube dried on a carbon-coated grid. (c–d) High-resolution TEM images of individual CdS nanoparticles embedded in the tube walls.[149] Reproduced by permission of The Royal Society of Chemistry.

Hybrid material composed of a hydrogel of sodium deoxycholate (NaDC) and single-walled carbon nanotubes (SWCNTs) with excellent viscoelastic properties and electrical conductivity has been reported by Tan and co-workers.[151] NaDC-functionalized SWCNTs were shown to be well-dispersed in a NaDC-hydrated matrix eventually forming a supramolecular hydrogel in such a matrix. The formed hydrogel could be extended 50-fold along the direction of additional stretching force. Rheological properties of this NaDC–SWCNT supramolecular hydrogel were shown to be 100 times larger compared to other small molecule–SWCNT gel systems being thus competitive with polymer–SWCNT hybrids. Excellent rheological properties together with good electrical conductivity make this gel a promising candidate for flexible, stretchable electronic applications.

1.4.4 Other nanoscale materials

Self-assembly of organic molecules provides a "bottom-up" approach for the synthesis of supramolecular structures with controlled sizes, shapes, and morphologies. As already mentioned earlier, the transcription of these self-assembled supramolecular objects into inorganic materials has attracted a lot of interest recently.[36] Particularly attractive are tubular structures of silica, which have potential applications in catalysis, separation, photonics, and bioengineering. Template-directed sol–gel polycondensation of tetraethoxysilane (TEOS) is a representative method to synthesize silica nanomaterials. Fang and co-workers have exploited the pH-dependent self-assembly of lithocholic acid in preparing micro- and submicro-scale silica structures from straight (Fig. 28), coiled, and helical tubes to single and double fan-like bundles using TEOS in

the presence of ammonia catalyst.[152] Also Huang and Weiss have reported the preparation of mesoporous rod-like silica and titania nano-objects using very dilute (0.1 wt%) aqueous solutions (0.1 M NaOH) of sodium lithocholate as templates.[153] The aggregates formed by the cholic acid self-assembly in the presence of benzylamine in aqueous solution have also been exploited as templates for the formation of hollow silica spheres.[154] Moreover, aqueous mixtures of different bile salts have been used as templates for the synthesis of sponge-like silica materials resembling the structure found in trabecular bone. The materials' ability to induce a bone-like apatite layer in contact with simulated body fluid has been investigated, as well.[155]

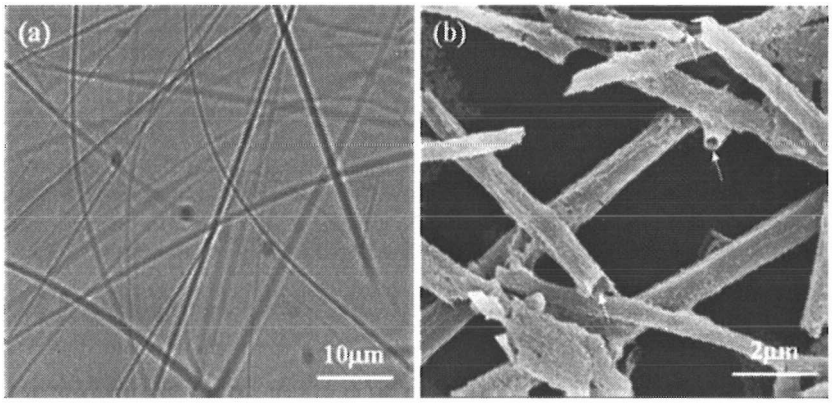

Figure 28. (a) Optical microscopy image of straight LCA microtubes in solution at pH 7.4. (b) SEM image of silica microtubes dried on carbon films. The arrows shown in (b) indicate the open ends of the tubes.[152] Reproduced by permission of The Royal Society of Chemistry.

Ammonium lithocholate (NH_4LC) nanotubes forming in strongly alkaline ammonia solutions have been used as templates to form short copper rods with external diameter of about 80 nm. The electroless plating method in which the Pd-catalyst is adsorbed on the surface of the nanotubes to catalyze the reduction of copper on the surface has been employed. The NH_4LC nanotubes carrying a net negative charge have been wrapped with poly(ethylene-imine) (PEI) polyelectrolyte to render the tubes positively charged before the copper metallization.[156]

With the helical structure being a central structural motif in biological systems and having appealing applications in nanoscience, it has been an attractive subject of research. Huang and co-workers have demonstrated the formation of well-defined right-handed helical nanoribbons in calcium cholate systems, where metal ions (Ni^{2+}, Zn^{2+}, Co^{2+}, and Cu^{2+}) are employed to drive the helix formation. These nanohelices have been further transcribed into helical silica materials *via* the traditional sol–gel process. Moreover, with the addition of Na_2S, helical ZnS semiconductor nanotubes have been obtained *via* self-templating approach in which the metal ions serve as both the inorganic precursor and as the constituent of the template (Fig. 29).[157] The authors have re-

cently presented the self-templating method as a general approach toward 1D inorganic nanotubes.[158]

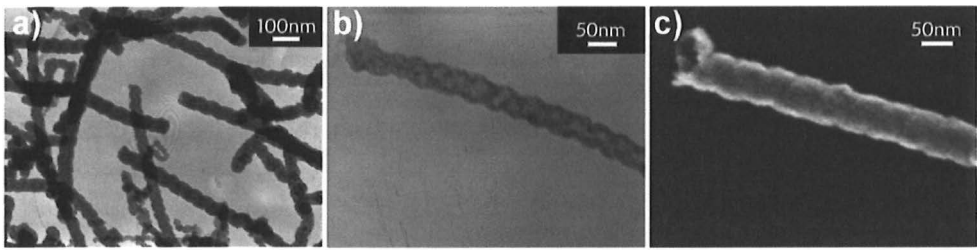

Figure 29. TEM (a,b) and SEM (c) images of ZnS semiconductor helical tubes.[157] Reprinted with permission. Copyright © 2009 American Chemical Society

As already discussed in section 1.4.1, Huang and co-workers have reported the formation of a variety of architectures by the self-assembly of lanthanide cholate.[117] They have also shown that these photoluminescent materials can serve as functional templates to prepare inorganic nanomaterials; novel lanthanide-doped silica nanotubes in which the lanthanide ions are embedded into the tube walls have been prepared by using sol–gel transcription of TEOS. In this approach, the lanthanide ions are efficiently uptaken by silica nanotubes, making the nanotubes photoluminescent. Moreover, the diameter of the silica nanotubes can be varied by adjusting the environmental temperature. Finally, by changing the doping ions or co-doping with multiple ions different kinds of lanthanide-doped silica nanotubes with tunable photoluminescent emission colors can be achieved.[159]

The self-assembly of amides of 3β-amino derivatives of deoxycholic and cholic acids in aqueous solutions has been extensively studied. These compounds have shown to form *e.g.* lamellar structures,[160] molecular tubes originating from vesicles,[161] and tubular structures through helical ribbons initially formed from planar sheets.[162] Additionally, a very dilute mixture of anionic and cationic derivatives of sodium cholate has been shown to form tubules, whose compositions and charges can be tuned by controlling the stoichiometry of the mixture. These new catanionic structures may have applications in controlled loading of charged molecules and macromolecules.[163]

Nanostructured silicon is of interest as a bio-investigation tool because of its photoluminescence at room temperature and slow degradation into safe components. However, a successful application of silicon nanocrystals requires tuning of certain characteristics, such as emission properties, toleration towards water and oxygen, and toxicity. Deoxycholate has been shown to function as an efficient coating agent for hydrophilic silicon nanocrystals, as reported by Scarpa and co-workers. In their work, the silicon nanocrystals were first made completely water soluble by covalent binding of an alkyl chain bearing a carboxyl group on the tail. The hydrophilic nanocrystals were then coated with sodium deoxycholate. The resulting silicon nanocrystals had an average diameter of 3–5

nm, could be dispersed in aqueous solutions, and showed stable photoluminescence.[164]

An organic lattice framework is a promising platform to achieve spatially oriented molecular arrays with a wide range of dye molecules. Hisaki and Miyata with their co-workers have demonstrated that inclusion crystalline lattice composed of deoxycholamide can be applied as a platform to arrange various dye molecules, such as anthracene and 1,6-diphenylhexatriene, into a tandemly aligned array without π–π stacking in the inclusion channel. Moreover, the density of the guest dyes included in the channels is controllable upon the change of the crystallization solvent: nonpolar solvents give inclusion crystals containing a small amount of dye molecules (Fig. 30a), while polar ones give inclusion crystals whose channels are filled by tandemly arrayed dyes (Fig. 30b). The results contribute to the development of efficient fluorescent solid materials.[165]

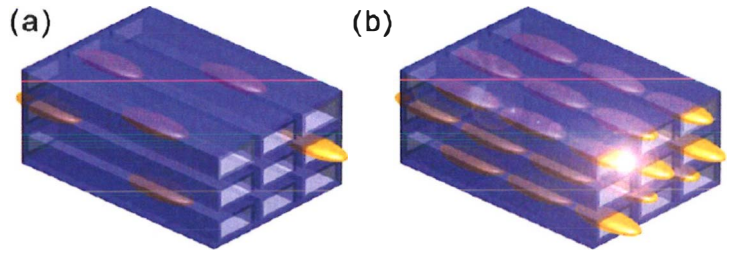

Figure 30. Schematic representation of inclusion crystals with isolated (a) and fully aligned (b) guest molecules in the channels.[165] Reprinted with permission. Copyright © 2011 American Chemical Society

2 EXPERIMENTAL PART

2.1 Aims and background of the study

Bile acids are fascinating compounds from a chemist's point of view because of their unique structural features, availability, low cost, and versatile derivatization possibilities. Further, bile acids are chemically well-characterized and their chemistry is understood in great detail. Thus, they have found numerous applications in the fields of pharmacology, supramolecular chemistry, and materials science.

The main objective of this research was to prepare amide conjugates of bile acids and biologically important small molecules, as well as to investigate the chemical and physical properties along with the structural details of the prepared compounds. The target compounds are biocompatible and exhibit potential applicability in the field of nanoscience, for example as nanoparticle coating or supramolecular gel-forming materials. Consequently, studies concerning the gel and nanoparticle formation and morphology, along with the phenomena underlying them, were of particular interest. Based on interesting preliminary self-assembly results of mainly cholic acid–amino acid derivatives reported by Sudhölter and co-workers[133] we were intrigued to investigate bile acid–amino acid based systems in more detail. Our aim was to utilize bile acids bearing a varying number of hydroxyl groups and amino acid alkyl esters with a variety of functional groups and different polarity profiles in order to see the effects of those parameters to the self-assembly properties of the compounds. Additionally, after positive gelation results obtained in our laboratory for hydroxy- and aminoalkyl amides of varying bile acids,[135,136] we were prompted to explore the self-assembly properties of structurally related cysteamine derivatives.

All of the 18 target compounds were prepared using simple synthetic methods and characterized utilizing NMR spectroscopy, mass spectrometry, and elemental analysis. X-ray diffraction and solid state NMR spectroscopy were employed to explore the solid state properties of the prepared compounds.

Self-assembly properties of all of the compounds were extensively investigated, and the formed systems studied by versatile methods.[II-IV] One of the compounds was exploited for preparing steroid-capped gold nanoparticles.[V]

2.2 Synthesis of bile acid amide conjugates[II-V]

The target compounds were synthesized by slightly modifying the mixed anhydride method described in the literature.[166] First, a mixed anhydride from bile acid and ethyl chloroformate was synthesized without isolating the product. Then, the freshly prepared bile acid anhydride was allowed to react with the amino acid alkyl ester or cysteamine. The reaction conditions somewhat varied between different syntheses, and more detailed information on the methods and specific conditions can be found in publications II–V. Unoptimized yields for the target compounds after column chromatographic purifications varied between 28–99%. The general depiction for the synthesis of the compounds studied in this research is presented in Scheme 1.

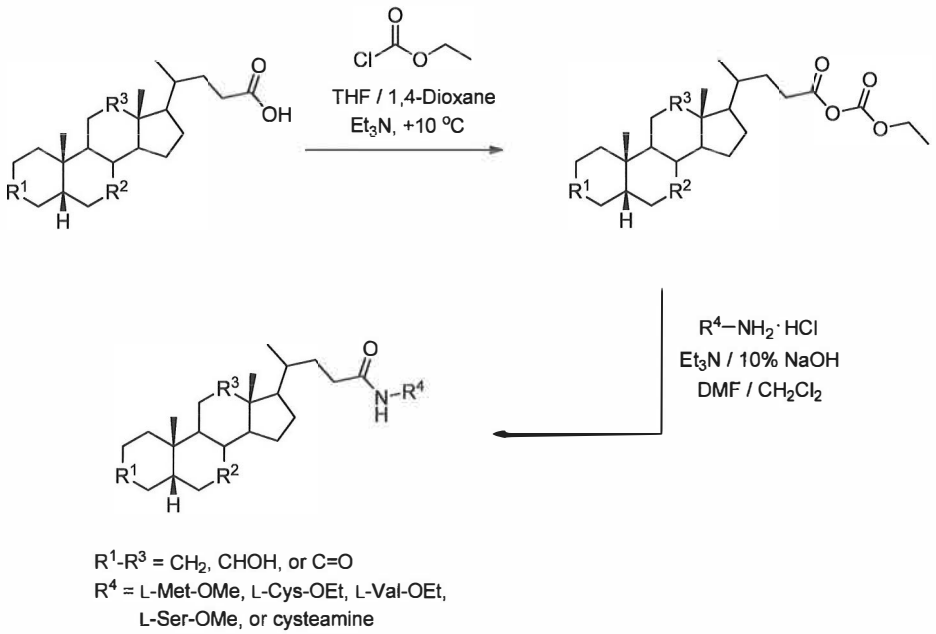

Scheme 1. General scheme for the synthesis of the investigated compounds.

Altogether 18 amide conjugates of different bile acids [LCA (**2**), CDCA (**3**), UDCA (**4**), DCA (**5**), CA (**6**), and dehydrocholic acid, DHCA] with different amino acid alkyl esters (L-methionine methyl ester,[II] L-cysteine ethyl ester,[III,V] L-valine ethyl ester,[III] and L-serine methyl ester[III]) or cysteamine[IV] were prepared. Structures of compounds **24–28** are presented in Figure 31.

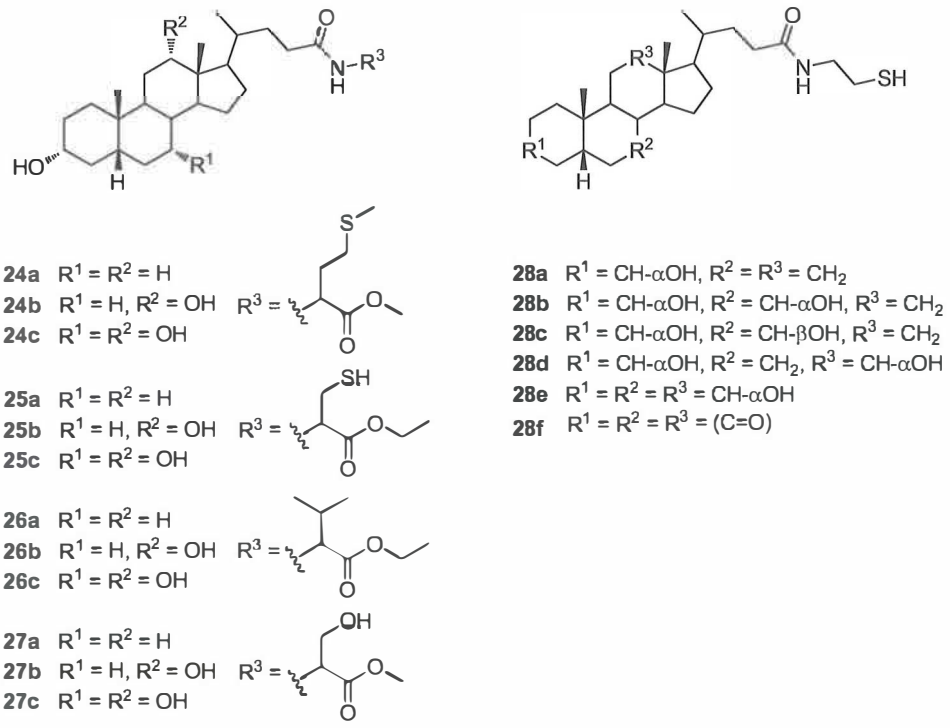

Figure 31. Chemical structures of the compounds prepared and investigated within this study.

2.3 Self-assembly studies[II-IV]

Self-assembly properties of compounds **24**–**28** were investigated in numerous solvent systems, and versatile self-assembled systems were detected. The number of the hydroxyl groups possessed by the steroidal skeleton and the character of the moiety attached *via* amidation to the carboxyl group of the bile acids were used as variables, when examining the self-assembly properties of the compounds. The detailed information on the results of the self-assembly studies can be found in the tables of publications II–IV.

Compounds **24a**, **24c**, **25c**, **26a**, **28a**, **28e**, and **28f** were shown to be capable of self-assembly leading to organogelation mostly in certain aromatic solvents, such as toluene, benzene, and chlorobenzene. Interestingly, all but one of the compounds showing gelation ability were derivatives of either lithocholic or cholic acid bearing one or three hydroxyl groups in their steroidal skeleton, respectively. The exception was the DHCA-derivative of cysteamine (**28f**). The deoxycholyl conjugates **24b**, **25b**, **26b**, **27b**, and **28d** having two hydroxyl groups in their steroidal part did not show gelation ability in the standard gelation tests. Their high solubility in the majority of the solvents tested was most probably prohibiting the self-assembly leading to gelation.

Regarding to the number of solvents gelated, the LCA- and CA-derivatives of L-methionine methyl ester (**24a** and **24c**, respectively) were shown to be the most "effective" gelators. Moreover, the transparent gels formed by compound **24c** in certain aromatic solvents were undoubtedly the strongest ones among all of the gels formed. Photographs of a gel formed by *N*-cholyl-L-(methionine methyl ester) (**24c**) in toluene are presented in Figure 1. The cholic acid conjugate of L-cysteine ethyl ester **25c** and cysteamine derivative of dehydrocholic acid **28f** turned out to be rather versatile organogelators forming gels not only in aromatic solvents, but also in CCl_4, diethylether (**25c**), and 1-octanol (**28f**).

Compound **25c** in water was not shown to form a real gel, but rather a certain kind of gel-like, viscous material. This was further studied by SEM by pipetting the hot solution of compound **25c** in water (2% w/v) on a sample stub and allowing it to dry. Isolated spherical structures of approximately 1 μm in diameter were discovered (Fig. 32A-B). Additionally, larger spherical objects of about 8 μm in size covered with the smaller sphericals were detected (Fig. 32C–D). With respect to the appearance and size the smaller vesicles resembled the ones formed by LCA in alkaline aqueous solution[85] discussed earlier in section 1.3.2.

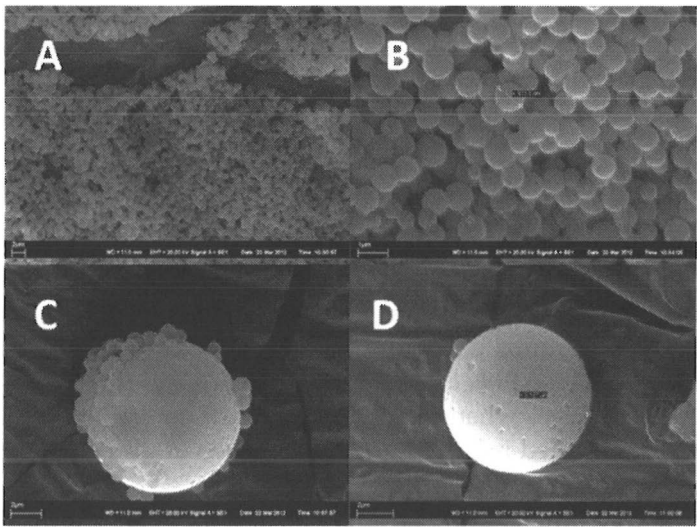

Figure 32. SEM images of self-assembled structures formed by compound **25c** in water (2% w/v). Scale bars: 2 μm (A, C, and D) and 1 μm (B).

Amides of bile acids with the relatively non-polar L-valine ethyl ester (**26a–c**) appeared to be highly soluble in the tested solvents, and formed only one gel (compound **26a** in CCl_4). The gel was also shown to form upon ultrasonic treatment, thus presenting an example of the physical stimuli-responsive systems triggered by a stimulus other than a thermal one. Compounds **27a–c**, for one, bearing the polar L-serine methyl ester, were poorly soluble in the studied solvent systems and none of the compounds showed the ability to promote ac-

tual gel formation. However, a couple of weeks after the self-assembly studies, formation of the so-called spherulitic structures in aromatic solvents was detected. Spherulites are generally described as polycrystalline moieties being composed of fibrillar crystal arrays radiating from a common central nucleus, thus creating a spherical aggregate.[167] They are ubiquitous in solids formed under highly non-equilibrium conditions, and are found in numerous systems.[168] Additionally, spherulitic microdomains are frequently encountered in the gel systems, and have been shown to function as the seeds for a slow crystallization process of the gel phase.[169] In the case of the DCA-derivative **27b** the isolated spherical structures were found to be attached to the wall of the test tube in each of the aromatic solvents studied (Fig. 33). For the solvents with lower solubility the spherulites were shown to be relatively small and most often entirely isolated (Fig. 33A), whereas in chlorobenzene bigger aggregates were observed (Fig. 33B). Moreover, one big spherulitic structure was detected in anisole (Fig. 33C). In the case of the LCA-derivative **27a**, for one, gel-like particles in solution, particularly in chlorobenzene and anisole, were observed. However, for neither of the compounds were these spherulitic structures able to grow sufficiently enough to be able to span the whole sample volume and cause the gel to form.

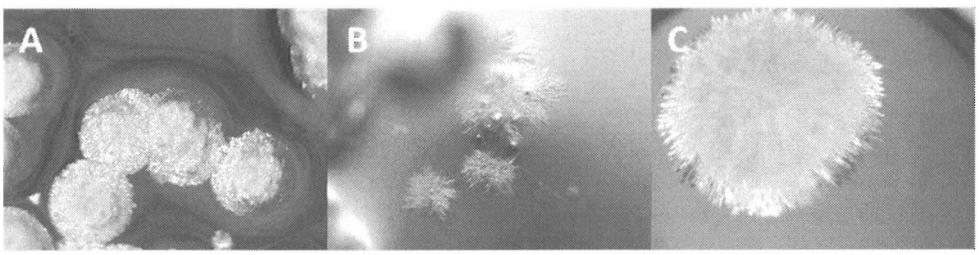

Figure 33. Optical microscopy images showing versatile spherulitic aggregates formed by compound **27b** in cumene (A; 50× magnification, polarized light), chlorobenzene (B; 30× magnification), and anisole (C; 15× magnification, polarized light).

Based on the results of the self-assembly studies it seems evident that the nature of the compound conjugated to carbon 24 of the bile acid moiety is the determinant factor for the gel-forming ability of the compounds. Though a few structurally related DCA-derived organogelators have been reported,[135,136] for this set of compounds no gels formed by the deoxycholyl derivatives in standard conditions were observed. Nevertheless, in the preliminary studies the DCA-conjugate of L-serine methyl ester **27b** showed capability of gel formation in aqueous mixtures of ethanol. Sudhölter and co-workers suggested based on their studies on certain *N*-cholyl amino acid alkyl esters[133] that the amide bond and several hydroxyl groups were the molecular requirements for the gelation to occur for this type of compounds. This has now been challenged by us with the LCA-derived organogelators **24a** and **26a**. However, in the case of bile acid–cysteamine conjugates **28a–f**, apart from a weak gel formed by **28a** in benzene; three functional moieties in the steroidal part of the compounds were

needed for the self-assembly leading to gelation to occur, as the gel-forming compounds were the CA- and DHCA-derivatives **28e** and **28f**, respectively.

2.3.1 Morphology of the gels

Morphology of the self-assembled supramolecular gels was mostly investigated utilizing SEM. Additionally, for CCl_4 gel of compound **26a** optical microscopy in order to monitor the gelation *via* formation of visible fibers was employed. Typically, two types of morphologies were detected among the gel, or xerogel, samples in SEM. Xerogels of compounds **24a**, **26a**, and **28f** revealed fibrous structures, whereas for the xerogels of **24c**, **25c**, and **28e** spherical structures were observed (Fig. 34). It is worth noting that ageing of the material can have effects on morphology. Also the cooling rate may play an important role in the appearance of xerogel samples. In our case, however, the samples were aged for a constant period of time prior imaging, and the cooling conditions for the samples were uniform.

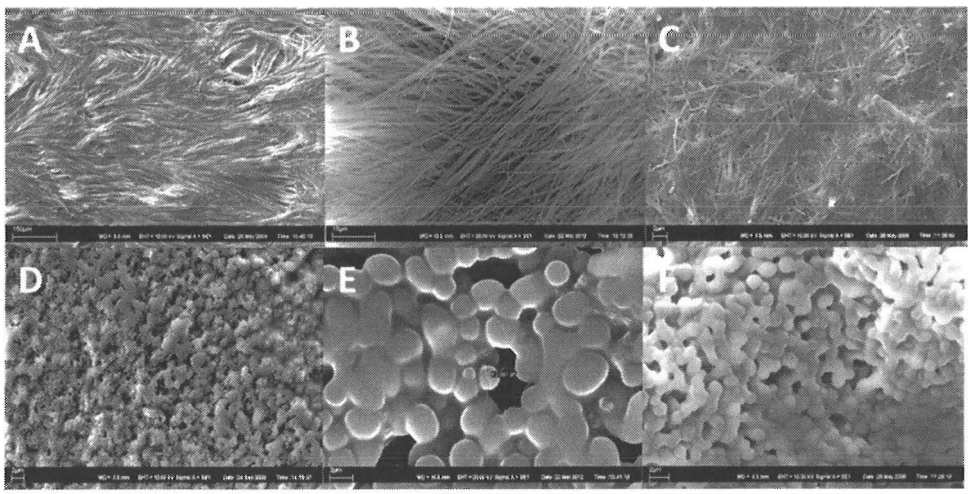

Figure 34. SEM images of the xerogels showing fibrous (A–C) and spherical (D–F) structures. A) **24a** in toluene (4% w/v), B) **26a** in CCl_4 (2% w/v), C) **28f** in 1-octanol (4% w/v), D) **24c** in toluene (2% w/v), E) **25c** in toluene (2% w/v), and F) **28e** in chlorobenzene (1% w/v). Scale bars: 100 μm (A), 10 μm (B), and 2 μm (C, D, E, and F).

The effect of the sample preparation protocol on the sample appearance was investigated for the gels of compound **25c** in *tert*-butylbenzene and CCl_4, as well as for compound **26a** in CCl_4. Portions of the pre-formed transparent gels of compound **25c** in *tert*-butylbenzene and CCl_4 at 0.75% w/v concentration were scooped on the sample stubs in addition to the samples prepared from the hot solution (2% w/v). Notable differences on the sample appearance were indeed observed by SEM. The scooped samples were shown to be composed of burl-like three-dimensional structures in both solvents (Fig. 35A and 35C), whereas in the samples prepared from hot solutions spherical interconnected

aggregates were observed (Fig. 35B, 35D, and 35F). Moreover, a few larger spherical aggregates of the size of tens of micrometers covered with micrometer-scale smaller sphericals in CCl_4 were found (Fig. 35E). Finally, a number of larger fully spherical objects of a couple of micrometers in size embedded in the main component composed of interconnected spherical aggregates were detected (Fig. 35F). However, it is questionable, whether the samples prepared from the hot solutions of *tert*-butylbenzene and CCl_4 represent the exact situation in the gel state, especially when the gelation was found to be rather a slow process and frequently take place only after vigorous shaking of the sample tubes. Either way, similar types of spherical structures were observed also for the 2% (w/v) samples of compound **25c** in *o*-xylene and mesitylene. Recently, also Steed and co-workers have evidenced shear-induced gelation.[170] Based on the cryo-SEM experiments performed for a pyridyl-urea based metallogel it was hypothesized that the mechanical shaking of the system breaks the initial fibers leaving reactive open ends, which then reassemble in a much more interconnected fashion forming a robust gel.

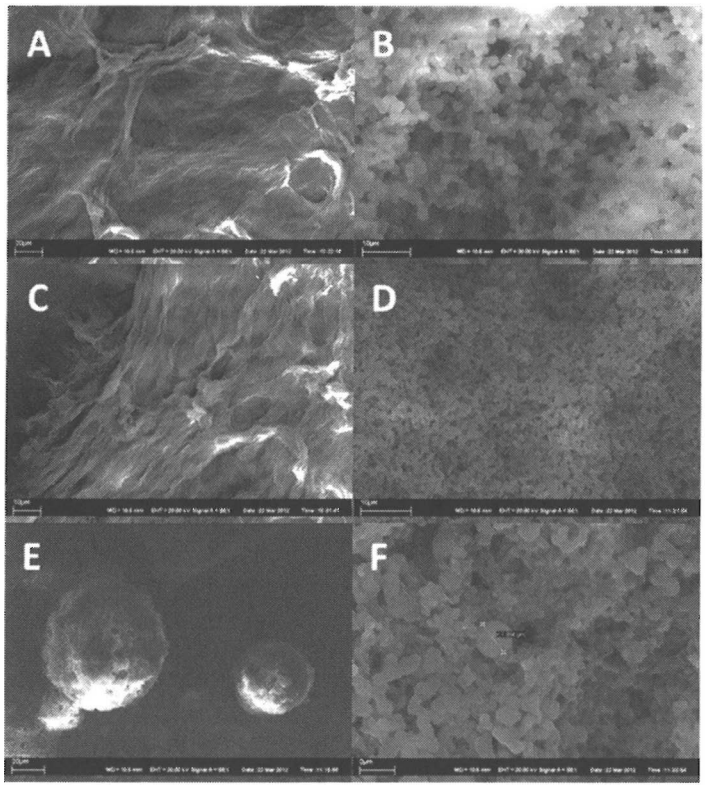

Figure 35. SEM images of the xerogels of compound **25c**. A) Sample prepared by scooping a portion of the transparent gel on a sample stub (0.75% w/v in *tert*-butylbenzene), B) Sample prepared from a hot solution (2% w/v in *tert*-butylbenzene), C) Sample prepared by scooping a portion of the transparent gel on a sample stub (0.75% w/v in CCl_4), D–F) Sample prepared from a hot solution (2% w/v in CCl_4). Scale bars: 20 μm (A), 10 μm (B, C, and D), 20 μm (E), and 2 μm (F).

When a small portion of the gel formed by compound **26a** in CCl_4 by sonication was scooped on the sample stub, a network of about 1 μm thick fibers not very uniformly oriented was observed (Fig. 36A). However, when the sample was prepared by heating the suspension to the boiling point of the solvent, and pipetting a small amount of the transparent solution on the sample stub, a network of uniformly oriented fibers was observed (Fig. 36D). Moreover, the xerogel sample was shown to be composed of isolated, flower-like structures composed of fibers, which had formed funnel-like pores possibly related to the evaporation of the solvent molecules during the drying process (Fig. 36B–C).

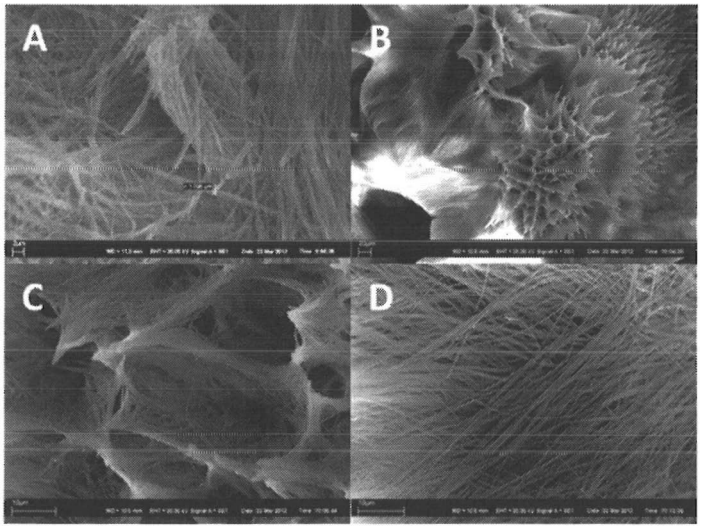

Figure 36. SEM images of the xerogels of compound **26a** in CCl_4 (2% w/v). Sample prepared by sonication (A) and sample prepared by placing the hot solution on a sample stub (B–D). Scale bars: 2 μm (A), 20 μm (B), and 10 μm (C and D).

As already mentioned, optical microscopy imaging was utilized to monitor the *in situ* gel formation in the case of compound **26a** in CCl_4. The gel formation was shown to occur *via* formation of fibers, yielding a gel with a clearly visible fibrous structure (Fig. 37).

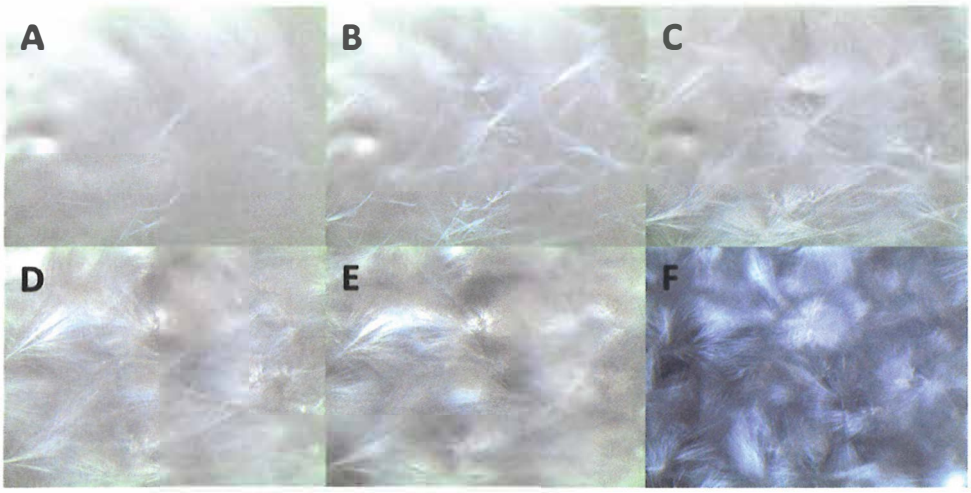

Figure 37. Optical microscopy images showing the evolution of the gel network of compound **26a** in CCl_4 (1% w/v). The images are taken with 20× magnification, and for image F polarized light has been used.

2.3.2 NMR spectroscopic studies for the gels

NMR studies for the gel state samples of LCA- and CA-derivatives of L-methionine methyl ester (**24a** and **24c**, respectively) were performed. In order to investigate the interactions involved in the gel formation, variable-temperature (VT) (30–70 °C) and concentration-dependent ^1H NMR experiments were employed.

For compound **24a** in its gel state (benzene-d_6, 2% w/v) at ambient temperature broad ^1H NMR signals appeared. By heating the sample in 5 °C steps, the signals became sharper and well-resolved spectral patterns were finally observed at 55 °C. Based on these experiments, the gel can be deduced to undergo a transition into the solution state between 50 and 55 °C. As the temperature was increased, no significant changes in the chemical shift values were observed (Fig. 38).

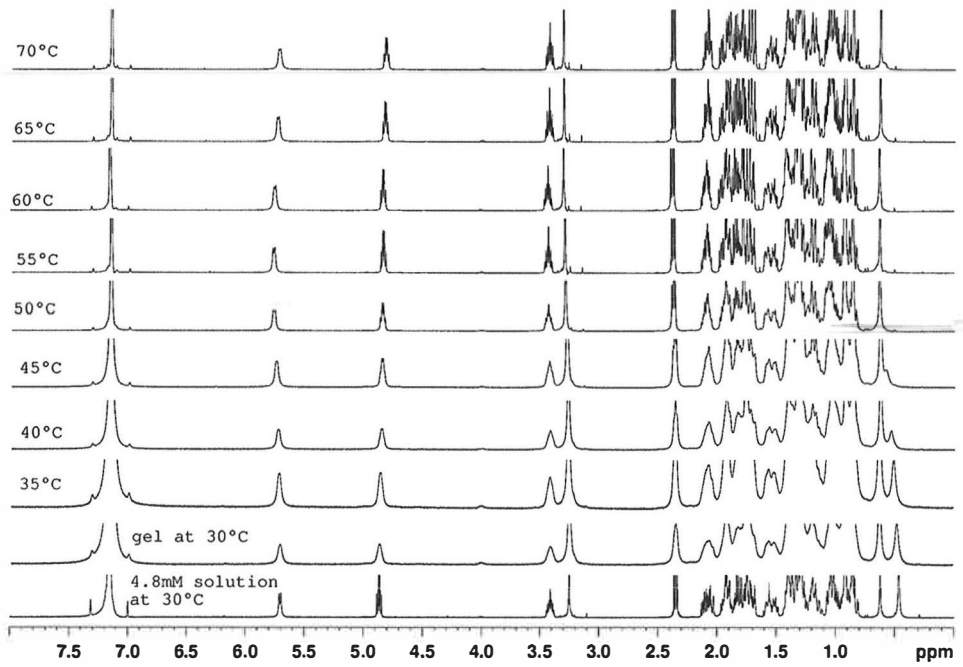

Figure 38. VT ^{1}H NMR spectra of 2% (w/v) benzene-d_6 gel of **24a**. For comparison, ^{1}H NMR spectrum of a dilute solution is presented undermost.

While performing NMR studies for the peptide-based organogelators, Miravet and co-workers observed that the ^{1}H NMR spectra of dilute solution and that of the gel displayed similar chemical shift values (with broadened signals in the gel sample).[171] Consequently, they hypothesized that the observed signals predominantly originated from the free molecules and the molecules in aggregated state were not observable by NMR. That is why concentration-dependent ^{1}H NMR experiments (Fig. 39) were performed by us. The experiments revealed that while the concentration in solution increases, the chemical shift of the NH proton moves to higher ppm-values, clearly indicating that hydrogen bonding plays a role in the self-assembly. However, at a concentration where the gel is formed (1.5% w/v), the amide proton again becomes more shielded, the chemical shift value being nearly identical to that of in 4.8 mM (0.25% w/v) free solution (the lowermost spectrum in Fig. 38). This observation coincides with the hypothesis of Miravet and co-workers[171] according to which the observed signals originate from the non-aggregated molecules of the sample.

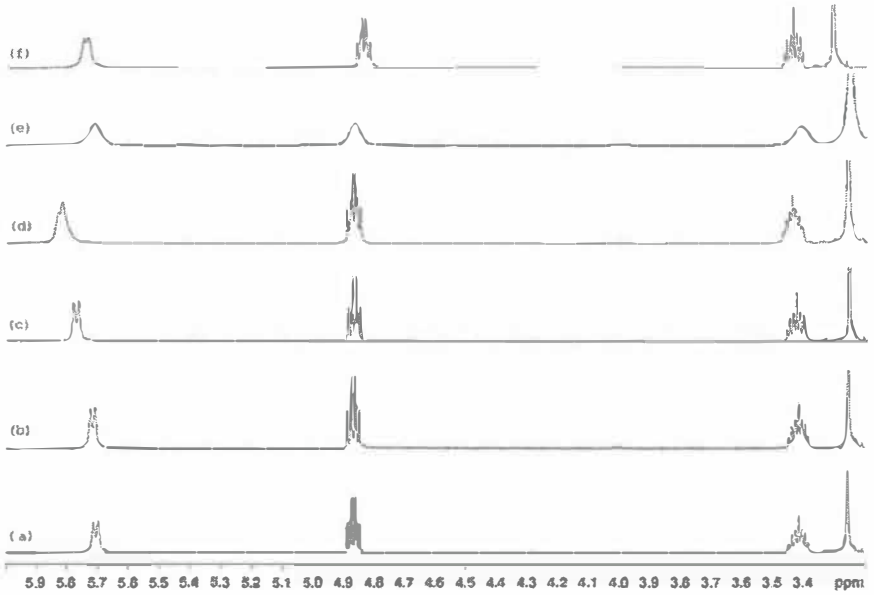

Figure 39. Concentration-dependent ^{1}H NMR spectra of **24a** in benzene-d_6 showing the position of the chemical shift of the amide proton (δ ~ 5.7 ppm) as a function of concentration. (a) 0.25% (4.8 mM); (b) 0.50%; (c) 1.0%; (d) 1.5%; (e) 2.0% (gel) at 30 °C, and (f) 2.0% at 60 °C.

The chemical shift value and the shape/splitting pattern of the amide proton of compound **24c**, for one, were shown to change significantly when transformed from the gel state (30 °C, δ 6.87) to the solution state (45 °C, δ 6.50) (Fig. 40). This suggests that there exists hydrogen bonding involving the amide protons in the gel. Deformation of the gel upon heating destroys the hydrogen bonding network and causes the amide proton to become more shielded.

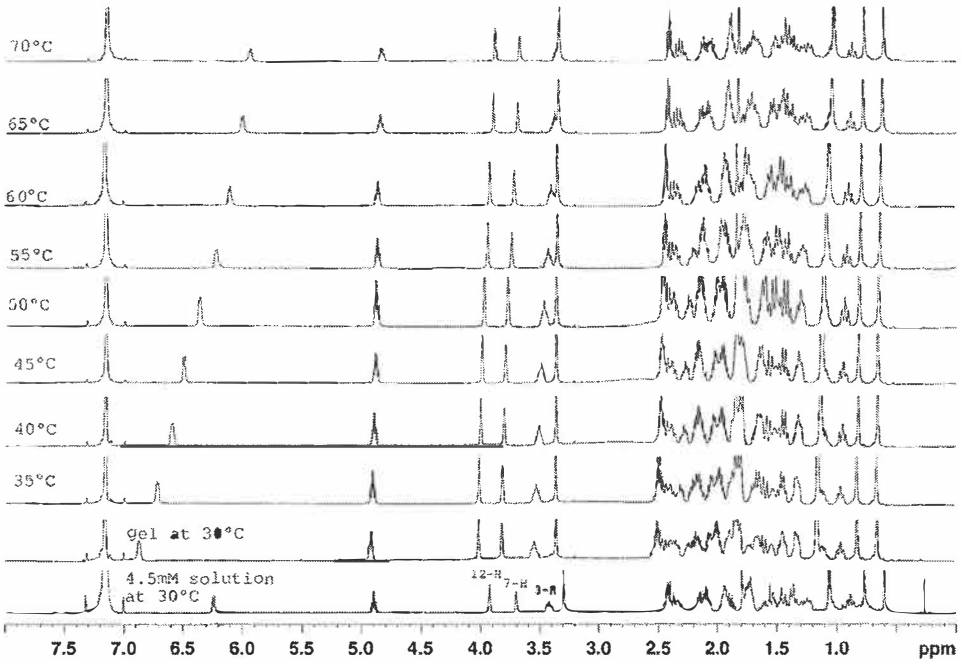

Figure 40. VT ^{1}H NMR spectra of 2% (w/v) benzene-d_6 gel of **24c**. For comparison, ^{1}H NMR spectrum of a dilute solution is presented undermost.

Concentration-dependent ^{1}H NMR experiments were carried out for compound **24c**, as well (Fig. 41). Deviating from the results obtained for compound **24a**, a steady movement of the chemical shifts of β-hydrogens (3β, 7β, and 12β-H's) as well as the amide proton to higher ppm values was observed even after the gel formation (0.5% w/v). Moreover, the NMR signals appeared as sharp and well-resolved all the way, even for the gel state sample. This indicates somewhat different behavior for the gel of **24c** in comparison to the one of **24a**.

In order to investigate the similarities/differences in the solid and gel state behavior of compounds **24a** and **24c**, ^{13}C CPMAS NMR experiments were performed. For compound **24a** (Fig. 42), solid state spectra of the product crystallized from acetonitrile and 2% (w/v) benzene gel closely resemble each other, suggesting a somewhat similar behavior in solid and gel states. CA-derivative **24c**, instead, seems to behave differently in the solid and gel states, as the spectra of the re-crystallized product (acetonitrile) and of the 4% (w/v) toluene-d_8 gel differ from each other (see publication II, Fig. 6).

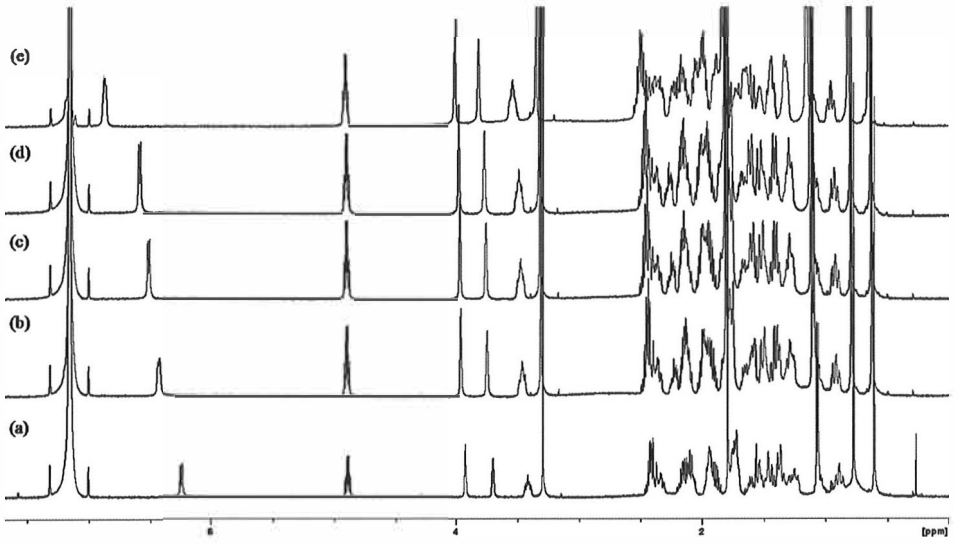

Figure 41. Concentration-dependent ^{1}H NMR spectra of **24c** in benzene-d_6. (a) 0.25% (4.5 mM); (b) 0.50%; (c) 0.75%; (d) 1.0%; (e) 2.0% at 30 °C.

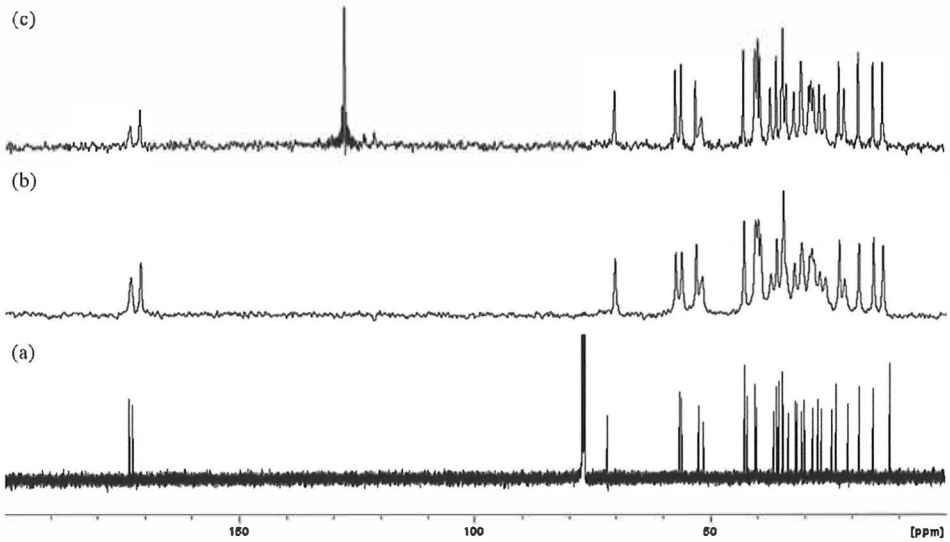

Figure 42. ^{13}C NMR spectra of compound **24a**. (a) Solution state; (b) CPMAS NMR spectrum of the synthesis product re-crystallized from acetonitrile; (c) CPMAS NMR spectrum of the 2% (w/v) benzene gel.

2.4 Solid state studies[II-IV]

During the course of the self-assembly studies many of the compounds were shown to crystallize from a variety of solvents. These observations were exploited in preparing samples for solid state studies. Solid state properties were investigated by means of both powder and single crystal X-ray diffraction along with solid state NMR spectroscopy. Single crystal structures for seven of the compounds were solved.

The crystallographic diagrams with thermal ellipsoids of compounds **24a**–**c** are presented in Figure 43. In compound **24b** there are two possible positions found for methyl C27 refined with population parameters of 0.81 and 0.19. Also the methyl C30 of **24b** points to a different direction compared to derivatives **24a** and **24c**, which can be observed from Figure 43. Anyhow, regardless of the small conformational discrepancy in derivative **24b**, the crystalline samples **24a**–**c** with similar unit cell parameters can be considered as isostructural materials.

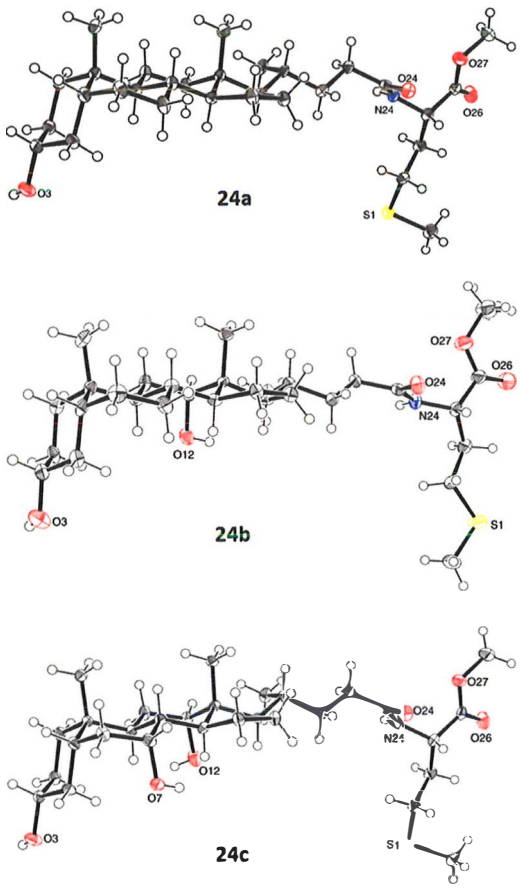

Figure 43. ORTEP[172] plots of asymmetric units of compounds **24a**–**c**.

Interestingly, it was revealed, that the single crystal structure of compound **24a** stands for a low-temperature form, which, dynamically in a reverse manner in solid state transforms to the room-temperature form (**24a-2**), the structure of which was determined utilizing powder diffraction data obtained from a xerogel sample of **24a**. In Figure 44 the overlaid molecular structures and packing modes of the two forms are presented.

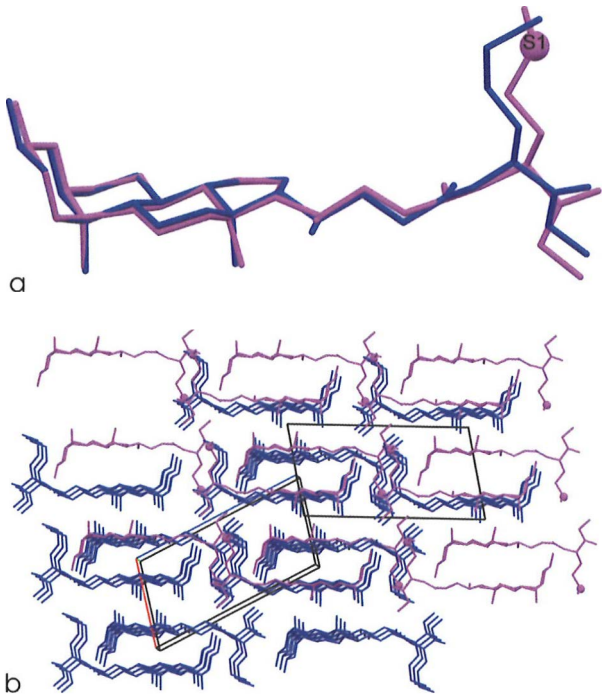

Figure 44. Overlays of (a) molecular structures and (b) packing modes of **24a** (blue structure) and **24a-2** (magenta structure) presented along the *b*-axis of the room-temperature structure **24a-2**. For clarity, the sulfur atom (S1) of **24a-2** is presented in a ball-style and hydrogen atoms are omitted.

In the single crystal X-ray diffraction analysis the molecular backbones of **25a**, **26a**, and **27c**·H_2O were found to show geometric parameters very typical to bile acid-based structures, deviating from each other only by the side chain conformation. The side chains of compounds **25a** and **26a** derived from lithocholic acid are fairly straight, and the overall side chain conformations between C13 and N24 as combinations of four dihedral angles are *ttt*i for **25a** and *tttt* (all-*trans*) for **26a** (*t* = *trans*, i = intermediate), respectively. The monohydrate of the cholyl derivative (**27c**·H_2O) shows twisted overall side chain conformation of *ttg*i (*g* = *gauche*), and the side chain is turned towards the hydrophobic β-face of the steroidal backbone. The hydrogen bonding interactions found for compound **25a** are both accepted by the same neighboring molecule, constructing along the *b*-axis a helical chain which is transversal to the longitudinal axis of

the molecule (Fig. 45). For compound **26a** the two donated intermolecular hydrogen bonds are directed towards the carbonyl acceptors (either O24 or O26) of the neighboring molecules, thus causing one molecule to be connected to four neighboring molecules by hydrogen bonding interactions. A helical chain motif along the *b*-axis formed by O3–H···O24 hydrogen bonds is found, resembling the motif observed for compound **25a**. In both of the compounds, the observed helical chains form bilayers throughout the structures, when connected to the adjacent chains.

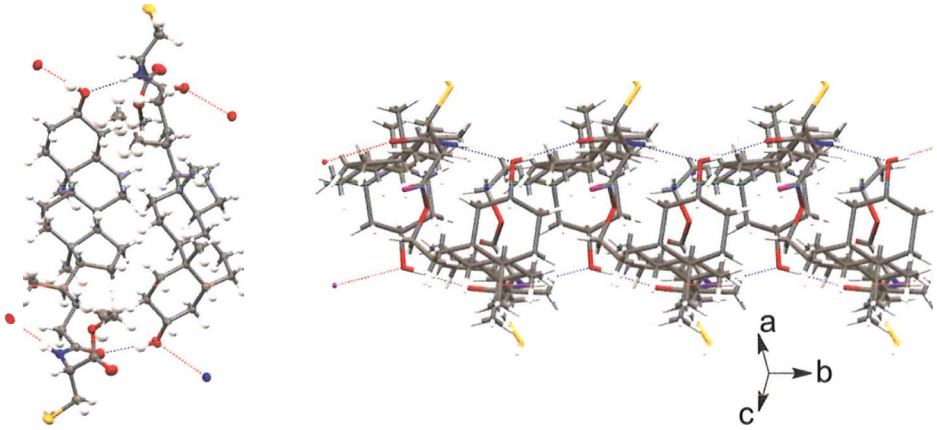

Figure 45. Left: Two interconnected molecules of compound **25a** showing the hydrogen bonds as dashed lines. Right: The helical motif formed along the *b*-axis of the single crystal structure of compound **25a**.

Due to two additional O–H donors in the steroidal skeleton and the presence of the water molecule, the monohydrate of the cholyl conjugate of L-serine methyl ester (**27c**·H_2O) has a notably richer hydrogen bonding network compared to those of compounds **25a** and **26a**. The water molecule is bound to the host by O12–H···O1 and O1–H···O7 interactions (Fig. 46), which is a common position for water in hydroxycholanoic acid-based structures.[173] The compound is found to assemble by two interlinked helical chain motifs. Similar layers possessed by **25a** and **26a** are not formed due to the twist of the side chain.

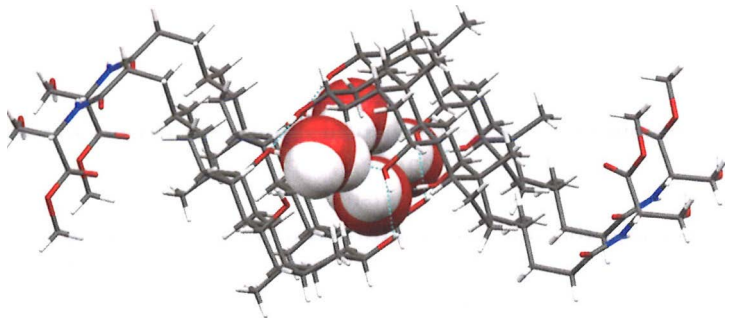

Figure 46. Binding of the water molecules by the steroidal parts of the molecules in **27c**·H_2O.

For the cysteamine conjugates of bile acids, crystals suitable for single crystal X-ray studies were obtained only for the cholyl derivative **28e**. The studies revealed that the structure of **28e** is a non-stoichiometric hydrate composed of a mixture of a hydrate (80%) and an anhydrous component (20%). Again, the steroidal skeletons show geometric parameters typical to bile acids. The torsion angles of the side chain are rather close to a perfect all-*trans* conformation. The hydrate and the anhydrous component are shown to differ in the conformation of the cysteamine moiety of the molecule. The sulfhydryl group of the hydrate is hydrogen-bonded to a water molecule. The molecules form bilayers along the *b*-axis by bringing the hydrophilic α-faces together with the help of hydrogen bonds. The bilayers further pack together *via* hydrophobic effects. The interactions involved are represented in Figure 47.

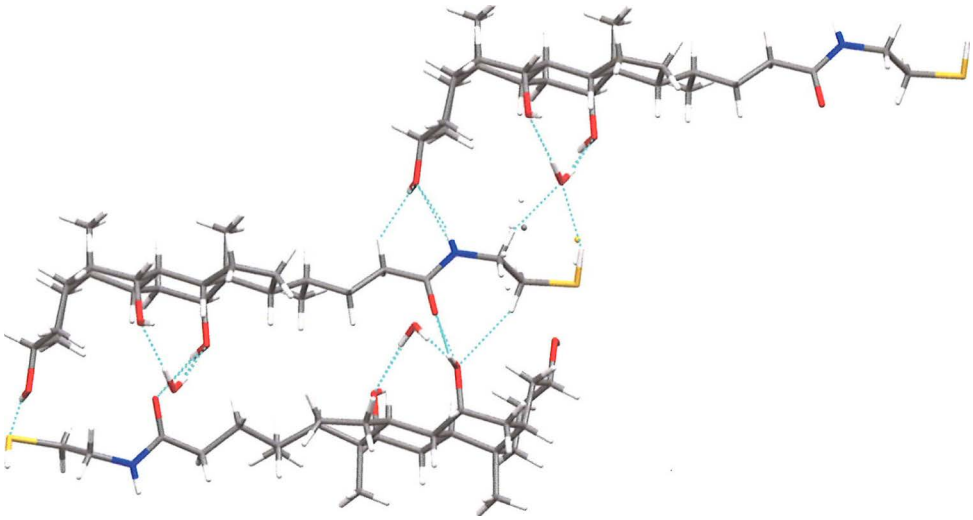

Figure 47. The interactions involved in the bilayer formation (between the molecules lowermost and in the middle) together with the contacts responsible for packing of the bilayers (between the molecules in the middle and uppermost) for compound **28e**.

Polymorphism is an ability of a compound or an element to exist in two or more crystalline forms that differ in the conformation and/or the arrangement of the molecules in the crystal lattice. Solvates (pseudopolymorphs), for one, are crystalline solid adducts containing either stoichiometric or non-stoichiometric proportions of solvent molecules within their crystal structure. When the incorporated solvent is water, the solvate is termed as a hydrate (as shown for compound **28e** earlier). The study of polymorphism is important especially from the pharmaceutical industry's point of view; different polymorphic forms of the same compound may significantly differ in certain physical, chemical, and biological properties.[174] The polymorphic behavior of commercial bile acids was recently studied by CPMAS NMR spectroscopy together with single crystal and powder X-ray diffraction.[175]

The possible polymorphism exhibited by selected compounds within the current study was investigated by means of solid state NMR spectroscopy and powder X-ray diffraction. ^{13}C CPMAS NMR studies were, for example, performed for the rather easily crystallized compound **28e**. The solid state NMR spectrum of the synthesis product (Fig. 48B) represents highly amorphous form giving very broad signals. However, in the spectrum of the re-crystallized compound (Fig. 48C) well-resolved signals with fairly narrow line-widths can be seen. Moreover, the spectrum reveals the so-called doublet-resonance pattern, suggesting the sample being either (a) mixture of different polymorphic forms, or (b) composed of a form having two non-equivalent molecules present in an asymmetric unit.

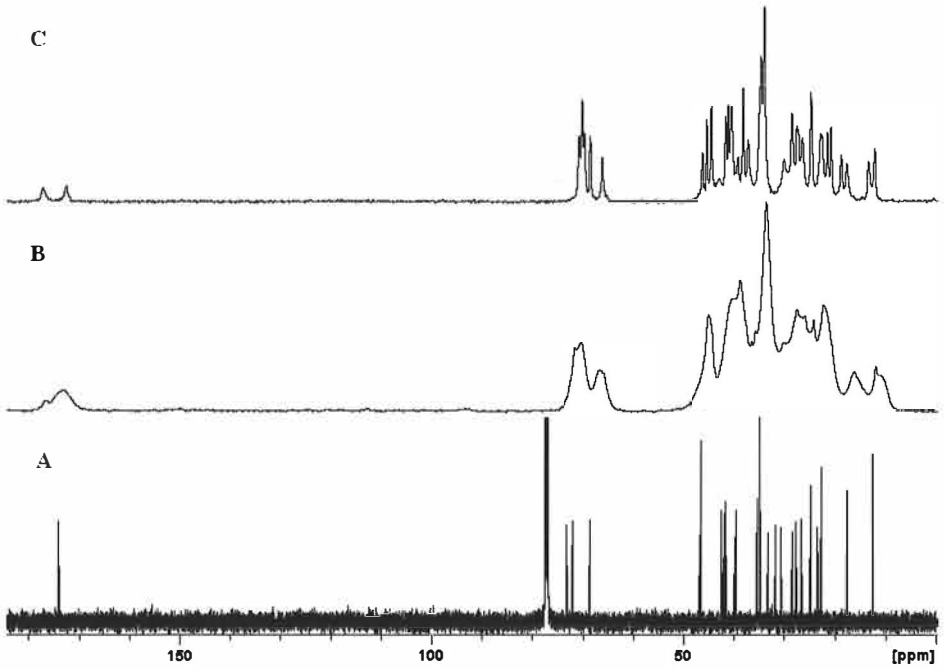

Figure 48. ^{13}C NMR spectra of **28e**: Solution state ^{13}C NMR spectrum in $CDCl_3$ (A), as well as ^{13}C CPMAS NMR spectra of the synthesis product (B) and the compound re-crystallized from acetonitrile (C).

In order to further investigate the phenomenon of polymorphism, powder X-ray diffraction (PXRD) data for the samples of **28e** were recorded (Fig. 49). As already noticed on the grounds of the solid state NMR experiments, the synthesis product turned out to be poorly crystalline, giving only a few reflections. The PXRD pattern of the single crystal data of **28e** was simulated, and the most intensive reflections in the simulated pattern were also found in the diffraction pattern of the synthesis product. This suggests that the synthesis product is, at least partly, composed of the mixture of the hydrate and the anhydrous component of **28e**. However, the PXRD pattern of the sample re-crystallized from acetonitrile differed completely from these patterns, suggesting that yet another

form of the compound exists. Unfortunately, the detailed structure of this form remains unknown, due to the lack of crystals suitable for single crystal analysis.

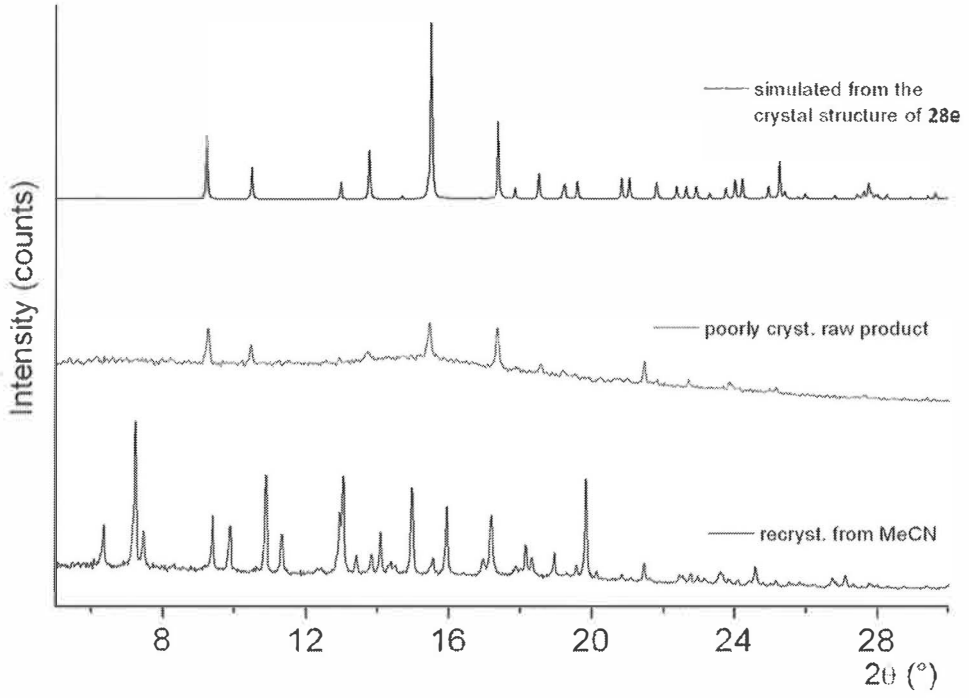

Figure 49. The experimental and simulated PXRD patterns of **28e**.

2.5 Biological studies of bile acid–cysteamine conjugates[IV]

Cysteamine (2-aminothiol) is the simplest stable aminothiol and a degradation product of the amino acid cysteine. The bitartrate salt of it (Cystagon) is used for the clinical treatment of nephropathic cystinosis, a rare autosomal recessive disease in humans.[176,177] The potential applicability of cysteamine *e.g.* in the treatment of malaria and Huntington's disease has recently been investigated.[178,179] However, because of certain problems in the applicability of cysteamine for drug purposes, efforts have been made to develop novel prodrugs of cysteamine.[180-182]

Lipinski's Rule of 5[183] is a rule discovered to evaluate druglikeness, or determine if a chemical compound with pharmacological or biological activity has properties that would enable it to function as an orally active drug in the human body. The Rule of 5 predicts that poor absorption or permeation is more likely when there are more than 5 hydrogen bond donors, 10 hydrogen bond acceptors, the molecular weight is greater than 500, and the calculated log*P* value is greater than 5. One violation to the above-mentioned criteria is generally

allowed. Compounds **28a–f** fulfill these criteria rather nicely. The molecular weight of the compounds varies between 435 and 461 Da, the number of hydrogen bond donors is from one to four, and the number of hydrogen bond acceptors from three to five. However, the log*P* values of compounds **28a–d** are somewhat higher than five (7.24 for **28a** and 5.36 for **28b–d**). Compounds **28e** and **28f**, for one, fulfill also the last rule, having log*P* values of 3.48 and 2.49, respectively.

Inspired by the calculations and the applicability of cysteamine for medical purposes, the preliminary toxicological evaluation for the compounds was performed. The standard model mouse fibroblast cell line, commonly used in accredited tests, was employed in the study. During MTT tests for compounds **28a–f**, some of the studied compounds may have reduced the MTT dye and thus false non-toxic results may have been observed. On this account the neutral red dye (NR) assay was used for further comparison. Table 1 contains the results obtained by using both methods. The results indicate that compounds **28a**, **28c**, and **28f** are relatively non-toxic in the conditions studied and thus show capability for further investigations for the use in pharmacological purposes.

Table 1 IC_{50} values determined for compounds **28a–f** by MTT method and incorporation of NR into living cells.

Compound	Tested range of concentrations (μg/mL)	IC_{50} (μg/mL) (MTT test)	IC_{50} (μg/mL) (NR test)
28a	0.4–50	-	-
28b	0.4–50	-	31.7 ± 5.4
28c	0.4–50	-	-
28d	0.4–50	-	7.8 ± 2.5
28e	0.4–50	12.2 ± 3.4	9.5 ± 1.5
28f	0.2–25	-	-

2.6 Synthesis and characterization of steroid-capped gold nanoparticles[v]

N-Lithocholyl-L-(cysteine ethyl ester) **25a** was exploited in preparing steroid-capped gold nanoparticles *via* a very straightforward single phase reduction process. The AuNPs were prepared by the $NaBH_4$ reduction of $HAuCl_4$ in the presence of **25a** in methanol, using 1:1, 2:1, and 1:2 molar ratios between the steroid and the gold salt. The prepared AuNPs were indispersible in most of the common organic solvents. However, they were easily dispersed in hexane, $CHCl_3$, and EtOAc in the presence of 5–10% of a polar co-solvent, such as MeOH and DMSO.

The synthesized AuNPs were characterized by elemental analysis, TEM, and UV spectrophotometry. The purity of the **25a**-capped AuNPs was exam-

ined by comparing the C:H ratios of the starting bile acid thiol and the final nanoparticles. The TEM images revealed mainly spherical particles with a diameter ranging from 4 to 17 nm. The individual NPs seemed to form agglomerates in methanol, as can be seen from the TEM image (Fig. 50). UV absorption spectra, for one, showed a surface plasmon resonance band, characteristic of colloidal gold, near 520 nm. The shapes of the observed plasmon resonance bands were dependent on the molar ratio of **25a** and the gold salt.

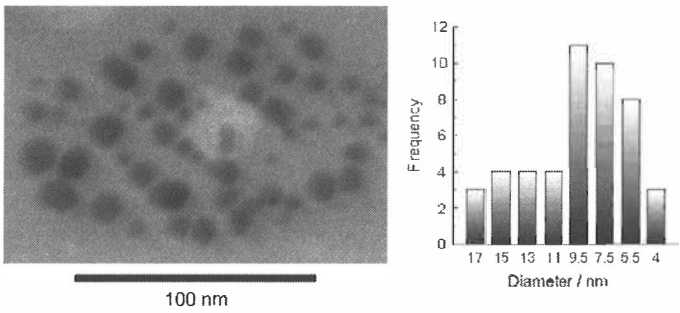

Figure 50. TEM image of an agglomerate formed by the **25a**-capped AuNPs (with 1:1 molar ratio of **25a**:$HAuCl_4$). Size distribution of the individual AuNPs is also shown.

Gold nanoparticles capped with the bile acid thiol were further analyzed by ^{13}C CPMAS NMR spectroscopy. The ^{13}C CPMAS NMR spectrum of the **25a**-capped AuNPs prepared with 2:1 molar ratio of **25a**:$HAuCl_4$ displayed the same chemical shifts as the liquid state spectrum of the organic ligand **25a**. This further supported the results obtained by elemental analysis, which suggested that **25a** was not decomposed during the nanoparticle formation.

3 SUMMARY AND CONCLUSIONS

In this thesis, the preparation of 18 bile acid amide conjugates of certain amino acid alkyl esters and drug molecule cysteamine is presented. All of the compounds have been extensively characterized by NMR spectroscopy and mass spectrometry thus providing a large amount of reference data for similar type of compounds. X-ray crystallography and solid state NMR spectroscopy have been employed to explore the solid state properties of the compounds. However, the weight of the research has been put on the self-assembly studies of the compounds, along with the investigations of the formed systems by versatile methods.

Compounds **24**–**28** formed a variety of self-assembled systems including supramolecular gels, vesicles, and spherulites. The number of the hydroxyl groups possessed by the steroidal skeleton and the character of the moiety attached *via* amidation to the carboxyl group of the bile acids were used as variables when examining the self-assembly properties of the compounds. Seven of the compounds were shown to be capable of self-assembly leading to organogelation mostly in certain aromatic solvents. All but one of the gelating compounds were derivatives of either lithocholic or cholic acid bearing one or three hydroxyl groups in their steroidal skeleton, respectively. Deoxycholyl derivatives bearing two hydroxyl groups in their steroidal part did not show gelation ability in the standard gelation tests applied. For the amino acid derivatives, three conjugates of the non-polar and hydrophobic L-methionine and L-valine alkyl esters were shown to be gelators, whereas the only compound bearing the polar and hydrophilic amino acid capable of gelation was the CA-derivative of L-cysteine ethyl ester. However, in the case of bile acid–cysteamine conjugates, apart from a weak gel formed by the lithocholyl derivative in benzene, three functional moieties in the steroidal parts of the compounds were needed for the self-assembly leading to gelation to occur, as the gel-forming compounds were the CA- and DHCA-derivatives. It thus seems evident that the nature of the compound conjugated to carbon 24 of the bile acid moiety is the determinant factor for the gel-forming ability of the compounds.

Morphologies of the self-assembled systems were investigated utilizing both optical and scanning electron microscopy. By SEM, mainly two kinds of morphologies for the gel samples were observed – fibrous structures or interconnected sphericals. Moreover, the sample preparation protocol was shown to affect the sample appearance. Variable-temperature and concentration-dependent NMR spectroscopy were exploited to investigate the interactions involved in the gel formation. Additionally, solid state NMR studies were performed for the native gel samples.

Solid state properties of the compounds were investigated by means of both powder and single crystal X-ray diffraction along with solid state NMR spectroscopy. Single crystal structures for seven of the compounds were solved. Moreover, the single crystal structure of compound **24a** was shown to represent a low-temperature form, which, dynamically in a reverse manner transforms to the room-temperature form (**24a-2**), the structure of which was determined utilizing powder diffraction data obtained from a xerogel sample of **24a**.

Inspired by the applicability of cysteamine for medical purposes, the preliminary toxicological evaluation for the compounds **28a–f** was performed. The standard model mouse fibroblast cell line, commonly used in accredited tests, together with the MTT tests and NR assay were employed in the study. The results indicated that compounds **28a**, **28c**, and **28f** are relatively non-toxic in the conditions studied and thus show capability for further investigations for the use in pharmacological purposes. Finally, compound **25a** was exploited in preparing steroid-capped gold nanoparticles *via* a very straightforward single phase reduction process.

To conclude, this thesis aims to highlight the importance of nanomaterials, such as supramolecular gels and gold nanoparticles, to modern chemical/materials science. Moreover, it shows that the steroidal bile acids found in the body of each of us may be exploited in a number of ways for a myriad of purposes. For the most part, the research described aims to provide useful information on the self-assembly properties of amide derivatives of bile acids gained by a varied range of experimental methods. However, despite of the number of studied compounds, general rules by which the molecular structure controls the gel-forming ability were hardly observed. This outlines the statement presented in the early part of the thesis, by which the rational design and synthesis of a gelator molecule typically is a challenging task. This is why an ever increasing effort could be expected to be put into the development of methodologies in order to get a deeper knowledge on the phenomena underlying gel formation at the molecular level. This is expected to provide novel tools for the design of functional and tunable systems that can be waited on to be increasingly composed of hybrid materials. Finally, the move from potential to active applications for all kinds of nanomaterials is to be expected. This can not, however, be achieved without a fruitful multidisciplinary collaboration between researchers in the field. Furthermore, the practical challenges, such as the stability of the supramolecular gels in a prolonged use or the toxicity of the

AuNPs during sustained and regular use of the AuNP formulations, are still to be solved.

REFERENCES

(1) Smith, D. K. In *Organic Nanostructures*, Atwood, J. L.; Steed, J. W. (Eds.), WILEY-VCH Verlag GmbH & Co. KGaA: Weinheim, 2008, pp. 111-154 and references cited therein.
(2) Sangeetha, N. M.; Maitra, U. *Chem. Soc. Rev.* **2005,** *34*, 821-836.
(3) Steed, J. W. *Chem. Commun.* **2011,** *47*, 1379-1383.
(4) Miravet, J. F.; Escuder, B. *Chem. Commun.* **2005,** 5796-5798.
(5) Dastidar, P.; Okabe, S.; Nakano, K.; Iida, K.; Miyata, M.; Tohnai, N.; Shibayama, M. *Chem. Mater.* **2005,** *17*, 741-748.
(6) Duan, P.; Liu, M. *Langmuir* **2009,** *25*, 8706-8713.
(7) Frkanec, L.; Žinić, M. *Chem. Commun.* **2010,** *46*, 522-537.
(8) Yan, N.; He, G.; Zhang, H.; Ding, L.; Fang, Y. *Langmuir* **2010,** *26*, 5909-5917.
(9) Mallia, V. A.; Terech, P.; Weiss, R. G. *J. Phys. Chem. B* **2011,** *115*, 12401-12414.
(10) Smith, D. K. *Chem. Soc. Rev.* **2009,** *38*, 684-694.
(11) Dastidar, P. *Chem. Soc. Rev.* **2008,** *37*, 2699-2715.
(12) Hirst, A. R.; Smith, D. K. *Chem. Eur. J.* **2005,** *11*, 5496-5508.
(13) Fages, F. *Angew. Chem. Int. Ed.* **2006,** *45*, 1680-1682.
(14) Piepenbrock, M.-O. M.; Lloyd, G. O.; Clarke, N.; Steed, J. W. *Chem. Rev.* **2010,** *110*, 1960-2004.
(15) Shapiro, Y. E. *Prog. Polym. Sci.* **2011,** *36*, 1184-1253.
(16) Banerjee, S.; Das, R. K.; Maitra, U. *J. Mater. Chem.* **2009,** *19*, 6649-6687 and references cited therein.
(17) Dawn, A.; Shiraki, T.; Haraguchi, S.; Tamaru, S.; Shinkai, S. *Chem. Asian J.* **2011,** *6*, 266-282.
(18) Yang, X.; Zhang, G.; Zhang, D. *J. Mater. Chem.* **2012,** *22*, 38-50.
(19) Simmons, B.; Li, S.; John, V. T.; McPherson, G. L.; Taylor, C.; Schwartz, D. K.; Maskos, K. *Nano Lett.* **2002,** *2*, 1037-1042.
(20) Kimura, M.; Kobayashi, S.; Kuroda, T.; Hanabusa, K.; Shirai, H. *Adv. Mater.* **2004,** *16*, 335-338.
(21) Bhat, S.; Maitra, U. *Chem. Mater.* **2006,** *18*, 4224-4226.
(22) Bhattacharya, S.; Srivastava, A.; Pal, A. *Angew. Chem. Int. Ed.* **2006,** *45*, 2934-2937.
(23) van Herrikhuyzen, J.; George, S.; Vos, M. R. J..; Sommerdijk, N. A. J. M.; Ajayaghosh, A.; Meskers, S. C. J.; Schenning, A. P. H. J. *Angew. Chem. Int. Ed.* **2007,** *46*, 1825-1828.
(24) Sangeetha, N. M.; Bhat, S.; Raffy, G.; Belin, C.; Loppinet-Serani, A.; Aymonier, C.; Terech, P.; Maitra, U.; Desvergne, J.-P.; Del Guerzo, A. *Chem. Mater.* **2009,** *21*, 3424-3432.
(25) Coates, I. A.; Smith, D. K. *J. Mater. Chem.* **2010,** *20*, 6696-6702.
(26) Love, C. S.; Chechik, V.; Smith, D. K.; Wilson, K.; Ashworth, I.; Brennan, C. *Chem. Commun.* **2005,** 1971-1973.
(27) Ray, S.; Das, A. K.; Banerjee, A. *Chem. Commun.* **2006,** 2816-2818.
(28) Vemula, P. K.; John, G. *Chem. Commun.* **2006,** 2218-2220.

(29) Vemula, P. K.; Aslam, U.; Ajay Mallia, V.; John, G. *Chem. Mater.* **2007**, *19*, 138-140.
(30) Mitra, R. N.; Das, P. K. *J. Phys. Chem. C* **2008**, *112*, 8159-8166.
(31) Basit, H.; Pal, A.; Sen, S.; Bhattacharya, S. *Chem. Eur. J.* **2008**, *14*, 6534-6545.
(32) Pal, A.; Chhikara, B. S.; Govindaraj, A.; Bhattacharya, S.; Rao, C. N. R. *J. Mater. Chem.* **2008**, *18*, 2593-2600.
(33) Srinivasan, S.; Babu, S. S.; Praveen, V. K.; Ajayaghosh, A. *Angew. Chem. Int. Ed.* **2008**, *47*, 5746-5749.
(34) Hirst, A. R.; Escuder, B.; Miravet, J. F.; Smith, D. K. *Angew. Chem. Int. Ed.* **2008**, *47*, 8002-8018.
(35) Truong, W. T.; Su, Y.; Meijer, J. T.; Thordarson, P.; Braet, F. *Chem. Asian J.* **2011**, *6*, 30-42.
(36) Llusar, M.; Sanchez, C. *Chem. Mater.* **2008**, *20*, 782-820.
(37) Hartgerink, J. D.; Beniash, E.; Stupp, S. I. *Science* **2001**, *294*, 1684-1688.
(38) Yoshimura, I.; Miyahara, Y.; Kasagi, N.; Yamane, H.; Ojida, A.; Hamachi, I. *J. Am. Chem. Soc.* **2004**, *126*, 12204-12205.
(39) Yamaguchi, S.; Yoshimura, I.; Kohira, T.; Tamaru, S.; Hamachi, I. *J. Am. Chem. Soc.* **2005**, *127*, 11835-11841.
(40) Steed, J. W. *Chem. Soc. Rev.* **2010**, *39*, 3686-3699.
(41) Foster, J. A.; Piepenbrock, M.-O. M.; Lloyd, G. O.; Clarke, N.; Howard, J. A. K.; Steed, J. W. *Nature Chem.* **2010**, *2*, 1037-1043.
(42) Escuder, B.; Rodríguez-Llansola, F.; Miravet, J. F. *New J. Chem.* **2010**, *34*, 1044-1054.
(43) Fukushima, T.; Aida, T. *Chem. Eur. J.* **2007**, *13*, 5048-5058.
(44) Jayawarna, V.; Ali, M.; Jowitt, T. A.; Miller, A. F.; Saiani, A.; Gough, J. E.; Ulijn, R. V. *Adv. Mater.* **2006**, *18*, 611-614.
(45) Liebmann, T.; Rydholm, S.; Akpe, V.; Brismar, H. *BMC Biotech.* **2007**, *7*, 88.
(46) Yang, Z.; Xu, K.; Wang, L.; Gu, H.; Wei, H.; Zhang, M.; Xu, B. *Chem. Commun.* **2005**, 4414-4416.
(47) Rajangam, K.; Behanna, H. A.; Hui, M. J.; Han, X.; Hulvat, J. F.; Lomasney, J. W.; Stupp, S. I. *Nano Lett.* **2006**, *6*, 2086-2090.
(48) Gao, Y.; Kuang, Y.; Guo, Z.-F.; Guo, Z.; Krauss, I. J.; Xu, B. *J. Am. Chem. Soc.* **2009**, *131*, 13576-13577.
(49) Silva, G. A.; Czeisler, C.; Niece, K. L.; Beniash, E.; Harrington, D. A.; Kessler, J. A.; Stupp, S. I. *Science* **2004**, *303*, 1352-1355.
(50) Sargeant, T. D.; Guler, M. O.; Oppenheimer, S. M.; Mata, A.; Satcher, R. L.; Dunand, D. C.; Stupp, S. I. *Biomaterials* **2008**, *29*, 161-171.
(51) Yang, Z.; Liang, G.; Ma, M.; Gao, Y.; Xu, B. *Small* **2007**, *3*, 558-562.
(52) Daniel, M.-C.; Astruc, D. *Chem. Rev.* **2004**, *104*, 293-346 and references cited therein.
(53) Giljohann, D. A.; Seferos, D. S.; Daniel, W. L.; Massich, M. D.; Patel, P. C.; Mirkin, C. A. *Angew. Chem. Int. Ed.* **2010**, *49*, 3280-3294.
(54) Turkevich, J.; Stevenson, P. C.; Hillier, J. *Discuss. Faraday Soc.* **1951**, *11*, 55-75.

(55) Brust, M.; Walker, M.; Bethell, D.; Schiffrin, D. J.; Whyman, R. *J. Chem. Soc., Chem. Commun.* **1994**, 801-802.
(56) Hostetler, M. J.; Green, S. J.; Stokes, J. J.; Murray, R. W. *J. Am. Chem. Soc.* **1996**, *118*, 4212-4213.
(57) Hostetler, M. J.; Templeton, A. C.; Murray, R. W. *Langmuir* **1999**, *15*, 3782-3789.
(58) Saha, K.; Agasti, S. S.; Kim, C.; Li, X.; Rotello, V. M. *Chem. Rev.* **2012**, *112*, 2739-2779.
(59) Huang, W; Chen, S.; Liu, Y.; Fu, H.; Wu, G. *Nanotechnology* **2011**, *22*, 025602.
(60) Zamborini, F. P.; Hicks, J. F.; Murray, R. W. *J. Am. Chem. Soc.* **2000**, *122*, 4514-4515.
(61) Wuelfing, W. P.; Zamborini, F. P.; Templeton, A. C.; Wen, X.; Yoon, H.; Murray, R. W. *Chem. Mater.* **2001**, *13*, 87-95.
(62) You, C.-C.; Miranda, O. R.; Gider, B.; Ghosh, P. S.; Kim, I.-B.; Erdogan, B.; Krovi, S. A.; Bunz, U. H. F.; Rotello, V. M. *Nat. Nanotechnol.* **2007**, *2*, 318-323.
(63) Upadhyayula, V. K. K. *Anal. Chim. Acta* **2012**, *715*, 1-18.
(64) Rana, S.; Bajaj, A.; Mout, R.; Rotello, V. M. *Adv. Drug Deliv. Rev.* **2012**, *64*, 200-216.
(65) Pissuwan, D.; Niidome, T.; Cortie, M. B. *J. Controlled Release* **2011**, *149*, 65-71.
(66) McIntosh, C. M.; Esposito, E. A.; Boal, A. K.; Simard, J. M.; Martin, C. T.; Rotello, V. M. *J. Am. Chem. Soc.* **2001**, *123*, 7626-7629.
(67) Joshi, H. M.; Bhumkar, D. R.; Joshi, K.; Pokharkar, V.; Sastry, M. *Langmuir* **2006**, *22*, 300-305.
(68) Singh, R.; Premkumar, T.; Shin, J.-Y.; Geckeler, K. E. *Chem. Eur. J.* **2010**, *16*, 1728-1743.
(69) Wu, B.; Kuang, Y.; Zhang, X.; Chen, J. *Nano Today* **2011**, *6*, 75-90.
(70) Mukhopadhyay, S.; Maitra, U. *Curr. Sci.* **2004**, *87*, 1666-1683.
(71) Monte, M. J.; Marin, J. J. G.; Antelo, A.; Vazquez-Tato, J. *World J. Gastroenterol.* **2009**, *15*, 804-816.
(72) Madenci, D.; Egelhaaf, S. U. *Curr. Opin. Colloid Interface Sci.* **2010**, *15*, 109-115.
(73) Roda, A.; Hofmann, A. F.; Mysels, K. J. *J. Biol. Chem.* **1983**, *258*, 6362-6370.
(74) Coello, A.; Meijide, F.; Rodríguez Núnez, E.; Vázquez Tato, J. *J. Pharm. Sci.* **1996**, *85*, 9-15.
(75) Funasaki, N.; Nomura, M.; Ishikawa, S.; Neya, S. *J. Phys. Chem. B* **2000**, *104*, 7745-7751.
(76) Garidel, P.; Hildebrand, A.; Neubert, R.; Blume, A. *Langmuir* **2000**, *16*, 5267-5275.
(77) Matsuoka, K.; Moroi, Y. *Biochim. Biophys. Acta* **2002**, *1580*, 189-199.
(78) Ninomiya, R.; Matsuoka, K.; Moroi, Y. *Biochim. Biophys. Acta* **2003**, *1634*, 116-125.
(79) Sugioka, H.; Matsuoka, K.; Moroi, Y. *J. Colloid Interface Sci.* **2003**, *259*, 156-162.

(80) Reis, S.; Moutinho, C. G.; Matos, C.; de Castro, B.; Gameiro, P.; Lima, J. L. F. C. *Anal. Biochem.* **2004**, *334*, 117-126.
(81) Mazer, N. A.; Carey, M. C.; Kwasnick, R. F.; Benedek, G. B. *Biochemistry* **1979**, *18*, 3064-3075.
(82) Campanelli, A. R.; Candeloro de Sanctis, S.; Giglio, E.; Viorel Pavel, N.; Quagliata, C. *J. Incl. Phenom. Mol. Recognit. Chem.* **1989**, *7*, 391-400.
(83) Blow, D. M.; Rich, A. *J. Am. Chem. Soc.* **1960**, *82*, 3566-3571.
(84) Terech, P.; de Geyer, A.; Struth, B.; Talmon, Y. *Adv. Mater.* **2002**, *14*, 495-498.
(85) Zhang, X.; Zou, J.; Tamhane, K.; Kobzeff, F. F.; Fang, J. *Small* **2010**, *6*, 217-220.
(86) Zhang, X.; Bera, T.; Liang, W.; Fang, J. *J. Phys. Chem. B* **2011**, *115*, 14445-14449.
(87) Tamhane, K.; Zhang, X.; Zou, J.; Fang, J. *Soft Matter* **2010**, *6*, 1224-1228.
(88) Enhsen, A.; Kramer, W.; Wess, G. *Drug Discovery Today* **1998**, *3*, 409-418 and references cited therein.
(89) Virtanen, E.; Kolehmainen, E. *Eur. J. Org. Chem.* **2004**, 3385-3399 and references cited therein.
(90) Salunke, D. B.; Hazra, B. G.; Pore, V. S. *Curr. Med. Chem.* **2006**, *13*, 813-847 and references cited therein.
(91) Sievänen, E. *Molecules* **2007**, *12*, 1859-1889 and references cited therein.
(92) Sharma, R.; Long, A.; Gilmer, J. F. *Curr. Med. Chem.* **2011**, *18*, 4029-4052 and references cited therein.
(93) Hofmann, A. F.; Hagey, L. R. *Cell. Mol. Life Sci.* **2008**, *65*, 2461-2483.
(94) Swaan, P. W.; Szoka Jr., F. C.; Øie, S. *Adv. Drug Deliv. Rev.* **1996**, *20*, 59-82.
(95) Balakrishnan, A.; Polli, J. E. *Mol. Pharmaceutics* **2006**, *3*, 223-230.
(96) Janout, V.; Regen, S. L. *Bioconjugate Chem.* **2009**, *20*, 183-192.
(97) Maitra, U. *Curr. Sci.* **1996**, *71*, 617-624.
(98) Nonappa; Maitra, U. *Org. Biomol. Chem.* **2008**, *6*, 657-669.
(99) Bortolini, O.; Fantin, G.; Fogagnolo, M. *Chirality* **2010**, *22*, 486-494.
(100) Miyata, M.; Tohnai, N.; Hisaki, I. *Acc. Chem. Res.* **2007**, *40*, 694-702.
(101) Tamminen, J.; Kolehmainen, E. *Molecules* **2001**, *6*, 21-46.
(102) Davis, A. P. *Coord. Chem. Rev.* **2006**, *250*, 2939-2951.
(103) Vijayalakshmi, N.; Maitra, U. *Org. Lett.* **2005**, *7*, 2727-2730.
(104) Ghosh, S.; Maitra, U. *Org. Lett.* **2006**, *8*, 399-402.
(105) Babu, P.; Sangeetha, N. M.; Maitra, U. *Macromol. Symp.* **2006**, *241*, 60-67.
(106) Zhu, X.-X.; Nichifor, M. *Acc. Chem. Res.* **2002**, *35*, 539-546.
(107) Zhang, J.-W.; Zhu, X.-X. *Sci. China, Ser. B Chem.* **2009**, *52*, 849-861.
(108) Schryver, S. B. *Proc. R. Soc. London, Ser. B* **1914**, *87*, 366-374.
(109) Schryver, S. B. *Proc. R. Soc. London, Ser. B* **1916**, *89*, 176-183.
(110) Schryver, S. B.; Hewlett, M. *Proc. R. Soc. London, Ser. B* **1916**, *89*, 361-372.
(111) Sobotka, H.; Czeczowiczka, N. *J. Colloid Sci.* **1958**, *13*, 188-191.
(112) Valenta, C.; Nowack, E.; Bernkop-Schnürch, A. *Int. J. Pharm.* **1999**, *185*, 103-111.

(113) Hishikawa, Y.; Sada, K.; Watanabe, R.; Miyata, M.; Hanabusa, K. *Chem. Lett.* **1998**, *27*, 795-796.
(114) Bhat, S.; Maitra, U. *Tetrahedron* **2007**, *63*, 7309-7320.
(115) Pal, A.; Basit, H.; Sen, S.; Aswal, V. K.; Bhattacharya, S. *J. Mater. Chem.* **2009**, *19*, 4325-4334.
(116) Tung, S.-H.; Huang, Y.-E.; Raghavan, S. R. *Soft Matter* **2008**, *4*, 1086-1093.
(117) Qiao, Y.; Lin, Y.; Yang, Z.; Chen, H.; Zhang, S.; Yan, Y.; Huang, J. *J. Phys. Chem. B* **2010**, *114*, 11725-11730.
(118) Bhowmik, S.; Banerjee, S.; Maitra, U. *Chem. Commun.* **2010**, *46*, 8642-8644.
(119) Banerjee, S.; Kandanelli, R.; Bhowmik, S.; Maitra, U. *Soft Matter* **2011**, *7*, 8207-8215.
(120) Bhowmik, S.; Maitra, U. *Chem. Commun.* **2012**, *48*, 4624-4626.
(121) Zhao, Y.-L.; Stoddart, J. F. *Langmuir* **2009**, *25*, 8442-8446.
(122) Das, S.; de Rooy, S. L.; Jordan, A. N.; Chandler, L.; Negulescu, I. I.; El-Zahab, B.; Warner, I. M. *Langmuir* **2012**, *28*, 757-765.
(123) Sangeetha, N. M.; Balasubramanian, R.; Maitra, U.; Ghosh, S.; Raju, A. R. *Langmuir* **2002**, *18*, 7154-7157.
(124) Babu, P.; Chopra, D.; Guru Row, T. N.; Maitra, U. *Org. Biomol. Chem.* **2005**, *3*, 3695-3700.
(125) Wang, X.; Lu, Y.; Duan, Y.; Meng, L.; Li, C. *Adv. Mater.* **2008**, *20*, 462-465.
(126) Maitra, U.; Mukhopadhyay, S.; Sarkar, A.; Rao, P.; Indi, S. S. *Angew. Chem. Int. Ed.* **2001**, *40*, 2281-2283.
(127) Mukhopadhyay, S.; Maitra, U.; Ira; Krishnamoorthy, G.; Schmidt, J.; Talmon, Y. *J. Am. Chem. Soc.* **2004**, *126*, 15905-15914.
(128) Terech, P.; Maitra, U. *J. Phys. Chem. B* **2008**, *112*, 13483-13492.
(129) Banerjee, S.; Vidya, V. M.; Savyasachi, A. J.; Maitra, U. *J. Mater. Chem.* **2011**, *21*, 14693-14705.
(130) Nonappa; Maitra, U. *Soft Matter* **2007**, *3*, 1428-1433.
(131) Nonappa; Lahtinen, M.; Behera, B.; Kolehmainen, E.; Maitra, U. *Soft Matter* **2010**, *6*, 1748-1757.
(132) Willemen, H. M.; Vermonden, T.; Marcelis, A. T. M.; Sudhölter, E. J. R. *Langmuir* **2002**, *18*, 7102-7106.
(133) Willemen, H. M.; Vermonden, T.; Marcelis, A. T. M.; Sudhölter, E. J. R. *Eur. J. Org. Chem.* **2001**, 2329-2335.
(134) Willemen, H. M.; Marcelis, A. T. M.; Sudhölter, E. J. R.; Bouwman, W. G.; Demé, B.; Terech, P. *Langmuir* **2004**, *20*, 2075-2080.
(135) Valkonen, A.; Lahtinen, M.; Virtanen, E.; Kaikkonen, S.; Kolehmainen, E. *Biosens. Bioelectron.* **2004**, *20*, 1233-1241.
(136) Löfman, M.; Koivukorpi, J.; Noponen, V.; Salo, H.; Sievänen, E. *J. Colloid Interface Sci.* **2011**, *360*, 633-644.
(137) Koivukorpi, J.; Kolehmainen, E. *Tetrahedron Lett.* **2010**, *51*, 1199-1201.
(138) Ikonen, S.; Nonappa; Valkonen, A.; Juvonen, R.; Salo, H.; Kolehmainen, E. *Org. Biomol. Chem.* **2010**, *8*, 2784-2794.
(139) Bhat, S.; Valkonen, A.; Koivukorpi, J.; Ambika, A.; Kolehmainen, E.; Maitra, U.; Rissanen, K. *J. Chem. Sci.* **2011**, *123*, 379-391.

(140) Maitra, U.; Chakrabarty, A. *Beilstein J. Org. Chem.* **2011**, *7*, 304-309.
(141) Tripathi, A.; Pandey, P. S. *Tetrahedron Lett.* **2011**, *52*, 3558-3560.
(142) Bhat, S.; Maitra, U. *J. Chem. Sci.* **2008**, *120*, 507-513.
(143) Kasthuri, J.; Rajendiran, N. *Colloids Surf., B* **2009**, *73*, 387-393.
(144)Chandirasekar, S.; Dharanivasan, G.; Kasthuri, J.; Kathiravan, K.; Rajendiran, N. *J. Phys. Chem. C* **2011**, *115*, 15266-15273.
(145) Qiao, Y.; Chen, H.; Lin, Y.; Huang, J. *Langmuir* **2011**, *27*, 11090-11097.
(146) Kumar, A.; Chhatra, R. K.; Pandey, P. S. *Org. Lett.* **2010**, *12*, 24-27.
(147) Zhang, J.; Wang, X.; Zhao, B.; Li, C. *Chem. Lett.* **2006**, *35*, 40-41.
(148) Zhang, J.; Zhao, B.; Meng, L.; Wu, H.; Wang, X.; Li, C. *J. Nanopart. Res.* **2007**, *9*, 1167-1171.
(149) Zhang, X.; Mathew, M.; Gesquiere, A. J.; Fang, J. *J. Mater. Chem.* **2010**, *20*, 3716-3721.
(150) Terech, P.; Talmon, Y. *Langmuir* **2002**, *18*, 7240-7244.
(151) Tan, Z.; Ohara, S.; Naito, M.; Abe, H. *Adv. Mater.* **2011**, *23*, 4053-4057.
(152) Zhan, X.; Tamhane, K.; Bera, T.; Fang, J. *J. Mater. Chem.* **2011**, *21*, 13973-13977.
(153) Huang, X.; Weiss, R. G. *J. Colloid Interface Sci.* **2007**, *313*, 711-716.
(154) Ren, Y.; Li, C.; Lu, Y.; Wang, X.; Zeng, X. *J. Mater. Sci.* **2010**, *45*, 6830-6833.
(155) Fernández-Leyes, M.; Verdinelli, V.; Hassan, N., Ruso; J. M.; Pieroni, O.; Schulz, P. C.; Messina, P. *J. Mater. Sci.* **2012**, *47*, 2837-2844.
(156) Terech, P.; Sangeetha, N. M.; Bhat, S.; Allegraud, J.-J.; Buhler, E. *Soft Matter* **2006**, *2*, 517-522.
(157) Qiao, Y.; Lin, Y.; Wang, Y.; Yang, Z.; Liu, J.; Zhou, J.; Yan, Y.; Huang, J. *Nano Lett.* **2009**, *9*, 4500-4504.
(158) Qiao, Y.; Wang, Y.; Yang, Z.; Lin, Y.; Huang, J. *Chem. Mater.* **2011**, *23*, 1182-1187.
(159) Qiao, Y.; Chen, H.; Lin, Y.; Yang, Z.; Cheng, X.; Huang, J. *J. Phys. Chem. C* **2011**, *115*, 7323-7330.
(160) Soto Tellini, V. H.; Jover, A.; Galantini, L.; Viorel Pavel, N.; Meijide, F.; Vázquez Tato, J. *J. Phys. Chem. B* **2006**, *110*, 13679-13681.
(161) Soto Tellini, V. H.; Jover, A.; Meijide, F.; Vázquez Tato, J.; Galantini, L.; Viorel Pavel, N. *Adv. Mater.* **2007**, *19*, 1752-1756.
(162) Meijide, F.; Antelo, A.; Alvarez Alcalde, M.; Jover, A.; Galantini, L.; Viorel Pavel, N.; Vázquez Tato, J. *Langmuir* **2010**, *26*, 7768-7773.
(163) Manghisi, N.; Leggio, C.; Jover, A.; Meijide, F.; Viorel Pavel, N.; Soto Tellini, V. H.; Vázquez Tato, J.; Agostino, R. G.; Galantini, L. *Angew. Chem. Int. Ed.* **2010**, *49*, 6604-6607.
(164) Froner, E.; D'Amato, E.; Adamo, R.; Prtljaga, N.; Larcheri, S.; Pavesi, L.; Rigo, A.; Potrich, C.; Scarpa, M. *J. Colloid Interface Sci.* **2011**, *358*, 86-92.
(165) Hisaki, I.; Murai, T.; Yabuguchi, H.; Shigemitsu, H.; Tohnai, N.; Miyata, M. *Cryst. Growth Des.* **2011**, *11*, 4652-4659.
(166) Bergström, S.; Norman, A. *Acta Chem. Scand.* **1953**, *7*, 1126-1127.
(167) Magill, J. H. *J. Mater. Sci.* **2001**, *36*, 3143-3164.

(168) Gránásy, L.; Pusztai, T.; Tegze, G.; Warren, J. A.; Douglas, J. F. *Phys. Rev. E* **2005**, *72*, 011605.
(169) Terech, P.; Sangeetha, N. M.; Maitra, U. *J. Phys. Chem. B* **2006**, *110*, 15224-15233.
(170) Piepenbrock, M.-O. M.; Clarke, N.; Steed, J. W. *Soft Matter* **2010**, *6*, 3541-3547.
(171) Escuder, B.; LLusar, M.; Miravet, J. F. *J. Org. Chem.* **2006**, *71*, 7747-7752.
(172) Farrugia, L. J. *J. Appl. Crystallogr.* **1997**, *30*, 565.
(173) Valkonen, A.; Lahtinen, M.; Kolehmainen, E. *Steroids* **2008**, *73*, 1228-1241.
(174) Vippagunta, S. R.; Brittain, H. G.; Grant, D. J. W. *Adv. Drug Deliv. Rev.* **2001**, *48*, 3-26.
(175) Nonappa; Lahtinen, M.; Ikonen, S.; Kolehmainen, E.; Kauppinen, R. *Cryst. Growth Des.* **2009**, *9*, 4710-4719.
(176) Gahl, W. A.; Thoene, J. G.; Schneider, J. A. *N. Engl. J. Med.* **2002**, *347*, 111-121.
(177) Gahl, W. A. *Eur. J. Pediatr.* **2003**, *162*, S38-S41.
(178) Min-Oo, G.; Fortin, A.; Poulin, J.-F.; Gros, P. *Antimicrob. Agents Chemother.* **2010**, *54*, 3262-3270.
(179) Dubinsky, R.; Gray, C. *Movement Disorders* **2006**, *21*, 530-533.
(180) Anderson, R. J.; Cairns, D.; Cardwell, W. A.; Case, M.; Groundwater, P. W.; Hall, A. G.; Hogarth, L.; Jones, A. L.; Meth-Cohn, O.; Suryadevara, P.; Tindall, A.; Thoene, J. G. *Lett. Drug Des. Discovery* **2006**, *3*, 336-345.
(181) McCaughan, B.; Kay, G.; Knott, R. M.; Cairns, D. *Bioorg. Med. Chem. Lett.* **2008**, *18*, 1716-1719.
(182) Omran, Z.; Kay, G.; Di Salvo, A.; Knott, R. M.; Cairns, D. *Bioorg. Med. Chem. Lett.* **2011**, *21*, 45-47.
(183) Lipinski, C. A.; Lombardo, F.; Dominy, B. W.; Feeney, P. J. *Adv. Drug Deliv. Rev.* **1997**, *23*, 3-25.

ORIGINAL PAPERS

I

Recent advances in steroidal supramolecular gels

by

Hana Svobodová, Virpi Noponen, Erkki Kolehmainen & Elina Sievänen

RSC Adv. **2012**, *2*, 4985 – 5007.

https://doi.org/10.1039/C2RA01343F

II

Bile acid–amino acid ester conjugates: gelation, structural properties, and thermoreversible solid to solid phase transition

by

Virpi Noponen, Nonappa, Manu Lahtinen, Arto Valkonen, Hannu Salo, Erkki Kolehmainen & Elina Sievänen

Soft Matter **2010**, *6*, 3789 – 3796.

https://doi.org/10.1039/B925795K

III

Self-assembly properties of bile acid derivatives of L-cysteine, L-valine, and L-serine alkyl esters

by

Virpi Noponen, Arto Valkonen, Manu Lahtinen, Hannu Salo & Elina Sievänen

submitted

https://doi.org/10.1080/10610278.2012.735365

IV

Bile acid–cysteamine conjugates: Structural properties, gelation, and toxicity evaluation

by

Virpi Noponen, Heini Belt, Manu Lahtinen, Arto Valkonen, Hannu Salo, Jitka Ulrichová, Adéla Galandáková & Elina Sievänen

Steroids **2012**, *77*, 193 – 203.

https://doi.org/10.1016/j.steroids.2011.11.006

V

Novel two-step synthesis of gold nanoparticles capped with bile acid conjugates

by

Virpi Noponen, Shreedhar Bhat, Elina Sievänen & Erkki Kolehmainen

Mater. Sci. Eng., C **2008**, *28*, 1144 – 1148.

https://doi.org/10.1016/j.msec.2007.10.001